Titre: Title:	Co-continuous polymer blends
Auteur: Author:	Jianming Li
Date:	2001
Type:	Mémoire ou thèse / Dissertation or Thesis
Référence: Citation:	Li, J. (2001). Co-continuous polymer blends [Thèse de doctorat, École Polytechnique de Montréal]. PolyPublie. https://publications.polymtl.ca/7077/

INFORMATION TO USERS

This manuscript has been reproduced from the microfilm master. UMI films the text directly from the original or copy submitted. Thus, some thesis and dissertation copies are in typewriter face, while others may be from any type of computer printer.

The quality of this reproduction is dependent upon the quality of the copy submitted. Broken or indistinct print, colored or poor quality illustrations and photographs, print bleedthrough, substandard margins, and improper alignment can adversely affect reproduction.

In the unlikely event that the author did not send UMI a complete manuscript and there are missing pages, these will be noted. Also, if unauthorized copyright material had to be removed, a note will indicate the deletion.

Oversize materials (e.g., maps, drawings, charts) are reproduced by sectioning the original, beginning at the upper left-hand corner and continuing from left to right in equal sections with small overlaps.

ProQuest Information and Learning
300 North Zeeb Road, Ann Arbor, MI 48106-1346 USA
800-521-0600

UNIVERSITÉ DE MONTRÉAL

CO-CONTINUOUS POLYMER BLENDS

JIANMING LI
DÉPARTEMENT DE GÉNIE CHIMIQUE
ÉCOLE POLYTECHNIQUE DE MONTRÉAL

THÈSE PRÉSENTÉE EN VUE DE L'OBTENTION
DU DIPLÔME DE PHILOSOPHIAE DOCTOR (Ph. D)
(GÉNIE CHIMIQUE)
SEPTEMBRE 2001

UNIVERSITÉ DE MONTRÉAL

ÉCOLE POLYTECHNIQUE DE MONTRÉAL

Cette thèse intitulée:

CO-CONTINUOUS POLYMER BLENDS

présetée par: LI Jianming

en vue de l'obtention du diplôme de: Philosophiae Doctor

a été dûment acceptée par le jury d'examen composé de:

M. CARREAU Pierre J., Ph. D., président

M. VLACHOPOULOS, John, Ph. D.,membre

M. FAVIS Basil D., Ph. D., membre et directeur de recherche

M. FISA Bohuslav, Ph. D., member

To my parents

To my family

ACKNOWLEDGEMENTS

I would like to express my heartfelt gratitude to my research and thesis director, Professor Basil D. Favis, for providing me with the opportunity to study under his supervision and to do this project on co-continuous polymer blends. I am also very indebted to him for his guidance, motivation and help during my study. His encouragement inspired me to go through all the difficulties in the project. His accurate, practical and realistic attitude toward scientific research will certainly hold positive influences on my career and personal life.

I would like to thank all the members in this research group for their valuable help and full cooperation during my study. My special thanks also goes to those who brought me companionship and friendship that make my daily life enjoyable and pleasureable.

All the research work for this project was performed in the Centre de Recherche Appliquée sur les Polymères (CRASP). I would like to express my sincere gratitude to the Professors and technical staff in the CRASP for their help in different aspects.

Finally, this thesis is dedicated to my parents. I also take this opportunity to show my gratefulness to my wife, Yuezhen, and my lovely daughter, Jing, for their loves and caring I have received. Their patience and encouragement are indispensable for the accomplishment of my study.

ABSTRACT

In the current work on the characterization of co-continuous morphology, the role of the type of polymer-polymer interface on morphology in co-continuous polymer blends, and the strategies of compatibilizing polymer blends have been studied. The work was done on a high density polyethylene (HDPE)/polystyrene (PS) materials. The research approach for this study is as following. Firstly, a characterization technique known as BET nitrogen adsorption technique has been introduced as a tool for characterizing the co-continuous morphological structure and to exploit co-continuous morphology effectively. Secondly, the role of the type of interface on morphology in co-continuous polymer blends has been systematically investigated with this newly introduced technique. Finally, to better control the morphology and interfacial properties of co-continuous blends the efficacy of the copolymer on compatibilization of immiscible polymer blends has been examined at different dispersed phase concentrations. Compatibilization versus micelle formation has been explored using a family of emulsification curves, and strategies for optimizing the migration of interfacial modifier to the polymer-polymer interface have been proposed.

The lack of adequate characterization technique has been a hindrance to the effective exploitation and study of co-continuous morphology in polymer blends. Thus, it is desirable to develop a new characterization technique to quantify the morphology of co-continuous polymer blends. A BET nitrogen adsorption technique which is adequate to measure the co-continuous structures has been developed in this study. The principle of the BET measurement technique is as follows: first, the blend sample to be tested for co-continuity was selectively extracted to remove one of the phases, thus resulting in a microporous specimen. Then this porous specimen was put into a testing cell. The nitrogen gas is then passed through the cell at the liquid nitrogen temperature. The nitrogen gas passing though the tube and sample condenses and adsorbs on the surface of the sample. Finally, knowing the amount of gas adsorbed and assuming a mono-layer

adsorption of the nitrogen molecules, the surface area of the sample can be estimated. While testing the sample, three assumptions should be made. (1) the geometrical shape of a pore is similar to an interconnected cylinder, (2) the total volume of the pore is equal to the volume of extracted phase, and (3) the total surface area is that of the pore wall. With the above assumptions the pore diameter can be readily calculated. In order to verify the accuracy of the pore diameter obtained by BET technique, a comparison experiment was performed. The blend of 60%HDPE/40%PS with co-continuity of about 90% was chosen for the measurement by BET and image analysis. For the sample of 60%HDPE/40%PS blend, image analysis gives a value of 15.0 μm for d_v and 7.2 μm for d_n, while the BET test gives a value of 6.2 μm. It was found that the pore diameters (d_n) obtained by these two different techniques are comparable. In fact, this correlation is expected since the BET technique measures a surface area parameter (monolayer adsorption of nitrogen on the HDPE surface) the cylinders of smallest diameter will dominate the surface area generation. In such a case the diameter obtained by the BET technique should correlate to the number average value. Immiscible polymer blends compatibilized by an interfacial agent will modify the interfacial situation. Under such a condition, blends with different compatibilization levels will result in a series of values of interfacial area. Because the BET technique is very sensitive to the surface (interface) variation, it is possible to examine the effect of an interfacial modifier on the microstructure of a co-continuous polymer blend with this technique. The blend of 50%HDPE/50%PS, which is a fully co-continuous sample, was chosen for the BET measurement. An emulsification curve is generated in co-continuous region. The emulsification curve of the co-continuous region demonstrated that the tracking of surface area via the BET technique provides a powerful tool for analyzing the efficacy of an interfacial modifier at emulsifying a co-continuous morphology. Indeed, the BET technique has filled the gap for the characterization of this complex morphology.

Most of the previous studies regarding co-continuous morphology are focused on the viscosity ratio and volume fraction of the blend. However, in practice other factors

(e.g. elasticity ratio, interfacial tension, processing conditions) are also found to have strong influence on the phase inversion and the development of co-continuity in an immiscible polymer blend system. The type of polymer-polymer interface also plays a very critical role in the development of co-continuous morphology and microstructure. Now, with an adequate characterization technique it should be possible to study the role of the type of polymer-polymer interface on morphology in co-continuous polymer blends. In this regard three different types of interface have been examined systematically in order to isolate the role of the interface in the development of co-continuous morphology during melt blending. The three types of interface are: compatible binary blends based on HDPE/SEBS and HDPE/SEB (Type I); an incompatible binary system comprised by HDPE/PS (Type II) and compatible ternary systems comprised by HDPE/PS compatibilized by SEBS in one case and by SEB in another (Type III). The Type I and Type III systems represent conventional approaches to preparing blend systems of low interfacial tension. The co-continuous morphology is analyzed using three techniques: microscopy/image analysis, solvent extraction/gravimetric analysis, and BET characterization of surface area and pore size. It is found that the co-continuous morphologies for the Type I systems exists over a very wide composition range (from 30% copolymer to 68% copolymer), and that the continuity - composition relationship is identical for both the triblock and diblock binary blends. However, the scale of the morphology is much finer for the blend with diblock copolymer than with triblock copolymer. The usual viscosity ratio models used to predict the region of co-continuity of blends could not describe these systems due to the breadth of the dual phase continuity region. Nevertheless, it is found that the viscosity ratio of the low interfacial tension binary blends has no effect on either the composition region of co-continuity or the microstructure of the co-continuous blend. The Type II system possesses a narrower region of dual phase continuity (from 40% PS to 66% PS) than the Type I. Out of these three systems, Type III system demonstrates the narrowest region of dual phase continuity (from 45%PS to 64%PS). Furthermore, the Type II system shows a clear dependence of pore size on the phase concentration, while the Type I and Type III

interface systems essentially maintain a constant pore size over a wide range of phase concentrations.

The wide region of dual phase continuity for the Type I system is consistent with an argument based on the formation of highly stable elongated structures during melt mixing. The low interfacial tension of those systems results in very effective deformation of the dispersed phase followed by long breakup times.

Using general arguments based on thread lifetime vs. droplet lifetime during melt processing, a mechanism for the formation of dual phase continuity is proposed. For the Type I system with low interfacial tension, the continuity development and microstructural features are consistent with a mechanism dominated by thread-thread coalescence (thread lifetime>droplet lifetime), while for Type II system with high interfacial tension, the formation and the morphology of the co-continuous structures is consistent with a mechanism controlled by droplet-droplet coalescence (droplet lifetime>thread lifetime). In the Type III system with a compatibilized interface, the continuity development and the microstructural features are controlled by reduced droplet-droplet coalescence. This latter case is considered to be only partially compatibilized due to the generation of fresh interface during the deformation process and hence it can be still considered that the droplet lifetime>thread lifetime. Nevertheless, due to the partial emulsification, the droplet coalescence process is significantly reduced. The relative presence of fibers or droplets during dynamic mixing is confirmed and analyzed quantitatively using a matrix dissolution/image analysis technique. It is clear from the above discussions that the formation of stable fibers is critical to the development of continuity. Fiber stability, in turn, is developed through two basic routes 1) deformation/disintegration phenomena and/or, 2) coalescence phenomena. In this work the observed microstructural features indicate that fiber formation in the Type I system is dominated by deformation/disintegration followed by thread-thread coalescence, while the fiber formation in the Type II and III systems is dominated by droplet-droplet

coalescence. It was also shown that the particular approach to achieving continuity has profound consequences on the resulting microstructure. A thread frequency ratio (TFR) is proposed as a basic general parameter to classify the relative presence of fibers to droplets during mixing and hence the type of continuity development and microstructure expected for a given system.

The addition of a block copolymer to immiscible blends with co-continuous structure can result in a finer and more stable interpenetrating morphology, better adhesion between the phases of the blends and consequently better properties of the final product. However, under certain circumstances a major drawback of this approach is the fact that the block copolymers may prefer to segregate and thus form micelles in one (or both) of the blend components, rather than to migrate to the interface, at a sub-critical concentration level. This phenomenon was found in studying co-continuous 50%HDPE/50%PS blends compatibilized by SEBS triblock copolymer. Knowing the value of the surface area, which can be directly obtained by BET, and the number of copolymer molecules used for emulsification, an estimated apparent interfacial area occupied per molecule, A_{app}, can be obtained. The A_{app} value for co-continuous 50%HDPE/50%PS/15%SEBS ($2.7nm^2$) is significantly lower than that obtained in PS/EPR blend compatibilized with same SEBS triblock copolymer ($13nm^2$). A systematic investigation was carried out on the HDPE/PS blend systems at different dispersed phase concentrations to detect the micelle formation of the copolymer at a sub-critical concentration level. Through an examination of evolution of the equilibrium dispersed phase size right at the interfacial saturation, as well as a comparison of the apparent interfacial area occupied by per modifier molecule (A_{app}) at the different dispersed phase concentrations, it is possible to estimate the interfacial coverage and thus detect the onset of micelle formation. The influence of the copolymer architecture and chemical composition on its migration to the interface has also been addressed. It is shown quantitatively that the affinity of the asymmetrical block copolymer (30PS:70EB) for the polyethylene matrix is responsible for the micelle formation before interfacial saturation.

Micelle formation at sub-critical concentration level can be virtually eliminated when PS is the matrix or when symmetrical block copolymers (50PS:50EB) are used. in such a case all of the interfacial modifier finds its way to the interface.

To conclude, the interfacial area of a co-continuous polymer blend can be readily obtained using BET technique. This parameter can be used to estimate the pore diameter of an extracted sample and thus it can be used to characterize the morphological properties of co-continuous blend. The development of the co-continuity and the formation of the microstructure are dependent mainly on the type of the polymer/polymer interface. Usually, for the type I interface and the type II interface the system possesses a wide region and a narrow region of dual phase continuity, respectively. While for the type III interface the system possesses the narrowest region of dual phase continuity. A thread frequency ratio (TFR) is proposed to catalogue the types of interface during continuity development. To stabilize the morphology of co-continuous polymer blends and control the interface properties, the addition of copolymer as an interfacial modifier significantly reduces the size of the dispersed phase and finesses the co-continuous structure. The micelle formation at a sub-critical concentration has been detected by using a family of emulsification curves. To inhibit this phenomenon, strategies to measure and optimize the migration of the interfacial modifier to the interface in immiscible polymer blend have been proposed. It is demonstrated that using the copolymer with a balanced block composition is an efficient approach to the better compatibilization of co-continuous polymer blends.

CONDENSÉ EN FRANÇAIS

Dans ce travail, sont étudiés la caractérisation de la morphologie co-continue, le rôle des différents types d'interface polymère-polymère sur la morphologie des mélanges de polymères co-continus et les stratégies pour compatibiliser ces mélanges. Ce travail a été mené sur un mélange modèle constitué de polyéthylène haute densité (HDPE) et de polystyrène (PS). L'approche de cette étude est la suivante : primo, une technique de caractérisation, appelée méthode d'adsorption d'azote BET a été introduite. Cette technique est adéquate pour caractériser la structure morphologique co-continue et rend possible l'exploitation efficace de la morphologie co-continue. Secundo, le rôle de chaque type d'interface sur la morphologie des mélanges de polymères co-continus a été systématiquement examiné avec la technique BET. Finalement, pour mieux contrôler la morphologie et les propriétés interfaciales des mélanges co-continus, l'efficacité de différents copolymères sur la compatibilisation des mélanges de polymères immiscibles a été étudiée pour diverses concentrations de phases dispersées. L'influence de la compatibilisation sur la formation de micelles a été explorée en produisant une famille de courbes d'émulsification et ainsi ont été proposées des stratégies pour optimiser la migration du modifiant interfacial à l'interface polymère-polymère.

L'absence d'une technique de caractérisation adéquate a été un obstacle pour l'exploitation efficace et l'étude de la morphologie co-continue des mélanges de polymères. Il a été nécessaire de développer une nouvelle technique de caractérisation pour quantifier la morphologie co-continue. La technique d'adsorption d'azote BET a été développée dans cette étude et a montré son adéquation pour évaluer les structures co-continues. Le principe de mesure BET est le suivant : tout d'abord, l'une des phases du mélange est extraite, donnant ainsi un spécimen microporeux. Ensuite, l'échantillon poreux est introduit dans la cellule d'essai. L'azote gazeux passe alors à travers la cellule à la température de l'azote liquide et est ainsi adsorbé sur les surfaces de l'échantillon

poreux. Finalement, connaissant la quantité de gaz adsorbé et en considérant l'adsorption d'une mono-couche de molécules d'azote, la surface totale de l'échantillon poreux peut être estimée. Lorsqu'un échantillon est testé, trois suppositions doivent être faites : (1) la forme géométrique d'un pore est un cylindre interconnecté; (2) le volume total de pore est égal à celui de la phase ayant été extraite; (3) la surface totale obtenue correspond à la surface de la paroi des pores. Avec les hypothèses ci-dessus, le diamètre de pore peut être facilement calculé. Afin de vérifier l'exactitude du diamètre de pore obtenu par la technique BET, une expérience de comparaison a été effectuée. Le mélange 60%HDPE/40%PS ayant une continuité de l'ordre de 90% a été choisi pour des mesures par BET et par analyse d'image. L'analyse d'image donne un diamètre moyen en volume d_v de 15.0μm et un diamètre moyen en nombre d_n de 7.2μm, tandis que l'essai BET donne une valeur de 6.2μm. Ainsi, on peut montrer que les diamètres de pore (d_n) obtenus par ces deux techniques sont comparables. En fait, cette corrélation était attendue puisque la technique BET mesure un paramètre de surface (adsorption d'une mono-couche d'azote à la surface du HDPE), les plus petits cylindres en diamètre dominant sur la génération de surface. Dans ce cas, le diamètre obtenu par la technique BET est pratiquement un diamètre moyen en nombre. Les mélanges de polymères immiscibles compatibilisés par un agent interfacial modifieront la situation à l'interface. Sous une telle condition, les mélanges avec différents niveaux de compatibilisation résulteront en une série de valeurs d'aire d'interface. Parce que la technique BET est très sensible à une variation de la surface (interface), il est possible d'examiner l'effet d'un agent interfacial sur la microstructure des mélanges de polymères co-continus avec cette technique. Le mélange 50%HDPE/50%PS, qui est complètement co-continu, a été choisi pour les mesures par BET. Une courbe d'émulsification de la région co-continue démontre que le suivi de l'aire de surface via la technique BET fournit un outil puissant pour l'analyse de l'efficacité des modifiants interfaciaux sur la morphologie co-continue. En effet, la technique BET a rempli une lacune pour la caractérisation de cette morphologie complexe.

Avec une technique de caractérisation adéquate, il devrait être possible d'étudier le rôle du type d'interface polymère-polymère sur la morphologie des mélanges de polymères co-continus. En fait, la plupart des études précédentes portant sur la morphologie co-continue tiennent seulement compte du rapport de viscosité et des fractions volumiques. En pratique, d'autres facteurs (rapport d'élasticité, tension interfaciale, conditions de mise en œuvre, par exemple) peuvent aussi avoir une forte influence sur l'inversion de phase et le développement de la co-continuité dans les systèmes de mélanges de polymères immiscibles. Les types d'interfaces polymère-polymère jouent un rôle très important dans le développement de la morphologie co-continue pendant le mélange à l'état fondu. Les trois types d'interface sont obtenus suivant les mélanges suivants : les mélanges binaires compatibles HDPE/SEBS et HDPE/SEB (Type I), un système binaire incompatible HDPE/PS (Type II) et des systèmes ternaires compatibilisés par le copolymère SEBS ou SEB (Type III). Les systèmes de Type I et de Type III représentent l'approche conventionnelle pour préparer des systèmes à faible tension interfaciale. La morphologie co-continue a été analysée par trois techniques : microscopie couplée à de l'analyse d'image, analyse gravimétrique après extraction par solvant et la caractérisation BET de l'aire de surface et de la taille de pore. Il a été trouvé que les morphologies co-continues pour les systèmes de Type I existaient sur une très large gamme de composition (de 30 à 68% de copolymère) et que la relation entre la continuité et la composition était identique quel que soit le copolymère, tribloc ou dibloc, utilisé. Cependant, la morphologie est beaucoup plus fine pour le mélange constitué du copolymère dibloc. Les modèles habituels comportant le rapport de viscosité servant à prédire la région de co-continuité ne peuvent décrire ces systèmes en raison de l'étendue de la région de co-continuité. Néanmoins, il a été trouvé que le rapport de viscosité des mélanges binaires de faible tension interfaciale n'avait d'effet ni sur la région de composition de la co-continuité, ni sur la morphologie du mélange co-continue. Le système de Type II possède une région de co-continuité plus étroite (de 40 à 66% de PS) que celle du Type I. Le système de Type III manifeste la région de co-continuité la plus étroite (de 45% à 64% de PS). Par ailleurs, le système de

Type II montre clairement une dépendance de la taille de pore suivant la concentration, tandis que les systèmes ayant des interfaces de Type I et III maintiennent une taille de pore essentiellement constante sur une large gamme de concentrations.

La large région de co-continuité pour le Type I est cohérente avec une formation de structures allongées extrêmement stables pendant l'étape de mélange à l'état fondu. La faible tension interfaciale de ces mélanges résulte en une déformation très efficace de la phase dispersée suivie par de longs temps de rupture.

En considérant la durée de vie des fils versus la durée de vie des gouttes pendant la mise en œuvre à l'état fondu, un mécanisme pour la formation de la co-continuité est proposé. Pour le système de Type I avec une faible tension interfaciale, le développement de la continuité et des caractéristiques structurales sont en accord avec un mécanisme dominé par une coalescence fil-fil (durée de vie d'un fil supérieure à celle d'une goutte), tandis que la formation et la morphologie du système de Type II co-continu avec une tension interfaciale élevée est en accord avec un mécanisme contrôlé par une coalescence goutte-goutte (durée de vie d'une goutte supérieure à celle d'un fil). Pour le système de Type III dont l'interface est compatibilisée, le développement de la continuité et de la microstructure sont contrôlés par une coalescence goutte-goutte réduite. Ce dernier cas est considéré comme étant seulement partiellement compatibilisé, en raison de la génération d'interface fraîche pendant le processus de déformation et de là, on peut encore considérer que la durée de vie d'une goutte est supérieure à celle d'un fil. Cependant, en raison d'une émulsification partielle, le processus de coalescence des gouttes est réduit de manière significative. La présence relative de fibres et de gouttes pendant l'opération dynamique de mélange a été confirmée et analysée quantitativement par une technique de dissolution de la matrice / analyse d'image. La discussion ci-dessus montre clairement que la formation de fibres stables est critique pour le développement de la continuité. La stabilité des fibres, à son tour, est développée suivant deux façons : 1) le phénomène de déformation/désintégration et/ou 2) le phénomène de coalescence. Dans

cette étude, les caractéristiques microstructurales observées indiquent que la formation de fibres dans le système de Type I est dominée par de la déformation/désintégration suivie par de la coalescence fil-fil, tandis qu'elle est dominée par de la coalescence goutte-goutte pour les systèmes des Types II et III. Il a été alors montré que l'approche particulière pour atteindre la continuité entraîne de profondes conséquences sur la microstructure résultante. Un rapport de fréquence de fil (TFR) est proposé comme paramètre de base pour classifier la présence relative de fibres et de gouttes pendant l'opération de mélange et ainsi, déterminer le type de développement de la continuité et de la microstructure attendue pour un système donné.

L'ajout d'un copolymère bloc dans des mélanges immiscibles co-continus peut résulter en une morphologie interpénétrée plus fine et plus stable, une meilleure adhésion entre les phases des mélanges et en conséquence, de meilleures propriétés du produit final. Cependant, dans certaines circonstances, une partie du copolymère bloc présente l'inconvénient de préférer s'isoler en micelles dans l'un ou les deux composants du mélange, au lieu de migrer à l'interface pour un niveau de concentration sous-critique. Ce phénomène a été observé dans l'étude des mélanges co-continus 50%HDPE/50%PS compatibilisés par le copolymère tri-bloc SEBS. Connaissant la valeur de l'aire de surface qui peut être directement obtenue par la technique BET et le nombre de molécules de copolymère utilisées pour l'émulsification, une aire interfaciale apparente estimée, occupée par molécule, A_{app}, peut être obtenue. Cette valeur A_{app} pour le mélange co-continu 50%HDPE/50%PS/15%SEBS ($2.7nm^2$) est significativement plus faible que celle obtenue pour le mélange PS/EPR compatibilisé avec le même copolymère tri-bloc SEBS ($13nm^2$). Une étude systématique a été conduite sur les systèmes HDPE/PS à des concentrations variables de phases dispersées, pour détecter la formation de micelle de copolymère à un niveau de concentration sous-critique. À travers le suivi de l'évolution de l'équilibre de la taille de phase dispersée appropriée pour saturer l'interface, aussi bien que par la comparaison d'aire interfaciale apparente occupée par molécule d'agent interfacial (A_{app}) à différentes concentrations de phase dispersée, il est possible d'estimer

le recouvrement de l'interface par l'agent interfacial et ainsi détecter le début de la formation de micelle. L'influence de l'architecture du copolymère et de sa composition chimique sur sa migration à l'interface a alors été détaillée : il est montré que quantitativement, l'affinité du copolymère bloc asymétrique (30PS:70EB) pour la matrice de polyéthylène est responsable de la formation de micelle avant la saturation de l'interface. La formation de micelles à un niveau de concentration sous-critique peut être pratiquement éliminée quand le PS est la matrice ou lorsque des copolymères blocs symétriques (50PS:50EB) sont utilisés. Dans de telles circonstances, la totalité du modifiant interfacial se dirige vers l'interface.

Pour conclure, l'aire de surface des mélanges de polymères co-continus peut être facilement obtenue par la technique BET. Ce paramètre peut servir à estimer le diamètre des pores de l'échantillon dont l'une des phases est extraite, et permet ainsi de caractériser les propriétés morphologiques du mélange co-continu. Le développement de la co-continuité et la formation de la microstructure dépendent principalement du type d'interface polymère-polymère. Pour l'interface de Type I, le système possède une large région de co-continuité, et le système de Type II, une plus faible. La plus faible est celle du système de Type III. Un rapport de fréquence de fil (TFR) a été proposé pour cataloguer les types d'interface pendant le développement de la continuité. Afin de stabiliser la morphologie des mélanges de polymères co-continus et contrôler les propriétés des interfaces, l'addition de copolymère comme modifiant interfacial réduit significativement la taille de la phase dispersée et affine la structure co-continue. La formation de micelles à un niveau de concentration sous-critique a été détectée par l'analyse d'une famille de courbes d'émulsification. Pour inhiber ce phénomène, des stratégies ont été proposées pour mesurer et optimiser la migration du modifiant interfacial à l'interface dans les mélanges de polymères. Il a été démontré que l'utilisation d'un copolymère ayant une composition en bloc équilibrée est une approche efficace pour obtenir une meilleure compatibilisation des mélanges de polymères co-continus.

TABLE OF CONTENTS

LIST OF FIGURES

LIST OF TABLES

CHAPTER 1. INTRODUCTION

Over the last two decades, the blending of two or more polymers to form a polymer blend has become an attractive route to develop new polymeric materials (Utracki 1989, Meijer et al., 1988, Paul and Bucknall, 2000).

Most polymer blends are immiscible. Considering the thermodynamics of mixing, the entropy of mixing of polymers becomes very small as a result of their macromolecular nature, thus even a mildly unfavourable enthalpy of mixing, which would not be enough to hinder mixing in small molecule miscibility because of the strong entropic driving force, is enough to render most polymer pairs immiscible (Akiyama, 1979, Olabishi, 1979). Therefore their blends are, in the vast majority of cases, two or multi-phase systems.

In two-phase blends, morphology plays an important role in determining properties. Most of such blends consist of a continuous phase of one component in which the second is dispersed. Clearly there is a tendency for the component which occupies the most space in the mixture to assume the role of a continuous phase. On the other hand, the component with the lower viscosity tends to encapsulate the more viscous component. Thus, which is the continuous phase depends primarily on composition and on the viscoelastic behaviour of the components. Moreover, there is frequently an intermediate region where there is no clear mandate for either component to be dispersed phase, so both components may form the continuous phase simultaneously. In this region, the two immiscible phases commingle in such a way that each phase remains continuously connected throughout the bulk of the blend. This morphological structure is called dual phase continuity or co-continuity. Obviously, such an interpenetrating network can be generated in many systems by a judicious control of microrheology and processing conditions.

Blends with co-continuous morphology are gaining attention because of an interesting feature of these morphologies is that both components, in all directions, can fully contribute to the properties of the blend (Gergen, 1987, Xie, 1991).

Polymer blends with co-continuous structure are of special interest for many types of applications, such as blends with barrier properties, conductive polymers, (Tchoudakov et al 1996, Levon et al 1993, Gubbels et al 1994), drug delivery in pharmaceutical field, scaffold for tissue engineering (Favis et al 2001) and materials with specific mechanical properties (Cook et al., 1996, Hourston et al., 1996).

Co-continuous morphologies are thermodynamically non-equilibrium structures. These structures can only be produced because the high viscosities of the polymer melts allow such a structure to be frozen in. Therefore, the structural instability is the one of their major disadvantages. Loss of co-continuity could result from prolonged exposure to melt temperature at low shear rate, since returning to conventional blend morphology, where droplets of one phase are dispersed in a matrix of the other phase, can lower interfacial area and thus free energy.

The conventional morphologies of polymer blends have been well reported in the literature (Elmendorp and Maalcke, 1985, and Favis and Willis, 1990), and their influences on physical properties of the materials have been significantly discussed in a number of publications (Yoshida et al., 1990, Shung, 1987, and Kamal et al., 1995). However, dual phase continuity and its influence on physical properties remain to be the least understood area in this field.

Although some work has been reported in the literature on predictions related to the position of co-continuity, very little has been known on controlling the scale of the co-continuous microstructure.

The ultimate objective of this study is to carry out fundamental studies related to controlling and characterizing the position and microstructure of co-continuous morphologies. This study will focuse on the investigation of the factors influencing the morphology of polymer blends, especially in the region of co-continuity. Strategies to control the morphology and interfacial properties of co-continuous blends will be developed.

CHAPTER 2. LITERATURE REVIEW

Polymer blends are physical mixtures of structurally different homo or copolymers. In order to tailor a polymer blend with a demanding morphological structure, it is of crucial importance to understand the fundamental parameters controlling the blend phase during melt processing. Theoretical and experimental studies indicate that composition, interfacial tension, processing conditions and rheological properties (viscosity and elasticity) of the components play important roles in determining the morphological structures of polymer blends.

2.1 Theory of Droplet Break-up and Coalescence

The development of morphology in two phase liquid/liquid systems, emulsions, and polymer blends has been a subject of extensive theoretical and experimental study for over 100 years. The main mechanism governing phase morphology development in immiscible polymer blends is believed to be the result of both droplet break-up and coalescence. Therefore, in order to obtain polymer blends with the desired morphology, a detailed knowledge of the blending condition and micro-rheological process (break-up and coalescence) is essential.

2.1.1 Newtonian Drop Break-up and Capillary Instability

When a neutrally buoyant, initially spherical droplet is suspended in another liquid and subjected to shear or extensional stress, it deforms and then breaks into small droplets. Taylor (1932, 1934) extended the work of Einstein (1906, 1911) on dilute suspensions of solid spheres in a Newtonian liquid, to dispersions of single Newtonian liquid droplet in another Newtonian liquid, subjected to well-defined deformational fields. Taylor (1932, 1934) observed that when the radius of the drop is great enough or when the rate of distortion is high; the drop breaks up. On the basis of Lamb's (Lamb 1932) general solution to Stoke's equation of creeping motion, Taylor calculated the velocity and pressure fields inside and outside the droplet and suggested that at low stress

in steady uniform shearing flow the deformation degree can be expressed by means of two dimensionless parameters: the capillary (or Taylor) number,

$$Ca = \frac{\eta_m \dot{\gamma} R}{\sigma} \qquad (2.1)$$

and the viscosity ratio:

$$p = \frac{\eta_d}{\eta_m} \qquad (2.2)$$

where η_d and η_m are the dispersed phase and matrix viscosity, respectively, $\dot{\gamma}$ is the shear rate, R is the radius of the drop, and σ is the interfacial tension. The parameter describing the critical condition of break-up is the critical capillary number Ca_{crit}. If the capillary number Ca is larger than the critical capillary number Ca_{crit}, the droplet can further deform and break up.

For simple shear flow, Taylor derived an equation for the value of Ca_{crit} in the case of Newtonian systems under simple shear flow (Equation 2.3)

$$Ca_{crit} = \frac{1}{2}\frac{16p+16}{19p+16} \qquad (2.3)$$

This relation is valid for small deformations in Newtonian fluids. Many researchers have followed up Taylor's work (Cox, 1969, Bentley et al., 1986, Flumerfelt, 1980, Rallison, 1981, Chin et al., 1979, Karam et al., 1986, Grace, 1982). Taylor predicted that no droplet break-up occurs when $p > 2.5$. This result compares well with simple shear experiments (Karam et al., 1986, Grace, 1982, Rumscheidt, 1961, Serpe et al., 1990) where no drop breakup was observed above $p = 4$.

For extensional flow, both experiments and theory indicate that the Ca_{crit} is lower than that in the case of simple shear flow. The flow in mixers used for polymer blending, is a mixture of simple shear flow and extensional flow. Thus Ca_{crit} for simple shear would predict the upper limit of the drop size for break-up in a dilute Newtonian system (Bentley et al., 1986). Grace (1982) has performed a monumental work on breakup of Newtonian drops in both simple shear and extensional flows. These results are

summarized in Figure 2. 1. It is clearly shown that breakup is possible in pure extensional flow at all viscosity ratios, but is impossible in shear flow simple flow above p = 4.

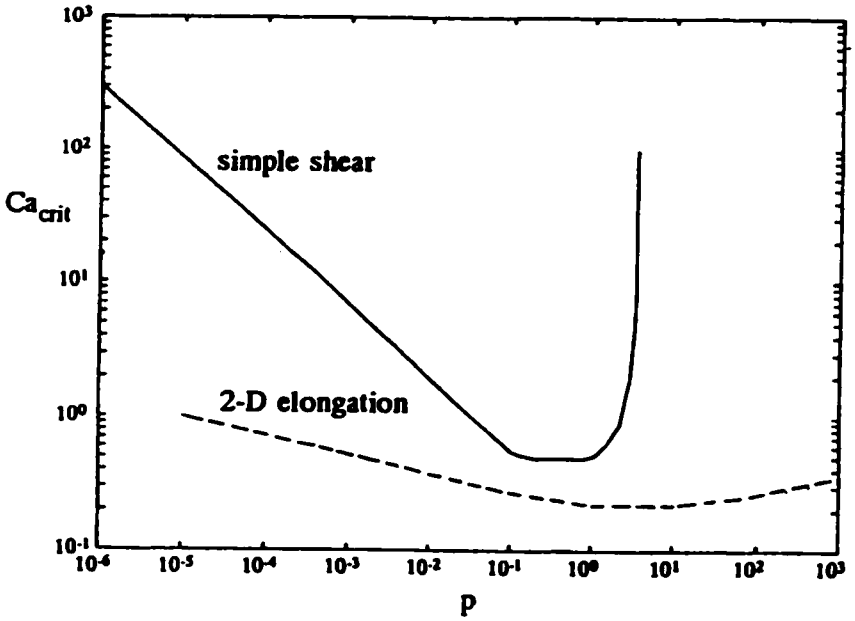

Figure 2. 1 Comparison of the effect of viscosity ratio on the critical capillary number in shear and elongational flows (Grace, 1982).

The study by Rumscheidt et al. (1961) indicates that two basic mechanisms are largely responsible for dispersing one liquid in another. One is steady break-up or drop splitting and the other is the disintegration of a deformed fine thread into a series of fine droplets. The latter phenomenon is known as a capillary instability and is often observed under transient shear conditions or after cessation of flow (see Figure 2. 2)

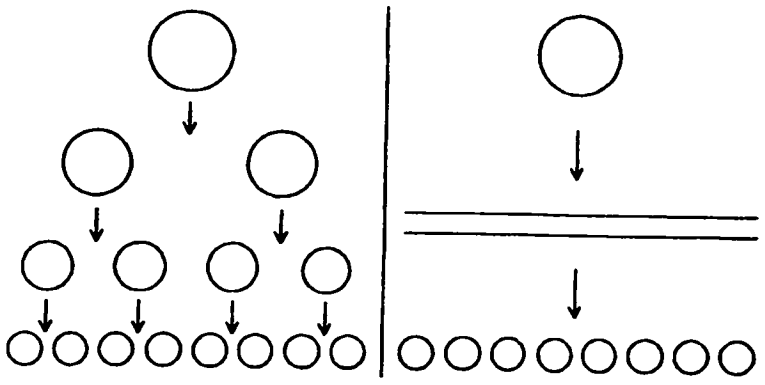

Figure 2. 2 Schematic presentation of the two dispersion mechanisms: on the left, the stepwise equilibrium mechanism of repeated breakup at Ca_{crit}, and on the right, the transient mechanism of thread breakup during extension. (Janssen and Meijer, 1993)

A capillary instability is defined as the instability of a cylindrical fluid thread in another fluid. It was initially Lord Rayleigh (1879) who suggested a model for the growth of a disturbance in a viscous jet in air. Later, Tomotika (1935) extended this theory to Newtonian fluids. Tomotika found that the time required for breakup through the capillary instability mechanism depends on parameters such as interfacial tension; viscosity ratio and initial thread diameter. According to his theory, the cylindrical thread will gradually distort sinusoidally and distortions with wavelength, λ, greater than the initial circumference of the thread, will grow exponentially with time as shown in equation (4)

$$\alpha = \alpha_0 \exp(qt) \qquad (2.4)$$

where, α is the distortion amplitude at time t, α_0 is the initial amplitude and q is the growth rate of this distortion, given by:

$$q = \frac{\sigma \Omega(X, p)}{2\eta_m R_o} \qquad (2.5)$$

where σ is the interfacial tension, η_m is the zero shear viscosity of the matrix and R_o is the initial radius of the thread. The function Ω can be calculated from Tomotika's original equation and has a particular value for a reduced wave number defined as $X=2\pi R_0/\lambda$ which depends on the viscosity ratio of the two liquids. For a given viscosity ratio (thread/matrix) there will be a dominant wavelength for which the amplitude grows fastest. Tomotika estimated that thread breakup occurs when $\alpha = 0.82R_0$. The time necessary to reach the breakup is then,

$$t_b = \frac{1}{q}\ln\left(\frac{0.82R_o}{\alpha_o}\right) \qquad (2.6)$$

Stone et al. (1986) observed another mode of break-up called end-pinching which is in competition with capillary instabilities. End pinching is a form of non-uniform fiber/thread break-up where fiber disintegration proceeds initially from the ends of the thread. This was found to be dependent on viscosity ratio and the initial L/D ratio of the elongated droplet. Break-up via end-pinching can lead to a distribution of particle sizes.

2.1.2 Drop Break-up in Polymer Blends

Several authors (Wu, 1987, Favis et al., 1987, Serpe et al., 1990, Everaert et al., 1999) have investigated the influence of viscosity ratio on the final phase morphology of non-Newtonian melt blending systems. In these studies, the minimum dispersed phase concentration was 5 wt %; thus, the low concentration limit was not found. Based on the experimental data of PA/rubber blends with varying viscosity ratios and interfacial tensions, Wu (1987) has formulated an empirical equation for the final particle diameter:

$$d = \frac{4\sigma p^{\pm 0.84}}{\dot{\gamma}\eta_m} \qquad (2.7)$$

In this equation, the plus (+) sign in the exponent applies to $p > 1$ and the minus (-) sign in the exponent applies to $p < 1$. All blends investigated by Wu contained 15 wt % of dispersed phase and the effective shear rate was arbitrarily chosen as 100 s^{-1}. This

relation obviously is not appropriate to the estimation of Taylor limit or to work on breakup of a single drop in a matrix (Cox, 1969, Bentley et al., 1986, Flumerfelt, 1980, Hinch et al., 1981, Rallison, 1981, Chin, 1979, Karam et al., 1986, Grace, 1982). In practice, it was shown that the dispersed phase concentration of 0.5 to 1 wt % can already give rise to flow induced coalescence (Sundararaj et al., 1995, Elmendorp,1986). Thus, coalescence is an important factor influencing the dispersed phase morphology.

2.1.3 Newtonian Coalescence

Coalescence in binary Newtonian liquid mixtures has been examined by several researchers (Coulaloglou et al., 1977, Jeelani et al., 1991, Chen et al., 1984, Allan et al., 1984). It was found that the contact time required for droplet coalescence increases when the droplet diameter increases, the matrix viscosity increases, and the density difference between the droplet and the matrix phases increases (Chen et al., 1984). Flow induced coalescence of the two Newtonian liquid droplets can be modeled as a three step mechanism as shown in Figure 2. 3.

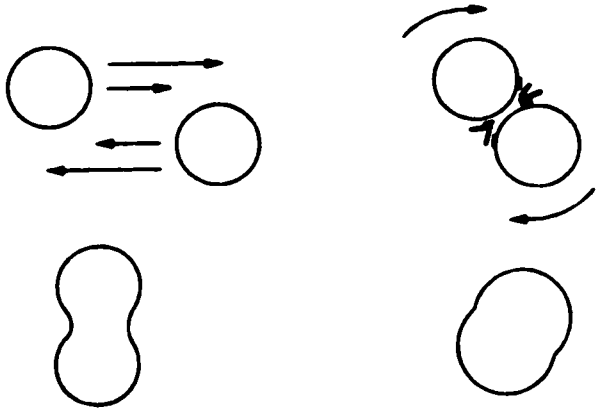

Figure 2.3 Idealized depiction of shear-induced coalescence of dispersed Newtonian droplets. The drops are brought close to each other by the shear field, and then the matrix film between the drops thins until the interface ruptures and coalescence occurs (Roland et al, 1984).

First, two droplets come close to each other and the pair rotates in the shear field. The film of the matrix phase between the two droplets drains, the film thickness decreases to a critical value and rupture of the interface occurs, resulting in coalescence. Unlike gravity induced coalescence, where the drops have time to equilibrate, contact times in shearing flows are small. Thus the film must drain out very quickly for a droplet pair to coalesce.

Modeling of drop sizes during mixing has been done using population balance ideas, similar to kinetic models (Ziff, 1986). Ramakrishna (1985) has given an excellent review of population balance modeling of drop sizes in all engineering fields. In Newtonian systems, the collision frequency (the number of times that particles meet) has been modeled satisfactorily, but coalescence probability (the probability that the meeting results in coalescence) is still very empirical (Muralidhar et al., 1988). Coalescence probability in viscoelastic polymer systems is even less understood.

2.1.4 Coalescence in Polymer Blends

Coalescence during mixing is governed by the interfacial mobility. The interfacial mobility of polymers is described by van Gisbergen (1991). A high polymer viscosity should give rise to a relatively immobile interface which should result in long drainage times for the intervening film. However, Elmendorp and van der Vegt (1986) found experimentally that polymers had a high coalescence probability during mixing and concluded that polymers had fully mobile interfaces. Though a polymer matrix will have a high viscosity relative to a Newtonian matrix, drop collision and film drainage in polymer blends will be much different from the Newtonian model due to the different rheological behavior of polymeric liquids. Elastic recoiling is expected to cause polymeric drops to separate during the initial step. However, Roland and Böhm (1984), found that, increasing shear rates, which intuitively one would expect to decrease coalescence, actually increased the amount of coalescence.

Several theories have been developed to interpret the coalescence effect. Tokita (1977) derived an expression for analysing the particle size of the dispersed phase in

polymer blends which incorporates a variable considering composition. The theory is based on the fact that an equilibrium drop diameter originates from continuous break up and coalescence of the dispersed particles. The total number of collisions per unit time can be expressed as Equation (2. 8) (Smoluchowski, 1916, 1917)

$$N_I = \frac{4n\varphi_d\dot{\gamma}}{\pi} \qquad (2.\ 8)$$

where, n is the number of particles. Under the assumption that coalescence is proportional to the total number of collisions, the decrease in the number of particles with time due to coalescence can be expressed as

$$\frac{dn}{dt} = -p_r N_I n \qquad (2.\ 9)$$

where, p_r is the probability that a collision will result in a coalescence. On the other hand, the increase in the number of particles with mixing time due to the drop breakup can be given as:

$$\frac{dn}{dt} = n\left[\frac{\eta_m\dot{\gamma}^2}{E_{DK} + 6\sigma_{12}/d}\right] \qquad (2.\ 10)$$

where E_{DK} is the macroscopic bulk breaking energy. At equilibrium, the rate of drop breakup and coalescence is equal: thus, from equations (2. 9) and (2. 10), the equilibrium drop size can be calculated as:

$$d_{eq} = \left(\frac{24p_r\sigma_{12}\varphi_d}{\pi}\right)\Big/\left[\eta_m\dot{\gamma} - \frac{4p_r E_{DK}\varphi_d}{\pi}\right] \qquad (2.\ 11)$$

Equation (2.11) indicates that the equilibrium drop diameter increases with concentration, interfacial tension, and decreases with shear stress. Generally, this agrees with earlier work by Taylor. This particular development is of interest because it includes in its

analysis a part considering the effect of composition on phase size. The role of composition in determining phase size is critical.

Fortelny et al. (1989, 1993), following a procedure similar to that of Tokita, proposed an equation taking into account both droplet break-up and coalescence to predict the equilibrium diameter of the dispersed phase,

$$r = r_c + \left(\frac{\sigma_{12}\,\alpha}{\eta_m\, f}\right)\varphi_d \qquad (2.12)$$

where r_c represents the critical droplet radius as calculated from Ca_{crit}; α is the probability that droplets will coalesce after collision; f is the function of the Taylor capillary number Ca, and rheological properties of the system. This relationship still contains several parameters which cannot easily be quantified for the blending of viscoelastic polymers.

Considering the properties of polymers, coalescence in polymer blends is much more significant than expected and it is clear that coalescence in polymer systems is not well understood.

2.2 The Concept of Percolation

The term percolation for the statistical-geometry model was introduced by Hammersley et al. (1957). However, earlier the essence of percolation theory was already incorporated in Flory's theory of gelation (1941). According to Hammersley's view, the sites (or bonds) of the lattice can be randomly occupied with a probability p. The percolation concept deals mainly with the value of the percolation threshold, p_c, at which an infinite connectivity of occupied sites (or bonds) first occurs, and the probability of finding such a connectivity as a function of p. Kirkpatrick (1973) pictured the occupied bonds as conductors and found that just above p_c the conductivity increases according to a power law $(p-p_c)^t$, where t is positive and depends only on the spatial dimension of the lattice.

The co-continuous structure is a unique feature of immiscible polymer blend morphology. The evolution of this structure undergoes the transition from one minor

phase dispersed in another matrix to dual phase continuity. The transition process can be explained by percolation theory. The development of percolation phenomena in a polymer blend system can be illustrated schematically in Figure 2.4. Starting with a simple homo-polymer, we begin adding particles of a second polymer represented as circles. At low volume fraction of minor phase, the particles are disconnected and separated from one another as shown in the composition represented by A. As the volume fractions of minor phase increase, the particles start to be interconnected with one another, as shown progressively by compositions B and C, and eventually, continuity is established throughout as shown in D. This is the essence of the percolation theory in polymer blend system. Stauffer (1980) presented a detailed review on scaling theory of percolation clusters. Through computer simulations (Monte Carlo method, series expansion, renormalization group technique and exact inequality), the results demonstrate that there is a qualitative difference of cluster structures above and below p_c and suggest

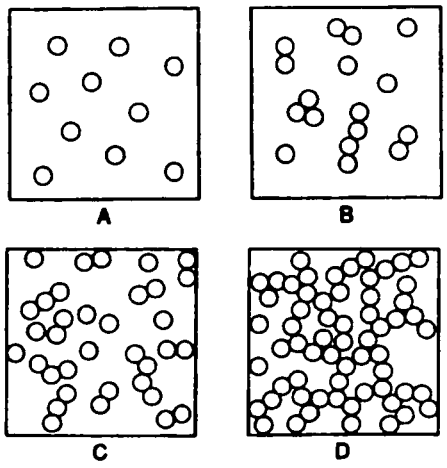

Figure 2.4 Schematic illustration of percolation theory (Hsu and Wu, 1993)

that for large clusters near the percolation threshold, p_c, the number of average clusters n_s, varies as an expression,

$$n_s \propto s^{-\tau} f(z) \qquad (2.13)$$

with $z = (p-p_c)s$

where, s, is the number of the sites, f(z), the scaling function and τ, σ, the free exponents. Some researchers (Margolina et al, 1988, 1990, Hsu et al, 1993, Arends, 1992) have applied the percolation concept to interpret the change in mechanical properties in the transition region as function of morphology in polymer blends, and they showed that

percolation concepts could be successfully used to analyse the data and explain the transitions.

2.3 Continuity and Phase Inversion

Usually, *continuity* can be defined as the volume of minor phase involved in the continuous path divided by the total volume of the minor phase, and the level of the continuity can be measured in this way. *Phase inversion* refers to a transition composition, at which a dispersed phase becomes a continuous phase (and vice versa). Strictly speaking, the terms between phase inversion and co-continuity should be different, co-continuity can exist in a composition range, whereas phase inversion occurs at a certain composition. But unfortunately, these two terms are frequently used interchangeably in the literature.

Several models have been proposed to predict the formation of interpenetrating co-continuous structures. Based on percolation theory Jorgensen and Utracki (1991) formulated an equation at which they suggested that, two types of domains, led by the coalescence and break up process in simple shear flow and low volume fraction, are coexistent. One is small and nearly spherical, and the other, larger and nearly cylindrical. The critical concentration at which percolation occurs can be expressed as follows,

$$\varphi_{cr} = 1/z \qquad (2.\ 14)$$

where,

z: average co-ordination number per domain, and $z = z(\varphi_L, \varphi_s, p)$

φ_L: fraction of cylindrical domains

φ_s: fraction of spherical domains

p: average number of spherical domains to which a cylinder can decompose

Using this model, they examined a polymethyl methacrylate (PMMA)/polystyrene (PS) blend system at a critical phase inversion point. The observed value is 0.113, compared with the predicted one of 0.109. Of course, this model can also be used to estimate the critical transition composition of spherical domains, especially, for the polystyrene/high density polyethylene (PS/HDPE) system. The observed value is 0.15, and predicted value is 0.156. The experimental result correlates well with the predicted value. From the above

two systems, it appears that the percolation threshold can be decreased when clusters are built up of non-spherical domains.

Arends (1992) investigated percolation in injection molded polymer blends (polycarbonate (PC)/ poly (styrene-co-acrylonitrile) (SAN)). He measured the variation of modulus of blend with the composition at the temperatures between the glass temperatures of two components. He compared the injection molded modulus to the compression molded one, and found that the former is a factor of three higher than the latter. He ascribed variation to be due to the difference in connectivity between minor components, and modelled the morphologies of these materials by using percolation concept. In his Monte Carlo simulation (see Figure 2.5), it can be observed that extrinsic factors, such as the state of dispersion, particle shape, orientation can significantly affect percolation threshold.

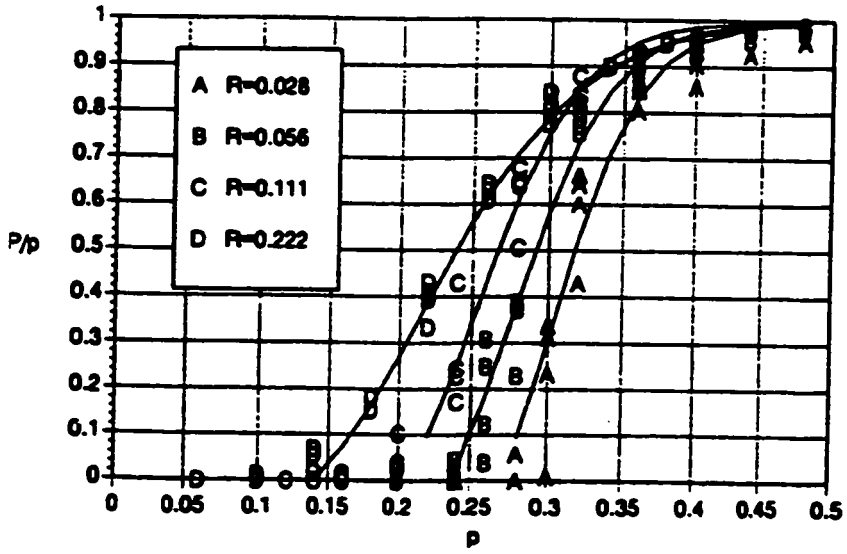

Figure 2.5 Effect of finite size on percolation : R is the ratio of inclusion to domain size in the percolation direction (Arends, 1992)

A parameter, R, is defined as the ratio of the inclusion length to the effective domain size in the percolation direction. It was found that for small R (0.028) the threshold approaches 0.31, and for large R (0.22), the threshold reduces to 0.22, indicating that the higher the R, the lower the critical concentration for percolation. It is quite evident that

the shape of the domain should have a significant effect on the percolation phenomenon. Increasing the inclusion length reduces the critical concentration for percolation.

2.4. Factors Influencing Dual Phase Continuity

It has been well documented that several basic parameters are very important in controlling the morphology a of polymer blend during processing, namely, composition, viscosity ratio of the molten components, melt elasticity ratio, interfacial tension and processing history (Allen, 1985, David, 1993, Jorgensen, 1991, Favis, 1992).

2.4.1. Viscosity Ratio and Composition

As mentioned earlier, many investigations have been carried out in the region of dual phase continuity, and a number of authors have formulated hypotheses for the formation of dual phase continuity. Among them, Avgeropoulos et al (1975) studied ethylene propylene dine/polybutadiene (EPDM/BR) system. They found that the ratio of mixing viscosity and the composition of the components affect the phase continuity of the system, and competition will thus exist between the compositional and rheological parameters. It appears that as the viscosity ratio (torque ratio) is near unity, the "conversion" region is characterized by samples with co-continuous phases.

Based on the observations made by Avgeropoulos, Paul and Barlow (1980) first formulated a model, indicating that the condition for phase inversion can be expressed as

$$\frac{\eta_1}{\eta_2} = \frac{\varphi_1}{\varphi_2} \qquad (2.\ 15)$$

where,

φ_X = composition at phase inversion

η_X = viscosity of phase x

Above equation has been corroborated by several researchers (Jordhamo, 1986, Miles, 1988, Elemans, 1988), but exceptions have also been reported (Ho et al., 1990, Favis, 1988, Bouilloux et al., 1997, Bourry et al., 1998). De Roover et al., (1997), studied blends of poly(m-xylene adipamide) with maleic anhydirde-functionalized polypropylene and found that the phase inversion region was controlled by the viscosity ratio of the components only during the early stage of the mixing process.

Another expression for the prediction of dual phase continuity was proposed by Metelkin and Blekht (1984). This expression is based on the theory of capillary instabilities by Tomokita (1935), and phase inversion concentration is given as:

$$\varphi_1 = \left[1 + \frac{\eta_1}{\eta_2} F\left(\frac{\eta_1}{\eta_2}\right)\right]^{-1} \qquad (2.\ 16)$$

where

$$F\left(\frac{\eta_1}{\eta_2}\right) = \left[1 + 2.25\log\left(\frac{\eta_1}{\eta_2}\right) + 1.81\left(\log\left(\frac{\eta_1}{\eta_2}\right)\right)^2\right]$$

Equation (2. 15) and (2. 16) have been discussed by Utracki (1989) and found to be consistent with each other.

Later, Utracki proposed an equation based on an emulsion model (1991)

$$\frac{\eta_1}{\eta_2} = \left[\frac{\varphi_m - \varphi_2}{\varphi_m - \varphi_1}\right]^{[\eta]\varphi_m} \qquad (2.\ 17)$$

where, φ_m refers to the volume fraction of the matrix at the percolation point, and $[\eta]$ refers to intrinsic viscosity. In this model, Utracki applied a correction related to the fact that co-continuity cannot occur when the volume fraction of either phase is below its percolation threshold. All the aforementioned models predict that the less viscous phase have the greatest tendency to be the continuous phase.

Favis (1988) investigated a blend of polycarbonate dispersed in polypropylene of viscosity ratio of 2, the phase size, (d_V, volume average diameter) increased from 1.2 at 10% to 5.8 μm at 40%. If the entire composition range is studied for a given blend, an intermediate region of phase inversion with dual phase continuous morphology is obtained. Jordhamo et al (1986) reported that the region of dual phase continuity of polybutadiene/polystyrene (PB/PS) obeyed the rheological viscosity/ volume fraction equation, shows,

$$(\eta_1/\eta_2)\,(\varphi_2/\varphi_1)\ \begin{cases} >1 & \text{phase 2 continuous} \\ =1 & \text{dual phase continuous} \\ <1 & \text{phase 1 continuous} \end{cases} \qquad (2.\ 18)$$

The ability of the low-viscosity component to encapsulate the high viscosity material may be related to its ease of deformability, which allows it to form highly extended bodies. Miles (1988) examined dual phase continuity in three thermoplastic blend systems, PS/PB, PS/PMMA and polymethyl methacrylate/ethylene propylene rubber (PMMA/EPR). Their experimental results were consistent with the above equation.

Recently, Willemse et al. (1999) developed a semi-empirical relation based on geometrical requirements for the formation of co-continuous structures:

$$\frac{1}{\varphi_d} = 1.38 + 0.0213\left(\frac{\eta_m \dot{\gamma} R_o}{\sigma}\right)^{1.2} \qquad (2.\ 19)$$

where φ_d is the volume fraction of the dispersed phase, η_m is the viscosity of the matrix, $\dot{\gamma}$ is the shear rate, σ is the interfacial tension and R_o is the radius of the thread. This relation gives the lower and upper limit, respectively, of the range of volume fractions within which a co-continuous structure can exist. However, this model cannot be used in a predictive manner because the thread radius has to be determined experimentally first.

As mentioned earlier, the effect of composition on the formation of dual phase continuity can be formulated by the hypothesis in forgoing discussion. Nevertheless, discrepancy often arises. Fortelny et al (1992) studied the composition dependence of phase structure of polypropylene(PP)/ethylene-propylene elastomer (EPR) blends with various rheological properties of the components. They discovered that neither the empirical rule, regarding the effect of the ratio of viscosities of the components on the ratio of their volume fractions at which the inversion of phases takes place, nor Van Oene's theory, regarding the effect of elastic properties of the components on phase structure of the blend, is generally valid.

2.4.2. Elasticity

The influence of the elasticity on the morphology of polymer blend remains poorly understood. One of the more classical studies in this area was carried out by Van Oene (1972). He formulated an expression to describe an elastic contribution to the interfacial tension under dynamic conditions.

$$\sigma_{eff} = \sigma + \frac{d}{12}\left[(N_1)_d - (N_1)_m\right] \qquad (2.20)$$

where,

σ_{eff}:effective interfacial tension

σ: interfacial tension

d: droplet diameter

N_{1d}: first normal stress difference (dispersed phase)

N_{1m}: first normal stress difference (matrix)

Van Oene predicted that normal forces exhibited by the droplet phase tend to stabilize themselves, while normal forces exhibited by the matrix tend to destabilize the dispersed phase, and he suggested that the interfacial tension should be replaced by an effective interfacial tension which involves first normal stress differences. Therefore it would be expected that the more elastic phase will tend to encapsulate the less elastic one at high concentrations in order to lower the overall surface energy. Favis et al (1988) investigated the polycarbonate/polypropylene blend system, they found that the more elastic polycarbonate encapsulates the less elastic polypropylene.

Thornton et al (1980) studied the melt elasticity of polystyrene (PS)/polymethyl methacrylate (PMMA) blend. Large maxima in the recoverable strain, in the time for the strain recovery to finish and in the melt tension were discovered at the region of co-continuity (weight percent composition of 40% polystyrene and 60% polymethyl methacrylate). They proposed a dual phase interpenetrating model to explain the above experimental phenomena.

Levitt et al (1996) designed a visualization apparatus to investigate polymer drop deformation in a polymer matrix. The apparatus provides a simple shear flow field and resolution comparable to an optical microscope. Several polymer blend systems (polypropylene (PP)/polystyrene (PS), polyamide (PA)/polystyrene (PS), and polymethyl methacrylate (PMMA)) were studied. Usually elasticity is expressed in terms of the primary normal stress difference, and their experiment was carried out at very low shear rate. Under such a condition, the primary stress difference is approximately twice the storage modulus, G' at low frequency. They observed that the minor phase changes from droplets to sheets, and then the sheets contract to fibers under the effect of interfacial tension. They proposed that the width of the flattened drops relies on the difference in elasticities between matrix and drop, and is proportional to the first normal stress difference of the two phases. They established an analytical relation between the first

normal stress difference of the phases and the degree of widening, and further concluded that the phenomena of widening results in area generation larger than the value calculated for the affine deformation.

Concerning the viscoelastic properties of polymers, Ghodgaonkar et al (1996) investigated the dispersed phase in polymer blends, and modeled the diameter of the dispersed phase quantitatively. Their model was based on a simple force proportionality. Polymers are viscoelastic, and thus the elasticity of the matrix and the elasticity of the dispersed phase affect the drop size. The droplets are deformed by shear stress, $\eta_m \dot{\gamma}$, and the matrix first normal stress, $T_{11\text{-}m}$. This deformation is opposed by the interfacial force. The predicted diameters are comparable to the experimental data. The PS/PP blend system (viscosity ratio p =0.87) shows a minimum drop diameter with shear rate. The diameter attains a minimum value at the shear rate between 100 to 162.5 s^{-1} and then increases at higher shear rates for the composition of PP 2%, 5%, and 8% in PS blend. The force balance best predicts the behaviour of the 2% PP in PS blend since the force balance is for a single polymer drop in a polymer matrix, and thus matches the results for the very dilute blend system. The minima are independent of the weight fraction of the dispersed phase in this region. However, no minimum was observed for 20% PP in PS blend, and they suggested that this may be due to greater coalesence at this high concentration. Droplets and fibers coexist, causing the morphology to be more complex.

Bourry et al (1997) have studied the level of cocontinuity for polystyrene (PS)/high density polyethylene (HDPE) blends prepared on twin-screw extruder. Considering the influence of the elasticity, they used following expression to measure the elasticity effect on PS/ HDPE blend system

$$\frac{\varphi_1}{\varphi_2} = \frac{G_2'(\omega)}{G_1'(\omega)} \qquad (2.21)$$

where,

φ_x: composition of phase inversion

G_x' : elasticity of phase x (storage modulus)

Observing the phase inversion in the PS/HDPE blend system, they found the predicted value from their equation is in accordance with the observed composition ($\varphi_{ps(th)}$=0.67, $\varphi_{ps(ex)}$=0.7) at high shear rate, while the viscosity ratio models failed. It is indicated that the viscosity ratio models can only predict accurately the observed phase inversion region

at very low shear rates, and fail to do so under the vigorous mixing condition of the twin-screw extruder. These results strongly suggest that elasticity can affect the phase inversion composition (see Table 2.1).

Table 2.1. Influence of elasticity on the prediction of the phase inversion point (Bourry and Favis, 1997)

Shear Rate	Viscosity Ratio	Paul and Barlow	Metelkin and Blekht	Utracki
rad/s	η^*_{PS}/η^*_{PE}	φ_{PS}	φ_{PS}	φ_{PS}
5	1.422	0.59	0.67	0.54
10	1.188	0.54	0.59	0.52
40	0.942	0.49	0.47	0.49
100	0.540	0.35	0.24	0.42
200	0.486	0.33	0.20	0.4
Observed:		0.7 ± 0.1		

More recently, Steinmann et al. (2001) proposed a relation based on elasticity ratio of blend components to predict the phase inversion concentration for their poly (methylmethacrylate) (PMMA)/polystyrene (PS) and poly (methylmethacrylate) (PMMA)/poly(styrene-co-acrylonitrile) (PSAN) blends:

$$\varphi_{pi} = -0.34\log\left(\psi_{eff,G'}\right) + 0.67 \qquad (2.22)$$

where, φ_{pi} is the volume fraction of the dispersed phase at the phase inversion and $\psi_{eff,G'}$ is the effective elasticity ratio. This model is in good agreement with their experimental data. However, in their experiment, Steinmann et al. estimated the co-continuity by TEM and a form factor parameter instead of using solvent extraction/gravimetric method. Therefore, the precise location of the phase inversion region in their study may be questioned.

2.4.3. Interfacial Tension and Interfacial Modifier

For polymer blends the interfacial tension has a remarkable effect on the

morphology. The domain size is dependent on the interfacial tension, i.e., the size of the dispersed phase usually decreases as the interfacial tension diminishes. Such an effect can be attained by the addition of interfacial modifier (Yoshida et al, 1990, Plochocki et al, 1990, Sakellariou et al, 1993). As mentioned earlier, most polymer blends systems are unstable, and the interface plays a very important role in controlling the morphology and final properties. The basic parameter which characterizes the interface is the interfacial tension. Mostly block copolymers, acting as compatibilizers, have been shown to be effective in reducing the minor phase size, and thus increasing the stability of the morphology of many blends. It is generally believed that this is a result of their ability to alter the interfacial situation (McNight et al 1985). Willis and Favis (1988) investigated this effect in detail for polyamide/polyolefin blends and reported a dependence best described as a rapid drop followed by little change in the phase size with interfacial modifier. They noticed that there appears to be a critical value of percent modifier after which very little change in size is observed. This type of dependence is analogous to the effect of surfactants on oil/water emulsions (Djakovic et al, 1987). This critical value also appears to depend on the interfacial area. The shape of the curve is also very similar to that obtained for the interfacial tension versus percent interfacial modifier as studied by Patterson et al (1971). For a mono-dispersed AB diblock copolymer in a homopolymer type A, Whitmore and Noolandi (1985) formulated an expression relating the critical micelle concentration, φ_c to the degree of polymerisation of copolymer, Z_C, degree of polymerisation of B block, Z_{CB}, Flory-Huggins interaction parameter, χ, and stretch factor, α_A, of copolymer.

$$\varphi_c^{crit} = 0.30 \frac{\chi Z_C}{(\chi Z_{CB})^{2/3}} \exp\left\{\chi Z_{CB} + 1.65(\chi Z_{CB})^{1/3} + \frac{1}{2}\left[1.65(\chi Z_{CB})^{1/3} + \frac{1.56}{(\chi Z_{CB})^{1/6}} - 3\right] + \frac{1}{2}\left[\alpha_A^2 + \frac{2}{\alpha_A} - 3\right]\right\} \qquad (2.23)$$

More recently Favis et al (1997) investigated the emulsification effect of styrene/hydrogenated butadiene copolymer on polystyrene/ethylene propylene rubber (PS/EPR) blends during melt processing. They proposed that the emulsification curve can even be used to estimate the interfacial area occupied per copolymer molecule (Figure 2.6).

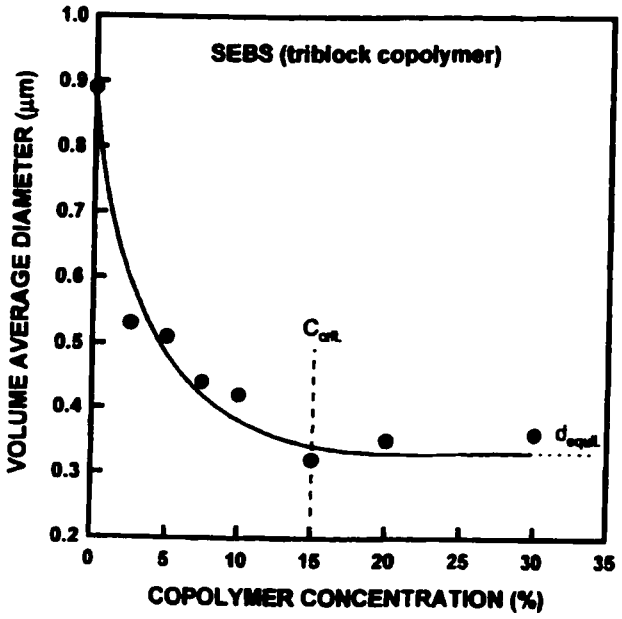

Figure 2.6 Emulsification curve for a 10%EPR/90%PS blend compatibilized by an SEBS triblock modifier of molecular weight 70K (Matos et al., 1995)

In addition they introduced a technique (combination of transmission electron microscopy (TEM) with electron energy-loss spectroscopy (EELS)) to trace the modifier in the minor phase, and they predicted that the thickness of the interfacial regions could even be potentially estimated by this method.

Wu (1987) studied polyamide/rubber (PA/Rubber) system and found that the particle size was directly proportional to the interfacial tension. The interfacial tension for the PA/rubber system used in his study was 9.7×10^{-3} N/m, with a number of average particle size for the minor phase of 4.2μm measured experimentally. The interfacial tension for a functionalised rubber/PA blend was 0.25×10^{-3} N/m, with a particle size of 0.08μm. Other researchers (Chappelear, 1964, Luciani, 1996, Watkins, 1993) also reported that the interfacial tension has a striking effect on the morphology.

Furthermore, Favis et al (1990) pointed out that the presence of good adhesion at the interface also serves to minimize coalescence effect as minor phase composition is increased. They proposed that if strong covalent interactions are present the particle size/composition dependence can be flat right up to the region of dual phase continuity, and this effect was demonstrated by Willis et al (1990) for styrene-maleic-

anhydride/bromobutyl rubber blends compatibilized with dimethylaminoethanol and also by Elmendorp and Van de Vegt (1986). In fact interfacial modification appears to be the dominant parameter in controlling the dispersed phase size. It can remarkably minimize the influence of composition. It can also substantially moderate the viscosity ratio effect. The phase size/viscosity ratio dependence is less pronounced for compatibilized systems. This may be explained from Taylor's theory, which states that it is more difficult to deform and disintegrate a small drop than a large one.

A variety of methods are available for determining the interfacial tension. Among them, the Pendant Drop (Roe et al, 1969, Kamal et al, 1994, Hu et al, 1995) and Spinning Drop (Patterson et al, 1971, Elmedorp et al, 1986) techniques are mostly used. The methods mentioned above are equilibrium ones and normally require long experimental times and involve complicated experimental procedures. De Chappelear (1964) was the first who applied Tomokita theory (1935) for measuring the interfacial tension between some melts. In this method, in the absence of an overall flow field, extended liquid threads in a liquid matrix exhibit sinusoidal disturbances which cause the threads to disintegrate into line of droplets. From the growth rate of these disturbances, the interfacial tension between the thread phase and the matrix phase is calculated. This method is fast and simple since it does not need density data for the two phases.

Elemans (1990) used this method to measure the interfacial tensions of LDPE/PS and HDPE/PS blend system. Further investigation was made on the influence of a diblock copolymer on these immiscible polymer blend systems. A considerable decrease in interfacial tension was observed, and this kind of effect is quite similar to the one reported by other authors (Anastasiadis et al, 1989, Hu et al 1995, Lepers et al, 1997, Cho et al, 1996, Liang et al 1997, and Mekhilef et al, 1997). More recently, Willemse et al. (1999), investigated the influence of the interfacial tension on the co-continuous morphologies of the PE/PS, PE/PA6 and PE/PP blends. They found that the composition range for full co-continuity is dependent on the interfacial tension. Increasing the interfacial tension shifts the limiting composition for onset of co-continuity to higher concentrations, thus narrowing the composition range. The interfacial tension influences the stability of the co-continuous morphology as well as the phase dimensions. The latter effect appears to be smaller than the former.

2.5 Stability of Co-continuous Polymer Blends

As mentioned earlier co-continuous morphologies are intrinsically unstable. A

transition from a co-continuous structure to dispersed phase one will occur on further processing. Mekhilef et al (1997) investigated the stability of co-continuous HDPE/PS blends under quiescent annealing conditions. They reported that composition plays a very important role in the stability of co-continuous morphology. Upon increasing the annealing time for the compatibilized and non-compatibilized 50%HDPE/50%PS blend, a significant coarsening was observed with increasing annealing time. However, co-continuity remains and both phases form a continuum. Of course, the compatibilized blends demonstrate more stability during annealing. Blends with other compositions (70%HDPE/30%PS and 30%HDPE/70%PS) in the range were also examined at the same condition; the morphologies changed from co-continuity to partial co-continuity with increasing annealing time.

Lee et al.(1998) studied co-continuous PMMA/PS blends with three different compositions (70%PMMA/30%PS, 50%PMMA/50%PS and 30%PMMA/70%PS). Upon annealing these blends under isothermal conditions at 170°C for varying periods, the co-continuous morphology evolved into a dispersed morphology, in which the major component formed the continuous phase and the minor component formed the discrete phase. When a symmetric 50%PMMA/50%PS was annealed the initially formed co-continuous morphology converted to a 'dual mode' of dispersed morphology.

In their study of the stability of co-continuous 50%PS/50%poly(ether-ester) blends in shear flow, Veenstra et al (1999) found that co-continuous morphologies in the blend break up into a droplet/matrix morphology when subjected a shear flow in a rheometer with a cone-plate configuration and are therefore not stable even though the blend is at a symmetric composition.

From the above it is shown that stabilizing co-continuous morphologies is a tremendous challenge. Addition of the block copolymer is an efficient way to stabilize the co-continuous morphology.

2.6 Mechanical Properties and Dual Phase Continuity

In many cases, mechanical properties of polymer blends may not follow an addition relation, and often it is found that properties such as tensile strength or elongation at break exhibit a minimum in the dual phase continuous region, i.e., these properties are inferior to both pure components. Frequently, this situation occurs at temperatures well below the glass transition of the specimen. This situation usually arises from a poor degree of interfacial adhesion between components that provides a

multiplicity of defects for early failure. Fayt et al (1989) investigated polyethylene/polystyrene blend system. They added poly (hydrogenated butadiene-b-styrene) copolymer (2~10%) to this system and found that both ultimate strength and elongation at break are significantly improved. Diblock copolymers are more effective than graft, triblock or star-shaped copolymers (Fayt et al 1990, 1987, 1986a, 1986b).

Ray and Khastgir (1993) investigated the correlation between morphology and mechanical properties of ethylene vinyl acetate (EVA) with 28% VA copolymer and LDPE blend. They observed that upon curing this blends, the tensile strength goes up dramatically, and a maximum value occurs for 50:50 composition. This composition is right in the range of dual phase continuity.

Favis et al (1997) investigated the morphology and dynamic mechanical properties of polyethylene/polystyrene blends over the entire compositions range for both non-compatibilized and compatibilized blends in the solid state. They discovered that a high synergy in storage modulus above the Tg of PS during dynamic mechanical testing. However, this synergetic effect is diminished for the compatibilized counterpart. They regarded that significantly lowered interfacial tension and enhanced morphological stability are the main factors.

Recently, Veenstra et al.(1999) investigated the mechanical properties of continuous polymer blends comprised by PP/SEBS and PS/poly(ether-ester). They also found that the storage moduli of co-continuous blends are higher than the moduli of the blends with droplet/matrix structure. However, no significant difference in tensile strength or impact strength was observed when co-continuous blends were compared to blends with a droplet/matrix morphology. A model was proposed by the authors to predict the moduli of polymer blends with co-continuous morphologies over the complete composition range.

2.7 Conclusion of Literature Review

Dual phase continuity describes a morphological structure where there is neither a matrix nor a dispersed phase. Intertwining and interpenetration are unique morphological features of the blend.

The main mechanism governing phase morphology development in immiscible

polymer blends is the result of competition between droplet breakup and coalescence. The formation of dual phase continuity can be well described by percolation concepts, and the model based on this concept can precisely predict the phase inversion composition at low shear rates.

The development of co-continuous structure undergoes the transition from one minor phase dispersed in another matrix to dual phase continuity. The transition process can be well documented by percolation theory.

Factors influencing morphological structures have been investigated by a number of studies. Viscosity ratio, elasticity ratio, composition, interfacial tension and processing condition play key roles in structure formation (see Figure 2.7). Usually these factors affect the morphological structures in a combined fashion, rather than individually.

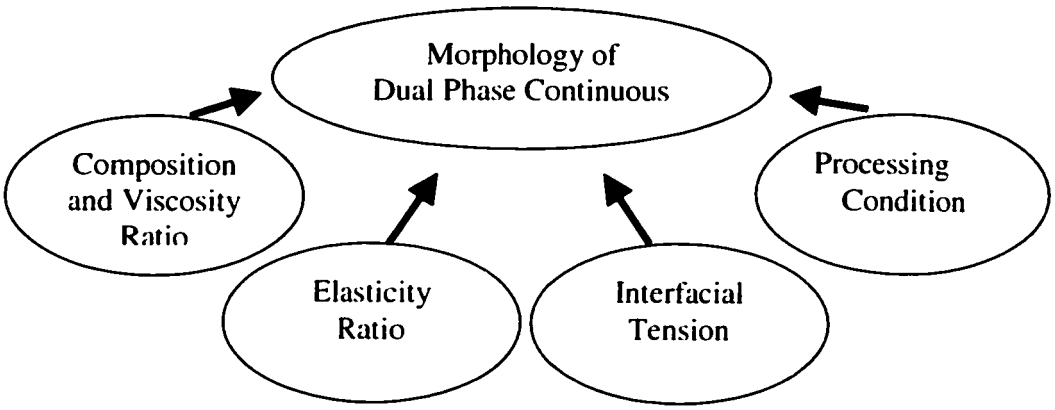

Figure 2.7 Factors influencing the morphology of dual phase continuity

Dual phase continuity possesses high interfacial area and thus high energy. Addition of interfacial modifier can remarkably reduce the interfacial tension, and minimize the interfacial energy, thus stabilizing the co-continuous morphological structures. Experimental results have indicated that mechanical properties can notably be improved by addition of interfacial modifiers.

From the above literature review, it appears that a number of issues remain unresolved.

Firstly, hypotheses formulated to predict the concentration region of phase inversion or the formation of dual phase continuity are not always consistent with experimental results, especially in the vigorous processing condition. These models focus principally on the viscosity ratio and volume fraction of blends. In effect, other factors, elasticity and interfacial tension which probably play a key role in the formation of dual phase continuous structures should also be considered. Furthermore, how do these factors influence the inversion composition and to what extent?

Secondly, it is well known that the morphology of the blend with a minor phase dispersed in a matrix can be well characterized. However, is it possible to quantify the structure in the co-continuity region? In that case there is no distinction of minor phase and matrix, and the structure is intertwining and interpenetrating.

Thirdly, the effect of interfacial modifier on immiscible polymer blends at low dispersed phase concentration, and the feature of emulsification curves have been reported in a great deal of papers. How can this phenomenon be studied in the region of co-continuity? Also, co-continuous morphologies possess very high interfacial areas and require large concentrations of interfacial modifier. Micelle formation and migration to the interface are serious concerns under these conditions. How can his be studied and how can the modification of co-continuous blends be optimised?

Finally, is it possible to formulate a mechanism that can be used to describe the microstructure and co-continuity development in immiscible polymer blend systems as a function of the type of interface?

It is the above unresolved issues that turn out to be the ultimate objective of this research: to carry out fundamental studies related to controlling and characterizing the position and microstructure of co-continuous morphologies and to formulate a mechanism regarding the microstructure formation and co-continuity development for immiscible polymer blend system during melt mixing.

CHAPTER 3. ORGANIZATION OF THE ATICLES

In the first paper "Characterizing co-continuous high density polyethylene/polystyrene blends", co-continuous blends of high density polyethylene/polystyrene were made to compare various microstructural characterization techniques. The surface area and pore dimensions of the blend system after solvent extraction of one of the phases were measured using the BET nitrogen adsorption technique and mercury porosimetry, respectively. Image analysis was also carried out as a third source of microstructural information. It is shown that the tracking of surface area via the BET technique provides a powerful quantitative tool to analyzing the efficacy of interfacial modifier at emulsifying co-continuous morphologies and to obtaining information on the fineness of the co-continuous structure.

The type of polymer-polymer interface plays a very critical role in the development of co-continuous morphology and microstructure. Now with the adequate characterization technique it is possible to study the role of type of polymer-polymer interface on morphology in co-continuous polymer blends. Three types of blend interfaces are examined systematically in the second paper "The role of the interface type on morphology in co-continuous polymer blends" in order to isolate the role of the interface on the development of co-continuous morphologies during melt mixing. A conceptual mechanism based on the experimental results has been formulated to describe the microstructure features and continuity development for three blend systems. In a compatible binary blend system, Type I, continuity development and microstructural features depend on thread-thread coalescence. In a non-compatible binary blend system, Type II, the continuity development and microstructure is found to be controlled by droplet-droplet coalescence. In a compatibilized ternary system, Type III, the essential features are dominated by reduced droplet-droplet coalescence.

Co-continuous morphologies possess very high interfacial areas and require large concentration of interfacial modifier. Micelle formation and migration to the interface are serious concerns under these conditions. The third paper, "Strategies to measure and optimize the migration of the interfacial modifier to the interface in immiscible polymer blends" focuses on quantification of the efficacy of compatibilizer migration to the interface using a family of emulsification curves. Through an examination of the evolution of the equilibrium dispersed phase size after interfacial saturation, as well as comparison of the apparent interfacial area occupied per modifier molecule (A_{app}) (or apparent areal density (Σ_{app})) at the different dispersed phase concentrations, it is possible to detect the onset of micelle formation and to estimate the interfacial coverage. This approach has been applied to HDPE/PS blends, using a variety of triblock and diblock copolymer interfacial modifiers for that system. It is shown that it is the affinity of the block copolymer for the matrix material that dominates migration efficacy to the interface. Micelle formation in the PS dispersed in the HDPE system can be virtually eliminated through the use of a symmetric (50:50) triblock or diblock copolymer.

An Annex is included, which represents an initial exploratory study on reactive compatibilization of co-continuous polyamide/polystyrene blends.

In short, this work provides a powerful tool to characterize the complex morphology for co-continuous blends, formulates a conceptual mechanism to explain the role of the interface type on morphology in co-continuous polymer blends, and generates strategies to measure and optimize the migration of the interfacial modifier to the interface in immiscible polymer blends.

CHAPTER 4. CHARACTERIZING CO-CONTINUOUS HIGH DENSITY POLYETHYLENE/POLYSTYRENE BLENDS***

Jianming Li and Basil D. Favis
Centre de Recherche Appliquée sur les Polymères, CRASP, Department of Chemical Engineering, École Polytechnique de Montréal, PO Box 6079,
Stn. Centre-Ville Montréal, Québec, Canada H3C 3A7

The lack of adequate characterization techniques has been a hindrance to the effective exploitation and study of co-continuous morphologies in polymer blends. In this paper we prepare co-continuous blends of high density polyethylene/polystyrene (HDPE/PS) in order to compare various microstructural characterization techniques. The influence of a triblock copolymer interfacial modifier, hydrogenated styrene-ethylene-butadiene-styrene (SEBS) on the system has also been investigated. The surface area and pore dimensions of the blend system after solvent extraction of one of the phases have been measured using the BET nitrogen adsorption technique and mercury porosimetry respectively. Image analysis was also carried out as a third source of microstructural information. It is shown that mercury porosimetry can lead to erroneous information while the BET method appears to be both rapid and consistent with SEM observation. The specific surface area of the compatibilized co-continuous blend system is 5 fold higher than that of its non-compatibilized counterpart, while the pore diameter of the extracted compatibilized blend is reduced 5 fold. Using the BET technique, it is possible to generate an emulsification curve in the co-continuous region, demonstrating the efficacy of the interfacial modifier in this complex system.

(Keywords: polymer blend; co-continuity; characterization; compatibilization)

4.1 Introduction

The blending of two or more polymers to form a polymer blend is now an established route to developing new polymeric materials[1-5]. Most polymer blends are immiscible due to thermodynamic reasons[6,7], essentially related to the negligible entropy, and unfavorable enthalpy of mixing. Consequently, polymer blending usually leads to a

*** published in polymer 42, 5047-5053 (2001)

heterogeneous system with a multiphase morphology. In a two-phase blend, at low concentration, the predominant morphology is of the dispersed droplet/matrix type. The further addition of minor phase will lead to a percolation point, and at higher concentrations phase inversion eventually occurs. At that point, the two immiscible phases commingle in such a way that each phase remains continuously connected throughout the bulk of the blend. This morphological structure is called dual phase continuity or co-continuity[8-11]. Solvent extraction of one of the components of a co-continuous blend results by definition in 100 % removal.

Polymer blends with a co-continuous structure are of special interest for many types of applications, such as blends with barrier properties, conductive polymers and impact resistant materials[12-14]. The microstructure of the network is a critically important physical characteristic of such materials. Conventionally, for the droplet-matrix morphology, scanning electron microscopy combined with image analysis is an adequate approach to measure the domain size and distribution of the dispersed phase[15]. However, it becomes laborious at best and impossible at worst to examine the microstructure in the region of co-continuity by such a method. This is easily understood since the image analysis approach is based on the analysis of two dimensional photomicrographs, while co-continuity is a complicated three-dimensional interpenetrating and intertwining structure. The lack of adequate characterization techniques has been a hindrance to the effective exploitation and study of co-continuous morphologies in polymer blends.

In this paper the BET method and mercury porosimetry will be compared as characterization techniques for analyzing co-continuous morphologies. Using the most appropriate technique, the efficacy of an SEBS copolymer interfacial modifier for the HDPE/PS co-continuous blend system will also be investigated.

4.2 Experimental

4.2.1 Materials

The materials used in this study were polystyrene (PS, MFI=8.0g/10min), high density polyethylene (HDPE, MFI=4.0g/10min) and a hydrogenated tri-block copolymer

(styrene-ethylene-butadiene-styrene, SEBS, containing 30wt% polystyrene) as interfacial modifier. Characteristic properties of HDPE, PS and SEBS are given in Table 4.1.

4.2.2 Sample preparation

The above materials were dry blended and dried under vacuum at 90°C overnight. A typical blending experiment consists of the following steps. With the temperature of the mixing chamber initially set at 195 °C and blades turning at 50 rpm, the resin mixture was fed into the chamber. Once all of the resin was added, the blend was allowed to mix for 5 min under a constant flow of dry nitrogen. Next, the melt was rapidly transferred to a press at 195 °C under very low pressure for 2 min. The compression molded sample was held in the hydraulic press under the same pressure until the sample had cooled down to room temperature. Finally, the sample was extracted with tetrahydrofuran (THF) to remove the polystyrene phase.

4.2.3 Microscopy

Plane surfaces were prepared for each specimen using a microtome equipped with a glass knife. While cutting, the samples were held below −150°C to minimize surface deformation. The microtomed surfaces were coated with gold and palladium, and observed under a Jeol JSM 840 scanning electron microscope at 10 and 15 kV.

4.2.4 BET measurement

A flowsorb 2300 BET instrument was used to measure the surface area of the specimen. Prior to testing, a given amount of nitrogen was introduced to the instrument through a septum to calibrate the system. Sample testing was conducted at liquid nitrogen temperature. In contrast to the conventional BET nitrogen adsorption technique, which requires vacuum apparatus, a dynamic BET technique[16, 17]which does not use vacuum was employed in this study. The gas mixture, which is composed of nitrogen and helium, continuously passes through the sample cell. Nitrogen gas, as an adsorbate, flows into the sample chamber, and is adsorbed on the adsorbent, (extracted blends where PS phase was removed), at the liquid nitrogen temperature. When the sample cell is immersed into and removed from the liquid nitrogen bath, adsorption and desorption of nitrogen gas respectively occur on the sample surface. The change in effluent gas composition during

adsorption and desorption is sensed by a thermal conductivity detector. The BET technique measures the total volume of nitrogen gas adsorbed on the surface. The volume of gas required to form an adsorbed monomolecular layer, is estimated using Equation (4.1) below [18].

$$\frac{p}{p^o\left[v\left(1-\left(\frac{p}{p^o}\right)\right)\right]}=\frac{1}{v_m c}+\frac{c-1}{v_m c}\frac{p}{p^o} \qquad (4.1)$$

Where, v_m is the volume of gas (at standard temperature and pressure (STP)) required to form an adsorbed monomolecular layer, v is the volume (STP) of gas adsorbed at experimental pressure, p. p^o is the saturation pressure, i.e. the vapor pressure of liquefied gas at the adsorbing temperature and c is a constant related to the energy of adsorption.

The determination of surface area from the BET theory is a straightforward application of Equation (4.1). Figure 4.1 shows the experimental curves of the multiple point method (use of several experimental pressures) for three different HDPE/PS/SEBS blends with PS and SEBS extracted. A plot of $p/[p^o (v(1-(p/p^o))]$ versus p/p^o yields a straight line with the slope $(c-1)/(v_m c)$ and intercept $1/(v_m c)$. If $c>>1$, the intercept is assumed to vanish and then Equation (4.1) reduces to:

$$v_m=v(1-(p/p^o)) \qquad (4.2)$$

This simplified equation allows for the estimation of v_m using a single experimental pressure (single point method). The surface area, S, of the sample is then calculated from

$$S=v_m N a/V_M \qquad (4.3)$$

where, N is Avogadro's number, a is the area of one adsorbed nitrogen molecule (16.2×10^{-20} m^2), and V_M is the molar volume of the gas. The single point method offers the advantages of simplicity and speed with little loss in accuracy. The c value obtained in this study is 58, confirming the condition of $c>>1$ and that the use of the single point method approach is justified.

In order to obtain the morphological parameters (surface area and pore diameter) in the co-continuous region, it is assumed that: (1) the geometric shape of the pore is an interconnected cylinder, (2) the total volume of the pore is equal to that of the extracted phase, (3) the total surface area is that of the pore wall. The total volume of the pore is:

$$V=n\pi d^2 l/4 \qquad (4.4)$$

where, n is the number of cylinders, d is the diameter of the cylinder, l is the length of cylinder and the total surface of the pore wall is:

$$S=n\pi dl. \qquad (4.5)$$

The pore diameter may be calculated from the following formula[19]

$$d=4V/S \qquad (4.6)$$

4.2.5 Mercury porosimetry

The porosity of the samples was also estimated by mercury intrusion porosimetry (Poresizer 9320). This experimental method involves the evacuation of all gas from the volume containing the sample. Prior to the measurement, the samples were dried overnight under vacuum. Mercury is then introduced into a sample container while under vacuum. Finally, pressure is applied to force mercury into the porous sample. The mercury volume forced into the pores is usually monitored in a penetrometer, which is a calibrated precision stem of a glass cell, containing the sample and filled with mercury. As intrusion occurs, the mercury level in the stem varies. A means of monitoring both the applied pressure and the intruded volume are integral parts of all mercury porosimeters. The experimental data treatment is based on the Washburn equation[20]

$$P\cdot r=-2\sigma\cos\theta \qquad (4.7)$$

where, P is the applied pressure, r is the radium of the pore, σ is the interfacial tension and θ is the contact angle. A mercury contact angle of 140° and an interfacial tension of mercury of 480 mN/m were used for all measurements. Analysis of the pore size and size distribution from mercury intrusion porosimetry is described in the results and discussion section.

4.3 Results and Discussion

4.3.1 System without interfacial modifier

Figure 4.2 shows the SEM micrographs of HDPE/PS samples (PS from 30 to 60% volume fraction). The PS was extracted from the blends. The morphological structure changes distinctly with composition. With increasing PS composition, the dispersed phase becomes more and more continuous due to coalescence. An interpenetrating structure occurs at a concentration of 50% PS (confirmed by extraction experiments), and at this composition, it becomes difficult to distinguish the dispersed phase from the matrix. According to Mekhilef et al.[21], the morphology at this composition demonstrates a coarsening effect upon annealing, but maintains the co-continuous type morphology.

Table 4.2 lists both the pore size and specific surface area data of the samples analyzed by the BET technique. The specific surface area depends on the blend composition and ranges from 0.32 to 0.82 m^2/g. The pore size of the sample is in the dimension range of 5.4 to 7.3 μm, which depends on the amount of PS. Table 4.3 lists the pore diameters of the extracted non-compatibilized network measured by the BET technique, mercury porosimetry and image analysis respectively. It can be seen that the BET results correlate well with the number average diameter measured by image analysis. The correlation of the BET data to the number average diameter is expected since the BET technique measures a surface area parameter (monolayer adsorption of nitrogen on the HDPE surface). The smaller diameter fibers will dominate the surface area generation. Mercury porosimetry, on the other hand, yields significantly smaller values. This is likely due to the creation of tiny pores in the material that are created due to the uneven distribution of the high operating pressure. Clearly, mercury porosimetry is not an effective technique for this non-compatible system.

4.3.2 System with interfacial modifier

Figure 4.3 shows the SEM micrographs of HDPE/PS/SEBS networks (polystyrene concentration varied from 30 to 60% volume fraction). The PS is extracted from the blends. In contrast to Figure 4.2 the morphological structure of compatibilized

samples changes only slightly with composition. Nevertheless, as shown in Figure 4.4 the specific surface area of the compatibilized network as measured by the BET technique increases with increasing PS composition. Comparing that data with Table 4.2, it can be seen that the specific surface area of the compatibilized 50HDPE/50PS blend is 5 fold higher than its non-compatibilized counterpart. Also, Tables 4.2 and 4.4 demonstrate that the pore size of the compatibilized 50HDPE/50PS blend was reduced by a factor 5 compared to the non-compatibilized blend. Table 4.4 also shows that a similar pore size is maintained with increasing PS composition for the compatibilized system which indicates that the porous volume increases without influencing pore diameter. Bourry and Favis[22] also found that addition of an interfacial modifier did not change the d_n pore size between 30-50 % PS. The effect of composition on morphology is greatly suppressed by the presence of interfacial modifier. This observation is also consistent with previous work on the compatibilization of dispersed particles. The addition of interfacial modifier significantly reduces the interfacial tension between HDPE and PS.[21] The copolymer locates at the interface between HDPE and PS, and there is miscibility of styrene block units with polystyrene on the one hand, and the miscibility of the hydrogenated ethylene-butadiene blocks with polyethylene, on the other. This effect allows for the stabilization of the phase morphology, and diminishes coalescence. The morphology of this compatibilized blend is thus very stable, and only slight coarsening occurs even after a long annealing time.[21]

The pore size and distribution of the samples were also estimated by mercury porosimetry, and all the pore size and distribution curves of the compatibilized samples are virtually identical. Figure 4.5 illustrates the pore size and distribution curve from mercury porosimetry of the compatibilized 50HDPE/50PS blend. Table 4.4 compares the pore diameters of the compatiblilized blends as estimated by the BET technique and mercury porosimetry. It is interesting to note that the data from the two different techniques are similar. It seems that for a more homogeneous morphology, as is the case of compatibilized blends, mercury porosimetry can also be used to obtain morphological data. In such a case, the operational pressure is more evenly distributed in the system, and

the risk of deforming the morphological structure during testing is reduced. Another possibility is that tiny pores are being created during the mercury porosimetry experiment, but since they are close to the actual pore sizes, they do not affect the measurement results. In any case, the overall results of this study clearly point to BET as the most reliable method. Although the micrographs in Figure 4.3 are too complex to analyze with high accuracy, it can be seen that the SEM pore size is in a range consistent with the values reported in Table 4.4.

4.3.3 Emulsification effect in the co-continuous region

Having determined the applicability of the BET technique, it was then desired to use it to examine the effect of an interfacial modifier on the microstructure of a co-continuous polymer blend. It is apparent from the previous discussion that the addition of SEBS as an interfacial agent results in a substantially finer network in the co-continuous region. The morphology evolution of the porous network (HDPE/PS: 50/50) due to the addition of interfacial modifier can be demonstrated through SEM observation by comparing Figure 4.2c and Figure 4.3c.

The relation of the specific surface area and pore size of the network as measured by BET to the amount of SEBS is depicted in Figure 4.6 (HDPE/PS: 50/50). The specific surface area of the network increases sharply in the range of 3 to 10 parts of SEBS modifier (based on the amount of HDPE). However, the specific surface area of the network reaches a plateau value at about 15 parts of SEBS. The use of morphology data to study emulsification phenomena has been reported for matrix/dispersed phase morphologies in several different systems [23-26]. In those papers the dependence of the particle diameter with interfacial modifier concentration is taken as an indication of the efficacy of the modifier in emulsifying the interface. So far, however there is little information reported on emulsification in the region of co-continuity, due to the difficulty of analyzing this type of complex morphology. The emulsification curve of the co-continuous region shown in Figure 4.6 demonstrates that the tracking of surface area via the BET technique provides a powerful tool to analyzing the efficacy of interfacial modifiers at emulsifying co-continuous morphologies. The possibility now exists to study

the relative efficacy of different modifiers and aspects such as areal density at the interface, modifier architecture and molecular weight on the emulsification of these morphologically complex systems. This subject will be studied in detail in upcoming work.

4.4 Conclusions

In this study, PS extraction followed by the use of a BET nitrogen adsorption technique is found to be an effective route to analyze the microstructure of highly continuous HDPE/PS polymeric blend networks. The specific surface area and the average pore size can be obtained in this way. It is shown that mercury porosimetry can lead to erroneous results. The emulsification of the co-continuous morphology with added SEBS interfacial modifier has also been studied quantitatively with the BET technique. It is shown that the tracking of surface area via BET provides a powerful quantitative tool to analyzing the efficacy of interfacial modifiers at emulsifying co-continuous morphologies.

Acknowledgement

The authors would like to express their appreciation to Professor D. Klvana and Dr. J. Kirchnerova for the use of the BET and mercury porosimetry equipment.

4.5 References

1. Utracki, L. A., *Polymer Alloys and Blends: Thermodynamics and Rheology*, Hanser Publishers Munich, 1990.
2. Favis, B. D., *The Canadian Journal of Chemical Engineering*, 1991, **69,** 615.
3. Sperling, L. H., *Polymeric Multicomponent Materials*, John Wiley & Sons Inc., New York, 1997.
4. Barlow, J. W. and Paul, D. R., *Polym. Eng. Sci.*, 1984, **24,** 525.

5. Han, C. D., *Multiphase Flow in Polymer Processing*, Academic Press, New York, 1981.
6. Olabishi, O., Robeson, L. M., and Shaw, M. T., *Polymer-Polymer Miscibility*, Academic Press, New York 1979.
7. Paul, D. R. and Newman, S., *Polymer blends*, Vols. 1 and 2, Academic Press, New York, 1978.
8. Lyngaae-Jorgensen J and Utracki, L. A., *Makromol. ChemiMacromol. Symp.*,1991, **48/49,** 189.
9. Avgeropoulos, G. N., Weissert, F. C.,. Biddison, P. H. and B hm, G. C. A., *Rubber Chem. Technol.* 1975, **49**, 93.
10. Tsebrenko, M. V., Razanova N. M. and Vinogradov, G. V., *Polym. Eng. Sci.*, 1980, **20,** 1203.
11. Mekhilef, N. and Verhoogt, H., *Polymer*, 1996, **37,** 4069.
12. Tchoudakov, R., Breuer, O., Narkis, M. and Siegmann, A., *Polym. Eng. Sci.*, 1996, **36,** 1336.
13. K. Levon, K., Marglina, A. and Patashinsky, A. Z., *Macromolecules*,1993, **26,** 4061.
14. Gubbles, F., Jérôme, R., Teyssié, Ph., Vanlathem, E., Deltour, R., Calderone, A., Parenté, V., and Brédas, J. L., *Macromolecules*, 1994, **27,** 1972 .
15. Favis, B. D. and Chalifoux, J. P., *Polymer*, 1988, **29,** 1761.
16. Loebenstein, W. V. and Deitz, V. R., *J. Res. Nat. Bur. Stand.*,1951, **46,** 51.
17. Nelson F. M. and Eggertsen, F. T., *Anal. Chem.*, 1958, **30,** 1387.
18. Brunauer, S., Emmett, P. H. and Teller, E., *J. Amer. Chem. Soc.*, 1938, **60,** 309.
19. Lowell, S and Shields, J. E., *Powder Surface Area and Porosity,* 3rd edition, T. J Press Ltd. Padstow, Cornwall 1991.
20. Washburn, E. W., *Phys. Rev.*,1921, **17,** 273.
21. Mekhilef, N., Favis, B. D. and Carreau, P. J., *J. Polym. Sci., Polym. Phys.*, 1997, **35,** 293.
22. Bourry, D. and Favis, B. D., *J. Polym. Sci., Polym. Phys.*, 1998, **36,** 1889.
23. Willis, J. M. and Favis, B. D., *Polym. Eng. Sci.*,1988, **28,** 1416.

24. Favis, B. D., *Polymer*, 1994, **35,** 1552.

25. Matos, M. and Favis, B. D., *Polymer*, 1995, **36**, 3899.

26. Cigana, P., Favis, B. D., Jérome, R. *J Polym. Sci., Polym. Phys* 1996; **34**, 1691

Figure captions

Tables

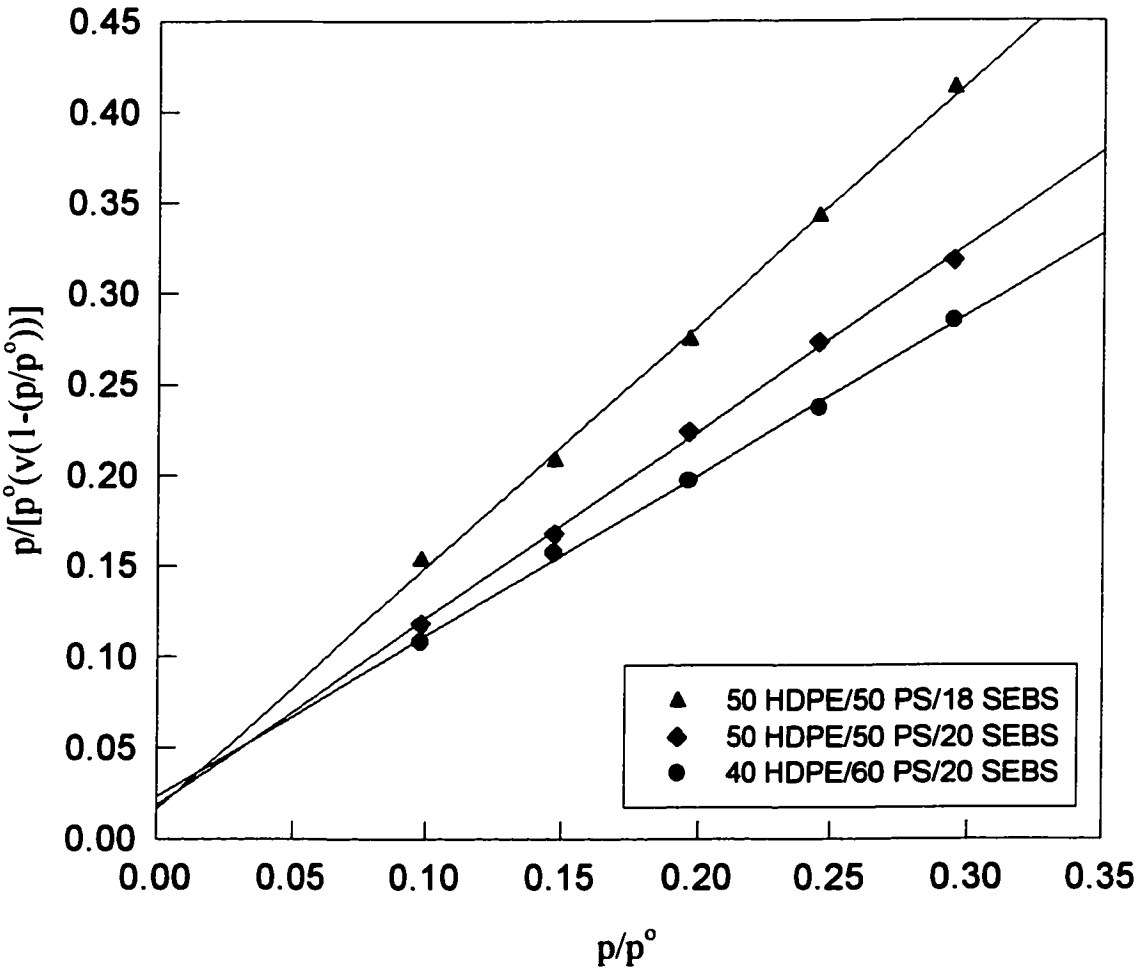

Figure 4.1. BET multiple point method for the extracted ternary blend systems.

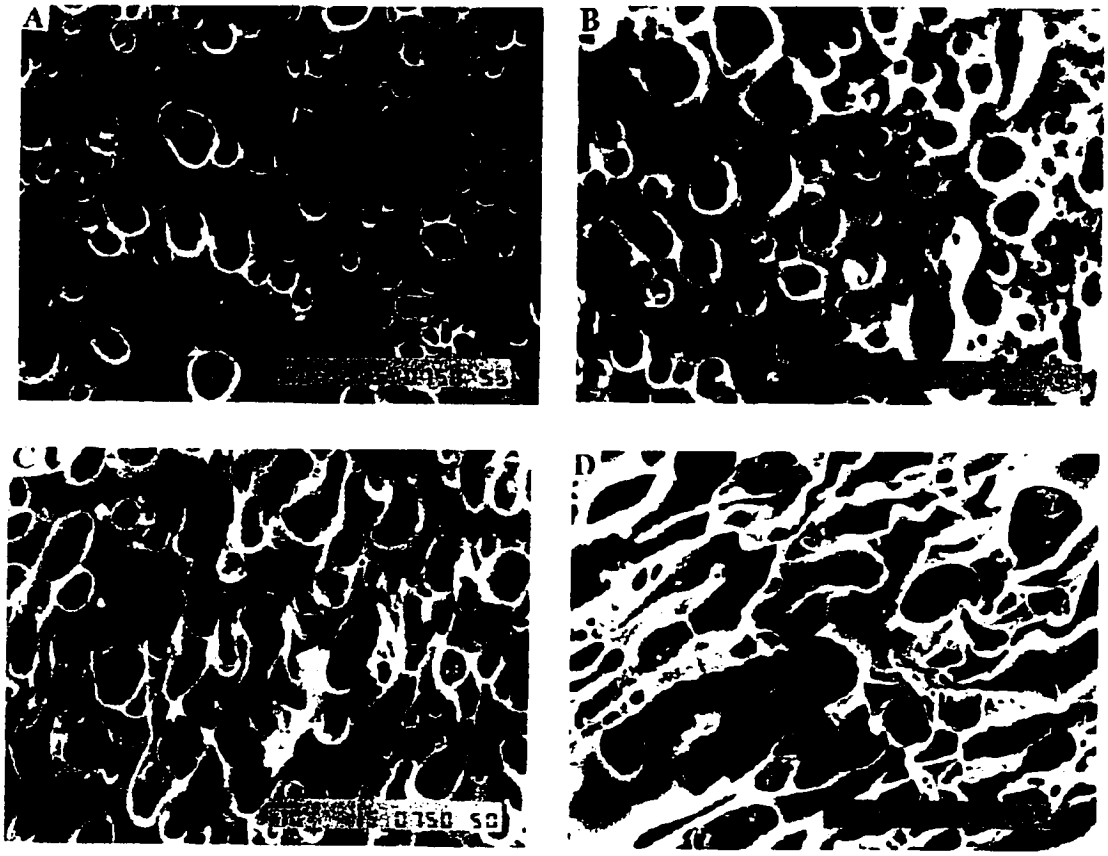

Scale bar — : 10 μm

Figure 4.2. Morphology evolution of non-compatibilized HDPE/PS blends with composition (a) 30 PS/70 HDPE, (b) 40 PS/60 HDPE (c) 50 PS/50 HDPE and 60 PS/40 HDPE.

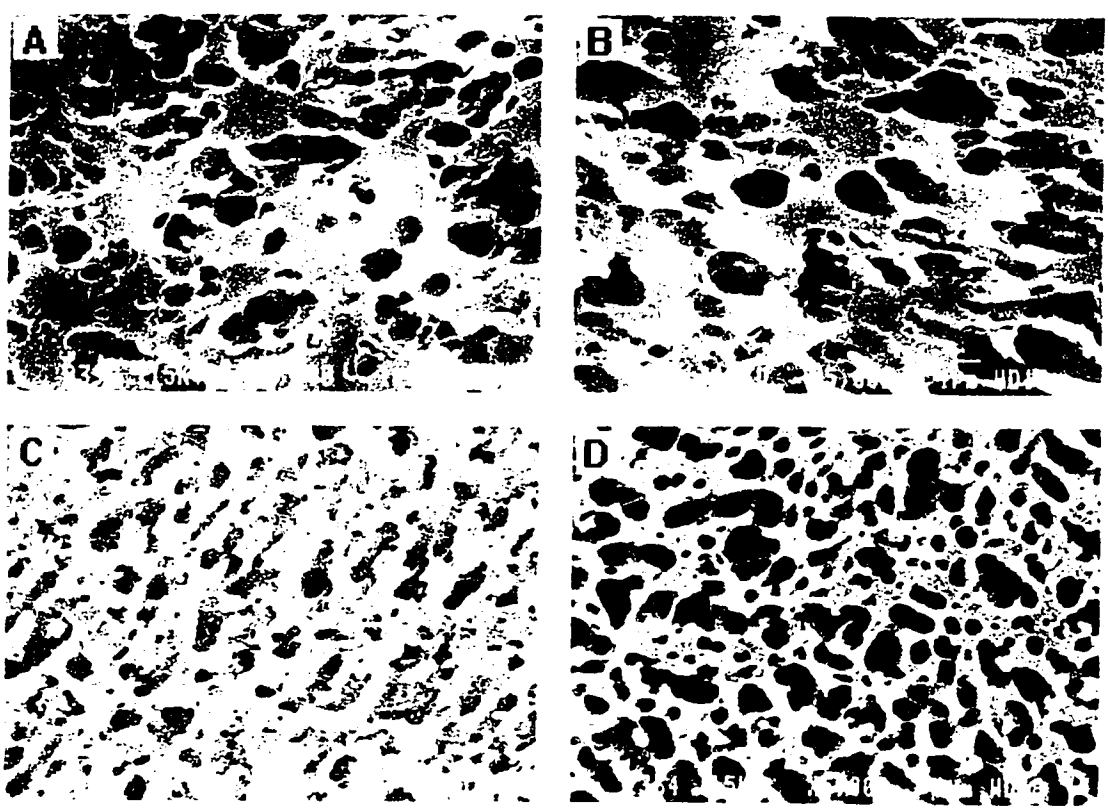

Scale bar : — 1μm

Figure 4.3. Morphology evolution of compatibilized HDPE/PS blends with composition. 20% SEBS interfacial modifier based on the minor phase was added. (a) 30 PS/70 HDPE/20 SEBS, (b) 40 PS/60 HDPE/20 SEBS, (c) 50 PS/50 HDPE/20 SEBS and (d) 60 PS/40 HDPE/20 SEBS.

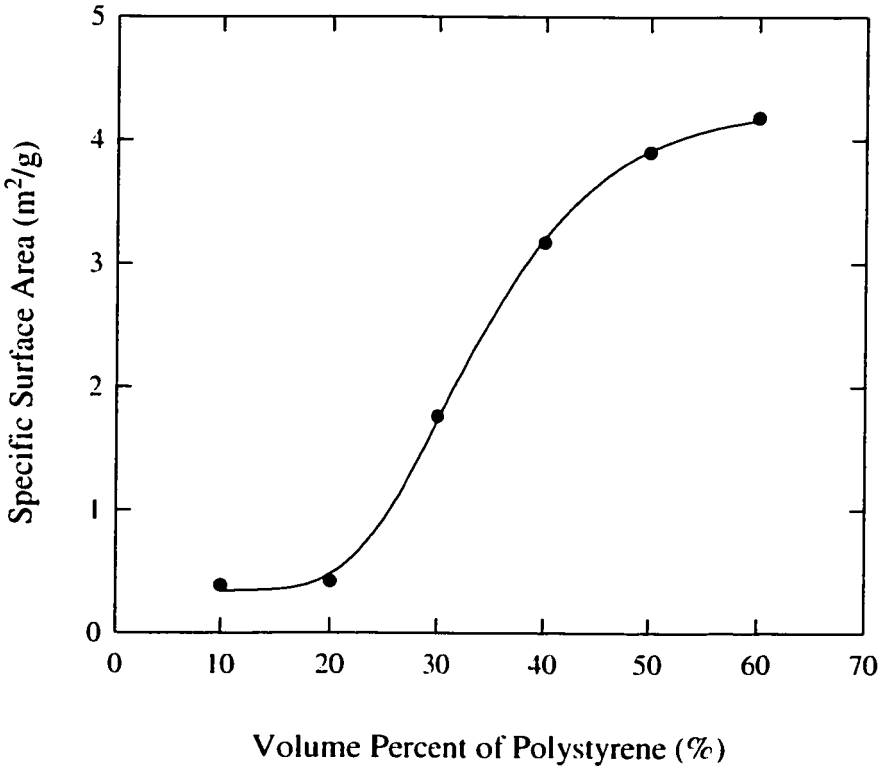

Figure 4.4. Effect of PS composition on the specific surface area for compatibilized blends. 20% SEBS interfacial modifier based on the minor phase was added.

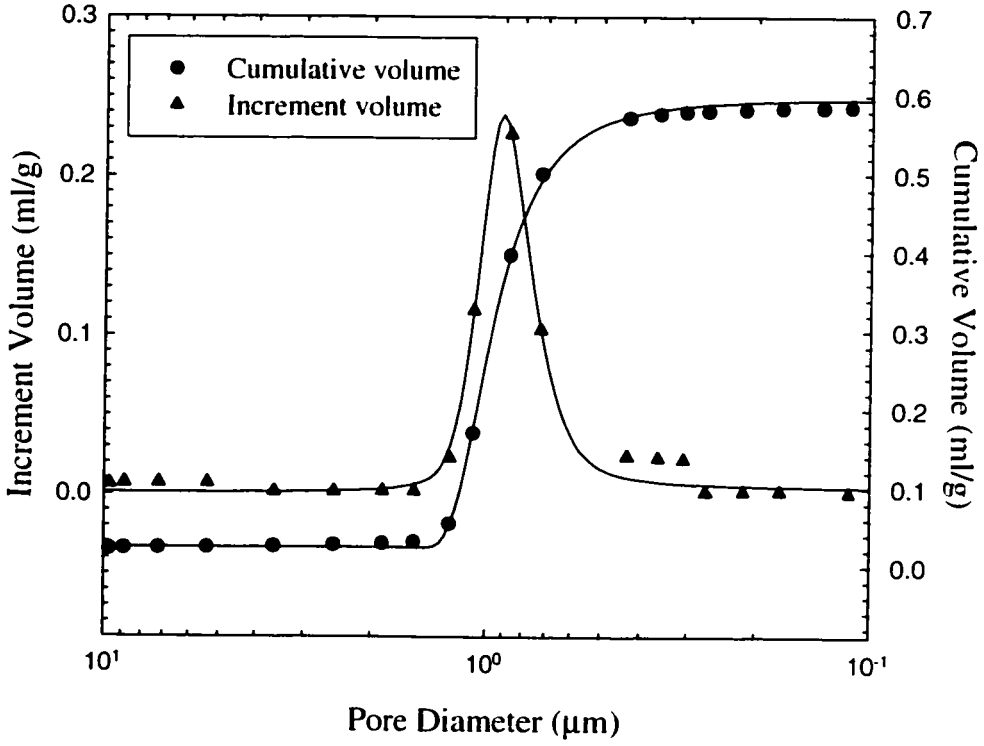

Figure 4.5. Pore size distribution of the extracted compatibilized blend (50HDPE/50PS/20SEBS) measured by mercury porosimetry.

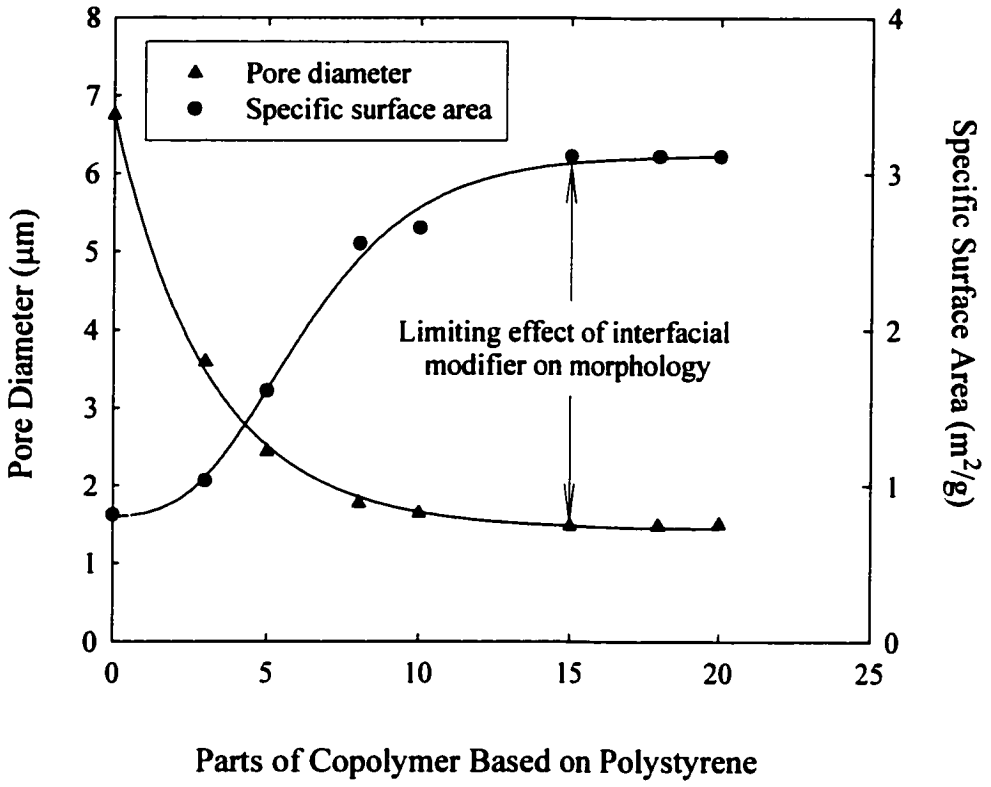

Figure 4.6. Effect of copolymer compatibilizer concentration on the specific surface area and pore size of extracted co-continuous blends (HDPE/PS: 50/50). The amount of SEBS added is based on the PS phase.

Table 4.1. Characteristics of materials

	Polystyrene	Polyethylene	SEBS[c]
M_w	215,000	79,000	S=7500 EB=35000
M_n	100,000	24,000	
Melt index (g/10 min)	8.0[a]	4.0[b]	---
Density (20°C) (g/ml)	1.04	0.962	1.000
Density (200°C) (g/ml)	0.974	0.754	---
Supplier	Dow	Dow	Shell

a 200°C/5.0 Kg
b 190°C/2.16 Kg
c 30% (wt) polystyrene

Table 4.2 Specific surface area and pore diameter of extracted noncompatiblized blends from the BET technique

	Specific surface area (m^2/g)	Pore diameter (μm)
HDPE/PS: 70/30	0.32	5.4
HDPE/PS: 60/40	0.43	6.2
HDPE/PS: 50/50	0.63	6.4
HDPE/PS: 40/60	0.82	7.3

Table 4.3 Pore size of noncompatibilized HDPE/PS blends by three different techniques

	Image analysis		BET technique (μm)	Mercury Porosimetry (μm)
	d_v (μm)	d_n (μm)		
HDPE/PS:60/40	15.0	7.2	6.2	0.6
HDPE/PS:50/50	17.3	7.6	6.4	1.3

Table 4.4 Pore size of extracted compatibilized blends by BET and Mercury Porosimetry respectively

Pore size of extracted polymeric blend (μm)		
	BET nitrogen Adsorption	Mercury porosimetry
HDPE/PS/SEBS: 70/30/20	1.4	1.0
HDPE/PS/SEBS: 60/40/20	1.5	1.2
HDPE/PS/SEBS: 50/50/20	1.3	1.0
HDPE/PS/SEBS: 40/60/20	1.3	1.5

CHAPTER 5.THE ROLE OF THE BLEND INTERFACE TYPE ON MORPHOLOGY IN CO-CONTINUOUS POLYMER BLENDS***

Jianming Li, Peilian Ma and Basil D. Favis
Centre de Recherche Appliquée Sur les Polymères (CRASP), Département de Génie Chimique, École Polytechnique de Montréal, P. O. Box 6079 Station Centre-Ville, Montréal, (QC) Canada H3C 3A7

ABSTRACT:

In this paper three different categories of blend interfaces are examined systematically in order to isolate the role of the interface in the development of co-continuous morphologies during melt mixing. They are: Type I) compatible binary blends based on HDPE/SEBS and HDPE/SEB; Type II) an incompatible binary system comprised of HDPE/PS; and Type III) compatible ternary systems comprised of HDPE/PS compatibilized by SEBS in one case and by SEB in another. The Type I and Type III systems represent conventional approaches to preparing blend systems of low interfacial tension. The co-continuous morphology is analysed using three techniques: microscopy/image analysis; solvent extraction/gravimetric analysis; and BET characterization of surface area and pore size. The relative presence of fibers or droplets during dynamic mixing is analysed quantitatively using a matrix dissolution/image analysis technique. A mechanism for the formation of dual phase continuity based on droplet and fiber lifetimes during melt mixing has been proposed. For the Type I compatible binary systems continuity development and micro-structural features are dominated by thread-thread coalescence. In the Type II incompatible HDPE/PS binary system continuity development and microstructural features are dominated by droplet-droplet coalescence. In the Type III compatibilized ternary systems continuity development and microstructural features are controlled by reduced droplet-droplet coalescence. Generation of fresh interface during droplet deformation results in a system that is only partially emulsified. A thread frequency ratio (TFR) is proposed as a basic

*** accepted for publication in Macromolecules

general parameter to classify the relative presence of fibers to droplets during mixing and hence the type of continuity development for a given system.

5.1 Introduction

When melt blending immiscible polymers, two major categories of morphologies are possible: a dispersed phase/matrix, or a co-continuous morphology. At compositions above the percolation threshold, various levels of continuity exist. Co-continuity is a special case of blend morphology in which each polymer is fully interconnected through a continuous pathway. Recently, much interest has been generated in polymer blends with a co-continuous morphology [1-14] due to a number of promising applications. [15-17]

One of the challenges in studying co-continuous systems is the use of appropriate characterization techniques. In the past, a significant amount of work used only microscopy as the principal method of analysis. Over the last ten years, however, it has become routine to combine microscopy with extraction/gravimetric analysis as a route to quantifying the level of continuity in a given system. This approach is quite rigorous at estimating the level of continuity, but does not provide any quantitative information on the scale of the co-continuous microstructure. Recently it has been proposed that BET analysis should be included as a necessary third technique towards the quantification of co-continuous structures. [7] It has been shown that the BET technique can be used to analyze the complex microstructure of co-continuous HDPE/PS blends following the extraction of the PS phase. Both the surface area and the pore size are estimated. Using this approach it has been possible to quantify the emulsification efficacy of an added interfacial modifier in the HDPE/PS dual phase continuous region. An emulsification curve, virtually similar in form to those observed in conventional droplet-matrix blend systems, is obtained.

Most studies on co-continuity have been carried out on immiscible binary blends and in particular with respect to the role of the viscosity ratio in determining the position of phase inversion. [1, 2, 8, 9, 10, 11] Very little work has been directed towards the role of the interface on co-continuous morphologies. Bourry and Favis [4] have shown that a

compatible ternary blend demonstrated an onset of percolation phenomena and continuity development at higher concentrations than the non-compatible binary blend. Willemse et al.[12] and Veenstra et al. [13] have recently shown that the co-continuous morphology in a homopolymer/copolymer system persisted over a wide composition range. This effect was shown to be related to very stable elongated structures which do not show breakup during processing and were obtained by processing SEBS type copolymers below its order/disorder transition temperature [13]. Verhoogt et al.[18] also demonstrated that binary blends of low interfacial tension could possess a wide region of dual-phase continuity.

The effect of interfacial tension on Tomotika-like capillary instabilities is well known in the scientific literature and it follows directly from that work that a reduction in interfacial tension should increase the stability of the capillary fiber. A number of papers studying the reduction in interfacial tension with interfacial modifier using the breaking thread technique have confirmed that point numerous times[5,19,20,21]. It is therefore difficult to argue with a concept of low interfacial tension binary blends demonstrating stable elongated structures and hence a wide region of dual phase continuity. It becomes more difficult, however, in light of the above, to explain why a number of papers have indicated that compatibilized ternary blends, of apparently low interfacial tension, demonstrate a narrower region of dual-phase continuity [22] and delayed percolation phenomena [4] than their high interfacial tension, incompatible binary blend counterparts. These latter systems appear to display anomalous behavior.

There is clearly a need to formulate a general conceptual mechanism of continuity development for the full range of possible polymer blend interfaces. Furthermore, what is the influence of the interface on the microstructure or phase size itself ? The objective of this work is to carry out a broad systematic study to contribute towards a general understanding of the role of the interface on continuity development in polymer blends. Both the continuity development and microstructural features are studied in detail for the three main categories of possible blend interfaces: I) compatible binary blends, II) incompatible binary blends and III) compatible ternary blend systems.

5.2 Experimental Procedure

5.2.1 Materials

The high density polyethylene (HDPE) and polystyrene (PS) used in this study were obtained from Dow Chemical of Canada. The copolymers were obtained from Shell USA. Kraton G1652 is a triblock copolymer of (styrene)-(ethylene-butylene)-(styrene) designated in this work as SEBS1, with a molecular weight of 35,000 for the center block and 7,500 for the PS blocks. Its composition is 30% PS. Cap 2825 is another triblock copolymer of (styrene)-(ethylene-butylene)-(styrene) (SEBS2), with a molecular weight of 39000 for the center block and 3000 for the PS blocks. Its composition is 13% PS. Two diblock copolymers were used in the study. One is Cap 4741, a diblock copolymer of (styrene)-(ethylene-butylene) (SEB1), with a molecular weight of 47,000 for the (ethylene-butylene block) and 20,000 for the styrene block. Its composition is 30% PS. Another diblock copolymer is a Cap 4745 (SEB2) containing 26% PS, with a molecular weight of 138,380 for the EB block and 48,620 for the PS block. The properties of the materials are listed in Table 5.1.

5.2.2 Blend Preparation

Binary blends and compatibilized ternary blends were prepared by melt mixing the polymers in a Brabender mixer, which is predominantly a shear mixing device. For the compatible ternary blend system the melt blending was achieved in two steps. In the first step the copolymer was melt blended with the dispersed phase (the volume percentage of copolymer is 20% based on the dispersed phase). The second step consisted of melt blending the dispersed phase (containing copolymer) with the matrix. A typical blending experiment consists of the following steps. With the temperature of the mixing chamber initially set at 195°C and blades turning at 50 rpm, the resin of mixture was fed into the chamber. Once all of the resin was added, the blend was allowed to mix for 5min under a constant flow of dry nitrogen. Next, the melt was rapidly quenched by liquid nitrogen to freeze-in the morphology. Finally, the quenched sample was treated with tetrahydrofuran (THF) to remove the copolymer or polystyrene phases.

5.2.3 Rheology

The polymers were pressed at 195°C in order to obtain the disks used for the rheological measurement. Rheological characterization of the specimens was carried out using a Bohlin constant stress rheometer (CSM) in the dynamic mode at 195°C under a nitrogen atmosphere and in the range of 0.01-30Hz frequency with a strain of 5%. A parallel plate configuration was used with a gap about 1.4 mm. The Cox-Merz rule is applicable to the materials measured.[13, 23]

5.2.4 Breaking Thread Method

The measurement of the interfacial tension by the breaking thread method is based on theories developed first by Lord Rayleigh [24] and later by Tomotika [25]. This method consists of sandwiching a thin filament between two films of the matrix. First, a thread of the SEBS2, which has a diameter of 20-60μm, was drawn from a few pellets on a hot plate, cut into 15mm long pieces and annealed in a vacuum oven (50°C) in order to ensure relaxation of any residual stress. Then, the thread is placed (at room temperature) between two films of HDPE, each with dimension of 10*10*0.3 mm. The system is enclosed between two glass sheets, placed under an optical microscope equipped with a Mettler FP82HT hot stage. The optical microscope was equipped with a video camera, and images of the developing oscillation were recorded on a VHS video recorder. An image processing system (Visilog 4.1.3) was used to measure the amplitude, α, which was calculated by measuring the evolution of the minimum and maximum diameters of one oscillation,

$$\alpha = \frac{D_{max} - D_{min}}{4} \tag{5.1}$$

In each experiment, the sample is first slowly heated to the melting temperature of the film matrix in order to avoid air bubble formation at the interface. The temperature is then increased just below the melting temperature of the thread and held for 5 min. Finally, the sample is rapidly heated to the test temperature. The expression of interfacial tension is given by

$$\sigma = \frac{q\eta_m D_o}{\Omega_m} \tag{5.2}$$

where q is the growth rate of the distortion, η_m is the viscosity of matrix, D_o is the initial thread diameter and Ω_m is a tabulated function and can be calculated from Tomotika's original equations. The growth rate of the distortion, q, can be calculated from the slope of the line, obtained by plotting log $(2\alpha/D_o)$ versus time according to the following expression

$$\alpha = \alpha_o \exp(qt) \tag{5.3}$$

where α_o is the initial distortion amplitude, and t is the time.

5.2.5 Microscopy

Prior to microscopic observation the samples were microtomed under liquid nitrogen to create a plane face using a Reichert Jung Supercut 2050 equipped with a glass knife. While cutting, the surface of the sample was held at approximately −150°C to reduce the degree of surface deformation. The microtomed samples were then subjected to the appropriate chemical treatment to dissolve one of the phases. Finally the samples were coated with gold and palladium, and observed under a JEOL JSM 840 scanning electron microscope operated at a working voltage of 10 or 15KV.

5.2.6 Image Analysis

For the dispersed phase in the composition of 30% and below, a semiautomatic method of image analysis consisting of a digitizing table and an in-house software was used to quantify the dispersed phase morphology. The number average, d_n, and volume average diameters, d_v, were obtained from the measurement of at least 200 diameters. Since the microtome does not necessarily cut the dispersed phase at the equator and since it is necessary to correct for polydispersity, a correction was applied in order to obtain the true diameter.[26] The maximum error for the measurement of d_n and d_v is about ±10%.

5.2.7 Solvent Extraction

Extraction of Dispersed Phase

Extraction of the dispersed copolymer phase was performed in a Soxhlet extraction apparatus with tetrahydrofuran (THF) for 36 hrs. A gravimetric method was used to calculate the extent of continuity of the removed phase (PS or copolymers),

$$\%\,Continuity = \frac{(Weight\ of\ copolymer\ or\ PS)_{initial} - (Weight\ of\ copolymer\ or\ PS)_{final}}{(Weight\ of\ copolymer\ or\ PS)_{initial}} * 100 \qquad (5.4)$$

The maximum error for the continuity measurement is ± 2%. Further details are given in previous work. [7]

Matrix Dissolution Technique

In order to determine the shape (fiber or droplet) of the dispersed phase during mixing, the extraction of the matrix (PS or copolymer) was performed followed by centrifugation and in some cases filtration. Initially the sample (about 1gram) was placed into a centrifuge tube filled with 50 ml THF. The tube containing the sample was then placed on a shaker for 48hrs. The sample was then centrifuged for one hour. The solution was poured away, fresh solvent was added to wash the precipitated HDPE and the sample was shaken again. This process was repeated three times which was sufficient to separate the HDPE dispersed phase from PS for the HDPE/PS and HDPE/PS/SEBS1 blends although the solution of the latter was slightly translucent in color. It was extremely difficult to remove all the copolymer matrix from 5HDPE/95SEBS blend. In this case the sample solution was diluted to one of 10th of its original concentration then followed by a filtration process. Finally, all the dispersed phase samples were carefully collected and dried in a vacuum oven for 72 hours at 40°C.

5.2.8 TFR (Thread Frequency Ratio) Measurement

The TFR measurement was undertaken for the dispersed phase obtained after matrix extraction. Five fields of view taken using the SEM and approximately 500 particles and threads were considered for a given sample. The t.f.(thread frequency) and the d.f.(droplet frequency) were obtained by counting the number of each respective

species. A droplet was considered to be a thread once it exceeded an aspect ratio of 3. The TFR was calculated according to Equation (5.7).

5.2.9 BET Measurement

A flowsorb BET instrument was used to measure the surface area and pore size of the extracted samples. Prior to testing, a given amount of nitrogen gas was introduced to the instrument through a septum to calibrate the system. Sample testing was conducted at liquid nitrogen temperature. Water was used to warm the sample tube to accelerate the desorption process. Adsorption and desorption data were recorded during the test. Bulk polyethylene samples were tested in order to correct for the case of nitrogen absorption. However, no absorption was registered by the apparatus under the same testing conditions as above. The maximum error for the surface area measurement is about ±5%. Further details of this technique are given in previous work. [7]

5.3 Results

5.3.1 Rheology

Figure 5.1 shows the complex viscosity as a function of frequency/shear rate for the raw materials used. The HDPE and PS show shear thinning behavior over almost the complete range of measured frequencies/shear rates, and Newtonian flow behavior is only observed at the lowest frequencies. The viscosities of triblock copolymer SEBS1 (containing 30% styrene) and diblock copolymer SEB1 (containing 30% styrene) are higher than those of polyethylene and polystyrene for the whole range of shear rates. SEBS1 displays the highest complex viscosity. There was no Newtonian behavior observed in the whole experimental shear rate range for SEBS1 and SEB1. However, the SEBS2 displayed a Newtonian plateau at low shear rates and shear thinning behavior at higher shear rates. The complex viscosity of SEBS2 is lower than those of HDPE and PS. Figure 5.2 illustrates the storage moduli of HDPE, PS, SEBS1, SEBS2 and SEB1. The storage moduli of SEBS1 and SEB1 is higher than those of HDPE and PS, while the storage modulus of SEBS2 is lower than those of HDPE and PS. The viscosity and

elasticity ratios of all the blends studied are given in Table 5.2. It will be demonstrated later that 50 rpm in the internal mixer corresponds to about 50 $s.^{-1}$

5.3.2 Fiber Stability and Interfacial Tension

The breaking thread experiment for an SEBS thread in HDPE is used to obtain the interfacial tension and also to demonstrate the stability (long breakup times) of the fiber under static conditions. Since a zero shear viscosity is required and SEBS2 was the only specimen which demonstrated a Newtonian plateau at low shear rates, it was used as the thread material. A typical example of the breakup behavior of an SEBS2 thread sandwiched in HDPE films at 195°C is illustrated in Figure 5.3. A sinusoidal distortion appeared after 30 minutes (Figure 5.3 (a)), and further developed after 90 and 120 minutes (Figure 5.3 (b) and (c)). The thread broke up into droplets after about 180 minutes (Figure 5.3 (d)). The resulting radius of the droplets is about 1.8 R_o.

By way of comparison, the breakup time for a PS thread of similar diameter in HDPE is approximately 22 minutes. This represents a factor 7 difference in thread stability.

Figure 5.4 shows typical results at 195°C for the relative amplitude log $(2a/D_o)$ versus time for SEBS2 imbedded in HDPE matrices. The required linear behavior of log $(2\alpha/D_o)$ versus t is observed. The slopes of the straight line, q/2.303, vary with the diameters of the threads as expected. With the value of the slope, the interfacial tension may be obtained by equation (2). The interfacial tension of HDPE/SEBS2 measured in this way is 0.72 mN/m. The interfacial tension for the very same HDPE/PS and HDPE/PS/SEBS1 has been studied previously and was found to be 5.6 and 1.0 mN/m,[5] respectively.

5.3.3 Continuity Development

Compatible Binary System

Figure 5.5 shows the %continuity/composition relationship for HDPE/SEB1 and HDPE/SEBS1 blends obtained after solvent extraction. There is no continuity present at 10% copolymer for either of the blends. When the copolymer composition is increased to 18%, the level of continuity achieves 50% for both blends. A co-continuous structure is

obtained in the range of 30-68% copolymer composition for both samples. Co-continuity in this binary blend system can be defined as the concentration range where both phases are 100% continuous. This is rigorously measured when selective solvents for each of the phases are available. In the case of HDPE/SEBS it is impossible to dissolve the HDPE without also dissolving out SEBS. For this reason we define a concentration region of co-continuity as existing from the onset of full continuity for SEBS (or SEB), using THF as a solvent, to the point at which the sample disintegrates in the presence of that same solvent. Sample disintegration in THF is a clear indication that SEBS (or SEB) is the matrix and HDPE is the dispersed phase. Both blends disintegrated at 70% copolymer after extraction, indicating that complete phase inversion is achieved between a composition of 68 to 70%. It is interesting to note that both blends demonstrate a virtually identical %continuity / composition relationship.

Non-compatibilized Binary System and Compatibilized Ternary System

The %continuity / composition relationships for HDPE/SEBS1, HDPE/PS and the HDPE/PS/SEBS1 blend systems are shown in Figures 5.6a and 5.6b. Figure 5.6b is an expanded view of the continuity development region. For the non-compatible blend system (HDPE/PS), zero continuity was observed up to a PS concentration of 10%. The continuity of PS is 25% at 18%PS and this increases to 84% at 30% PS. A fully continuous structure is obtained at about a volume concentration of 40% PS. This continuous structure disintegrates at 68% PS once again indicating phase inversion. For the compatibilized ternary system (HDPE/PS/SEBS1), the continuity level is lower when compared with both the compatible and non-compatible binary systems at the same composition in Figure 5.6a and 5.6b. The compatibilized ternary blend system (HDPE/PS/SEBS1) displays zero continuity up to 15% PS. A level of 15% continuity is observed at 18% PS. The continuity increases to 80% at 30% PS and a fully continuous structure is obtained at about 45% PS. The extracted structure disintegrates at 66% polystyrene. It is interesting to note that a narrowing of the co-continuous range, as compared to the non-compatibilized binary blend, is observed for the compatibilized

ternary system despite its low measured interfacial tension. An explanation of this effect will be elaborated on in the discussion section.

5.3.4 Pore Size

Compatible Binary System (Type I)

The variation of specific surface area, as measured by BET nitrogen adsorption technique, of HDPE/SEBS1 and HDPE/SEB1 with copolymer composition is shown in Figure 5.7. The specific surface area of both samples increases with increasing copolymer composition. The specific surface area of extracted 80HDPE/20SEBS1 is 1.32 m^2/g, while that of 80HDPE/20SEB1 is 2.43 m^2/g. The specific surface area for 40HDPE/60SEBS1 is 10.64 m^2/g and 16.00 m^2/g for 40HDPE/60SEB1. Clearly, the specific surface area of the SEB1 system is significantly higher than that of the SEBS1 system at the same copolymer concentration.

Figure 5.8 illustrates pore diameters for both extracted compatible blend systems. The pore diameter is estimated from the specific surface area assuming a cylindrical pore shape as reported previously. [7] For the HDPE/SEBS1 blend the pore size is about 0.60 μm, while the pore size of the HDPE/SEB1 blend is only around 0.30 μm. HDPE/SEBS1 and HDPE/SEB1 clearly demonstrate little change in pore size with composition. It is interesting to observe that although the surface area of extracted HDPE/SEB1 increases about 10 fold with composition, there is little change in pore size. These results indicate that the effect of increasing composition in a compatible binary blend is to create a more dense continuous network of virtually equivalent pore size.

Figures 5.9 and 5.10 show SEM micrographs of both compatible binary blends in the composition range of 30-60% copolymer. As expected, the two-dimensional micrographs (Figures 5.9 and 5.10) are limited in their information related to dual phase continuity (a three dimensional structure), however, it is clear that a much finer microstructure is observed for the extracted blend containing diblock copolymer (HDPE/SEB1). It is also apparent that the pore size of each blend does not change significantly with concentration. Both these observations support the BET results from above.

Non-compatible Binary System (Type II) and Compatible Ternary System (Type III)

Figure 5.11 demonstrates the pore size /composition relationship for two compatible ternary systems. Very similar pore sizes are obtained for diblock or triblock modifiers and very little change in pore size is observed with composition. Figure 5.12 illustrates the pore size / %composition relationship for all the blend systems studied. For the non-compatible binary system (HDPE/PS), the pore size increases significantly with composition (from 2.0 μm at 10% PS to 6.3 μm at 60% PS).

The pore size data were obtained from image analysis (when the minor phase was less than and equal to 30%) and with the BET technique (when the minor phase was equal to and above 30%). The good correspondence between the data from the two different techniques has been discussed in a previous publication. [7]

5.3.5 Summary of the Main Features for the Three Types of Blend Interface Categories

The main microstructural features for the three blend interface categories can be summarized from Figures 5.6b, 5.8, 5.9, 5.10, 5.11 and 5.12.

Compatible Binary Blend (HDPE/SEBS1; HDPE/SEB1) (Type I)

In a compatible binary system the main features are: (a) the onset of percolation and continuity development occur at low composition, (b) the full continuity of the minor phase is attained at low composition and maintained over a wide composition range, and (c) the pore size of the blend changes little with increasing %minor phase.

Non-compatible Binary Blend (HDPE/PS) (Type II)

The non-compatible binary blend shows that: (a) the onset of percolation and continuity development take place at a higher composition than Type I, (b) the full continuity is maintained in a narrower composition range than Type I, and (c) the pore size of blend increases significantly with minor phase.

Compatibilized Ternary System (HDPE/PS/SEBS) (Type III)

The compatibilized ternary system demonstrates that: (a) the onset of percolation and continuity development take place at higher composition than Type II, (b) the full continuity region is narrower than Type II, (c) there is little change of pore size with composition, and (d) the pore size is greater than Type I, but less than Type II.

A general conceptual mechanism which accounts for all of the above effects will be presented in the discussion section.

5.4 Discussion

5.4.1 Position of the Region of Dual-Phase Continuity

It has been shown in previous papers that both the viscosity ratio and the elasticity ratio can have an influence on the position of the region of dual-phase continuity.[4, 27] It has been suggested that the more elastic material could tend to preferentially encapsulate the less elastic material in order to reduce the dynamic interfacial tension and hence the surface free energy of the system. These results were reported by Bourry and Favis [4] and Favis and Chalifoux [27] and were based on the theoretical developments of Van Oene.[28] Van Oene studied the contribution of the elasticity of the components in a blend system on the dynamic interfacial tension.

The region of dual-phase continuity for the three types of blend systems are shown in Figures 5.6a and 5.6b. It is important to note that the arrows in Figure 5.6a refer to the point of disintegration of the blend after extraction in THF (70% for HDPE/SEBS1; 68% for HDPE/PS; 66% for HDPE/PS/SEBS). That point indicates the case where polystyrene is the matrix, an indication that phase inversion has already occurred. In order to ascertain the highest composition at which the extracted blend maintains its integrity, for all three blend types, blends were prepared in the composition range of 60% PS and higher in steps of 2%. That value was 68% for HDPE/SEBS1, 66% for HDPE/PS and 64% for HDPE/PS/SEBS1. Those values indicate the upper limit of co-continuity. The range of co-continuity for HDPE/SEBS1 is therefore 30-68%; for HDPE/PS it is 40-66% and for HDPE/PS/SEBS1 it is 45-64%. For the Type I case, the

wide breadth of the region of dual-phase continuity makes it difficult to comment on if the SEBS1 demonstrates preferential encapsulation. For the purposes of commenting on the position of the region of dual-phase continuity, we will limit the discussion to the Type II HDPE/PS system. The Type II HDPE/PS system with its region of dual-phase continuity from 40-66% PS is best described as showing no preferential encapsulation of any of the components.

In order to estimate the appropriate viscosity and elasticity ratios for the HDPE and PS in the mixing chamber, a torque study of the pure components was carried out in the Brabender mixer. Previous studies from this laboratory [29] have clearly shown that the torque ratio (torque of PS/torque of HDPE) from the Brabender mixer can be closely related to the complex viscosity ratio from rheological equipment. The torque data are reported in Table 5.3 and the torque ratio for PS/HDPE is 1.0. From the rheological curves shown in Figure 5.1, a complex viscosity ratio of 1 corresponds to a shear rate of 50 s^{-1}. At 50 s^{-1} the elasticity ratio from Figure 5.2 and Table 5.2 is 1.55. Hence, the elasticity ratio would predict a slight tendency of PS to encapsulate HDPE while the viscosity ratio would predict no preferential encapsulation. The wide region of dual-phase continuity again makes it somewhat difficult to comment any further.

It is interesting to note that Bourry and Favis [4] observed a region of dual-phase continuity for the very same HDPE/PS blends from 60-80% PS for blends prepared on the twin-screw extruder at 200°C and 100 rpm. Both the solvent extraction and morphology experiments clearly demonstrated a tendency of HDPE to preferentially encapsulate PS in that work. In this current study, a shift of approximately 20 composition units has occurred in this work using the Brabender mixer. The region of dual-phase continuity is shifted to lower %PS. Since the twin-screw is operating at a significantly higher rpm and since it also uses mixing elements such as kneading blocks which create zones of high shear, it is safe to assume that the twin-screw extruder, under the conditions used by Bourry and Favis, represents a higher shear rate mixing approach than the Brabender. If one compares the change in viscosity and elasticity ratios with shear rate shown in Table 5.4 it can be seen that lower shear rates result in a higher

G'_{PS}/G'_{HDPE} and a higher η_{PS}/η_{HDPE} as well. Lowering the shear rate should shift the region of dual-phase continuity to higher %PS if the viscosity ratio model dominates and to lower %PS if the elasticity ratio model dominates. Comparison of the rheological data of the two studies also indicates that a temperature reduction of 5 degrees (195°C in this work) increases both the elasticity ratio and the viscosity ratio. Lowering temperature has the same effect on the region of dual-phase continuity as lowering the shear rate, which should shift the region of dual phase continuity to higher %PS if the viscosity ratio model dominates and to lower %PS if the elasticity ratio dominates. Hence this study coupled with the work by Bourry and Favis [4] indicates that the observed shift in the region of dual-phase continuity to lower %PS is consistent with an elasticity ratio argument and goes in the opposite direction to the prediction of the viscosity ratio model.

5.4.2 A Conceptual Mechanism for the Formation of Dual Phase Continuity Compatible Binary System (Type I)

The compatible binary system possesses a low interfacial tension (interfacial tension is in the range between 0.7 and 1.0 mN/m). This low interfacial tension value (five times less than the non-compatible binary system) results in a large capillary number [30, 31] (Equation (5.5)) and long breakup times [30, 31] (Equation (5.6)).

$$Ca = \frac{\eta_m \dot{\gamma} R}{\sigma} \tag{5.5}$$

where η_m is the matrix viscosity, σ is the interfacial tension, $\dot{\gamma}$ is the shear rate and R is the radius of the drop.

$$t_b = \frac{2\eta_m R_o}{\Omega_m \sigma} \ln\left(\frac{0.82 R_o}{\alpha_o}\right) \tag{5.6}$$

where α_o is the initial distortion amplitude, R_o is the initial radius of the thread, and Ω_m is a function related to viscosity ratio. Evidence of long breakup times is shown in Figure 5.3 where it is demonstrated that HDPE/SEBS2 broke up only after 3 hours under static conditions. Although static breakup of capillary instabilities is not the same as in the

dynamic situation, it gives an indication of tendencies. Such a system should readily deform into a stable thread during melt mixing as observed by a number of authors [12, 13, 25]. In such a case the thread lifetime is expected to be longer than the droplet lifetime even at low dispersed phase concentrations. Thread and droplet lifetimes can be defined as the time with which the particular shape is observed during the full course of melt mixing. The thread and droplet lifetimes can be directly related to the frequency at which they appear in blend systems. The longer the lifetime of the thread or droplet, the higher the respective frequencies. Direct evidence of long thread lifetimes or higher frequencies at low dispersed phase concentration is demonstrated in Figure 5.17a where the matrix phase of the 5 HDPE/95 SEBS1 blend is dissolved away and the dispersed phase is visualized by SEM after a combination of centrifugation and filtration as explained in the Experimental. The micrograph of 5 HDPE/95 SEBS1 in Figure 5.17a clearly shows that the dispersed phase is in an elongated fiber form. It was impossible to carry out the 5 SEBS1/95 HDPE experiment since there was no way to dissolve the matrix without dissolving the dispersed phase. Nevertheless all the features of low interfacial tension resulting in a high capillary number and long breakup times are equally present in the 5 HDPE/95 SEBS1 or 5 SEBS1/95 HDPE samples. In the case where the thread lifetime is greater than the droplet lifetime, continuity will develop principally through thread-thread coalescence. Figure 5.14 gives a schematic illustration of this process. For the case of stable threads, coalescence is limited locally to the crossover points as observed by Willemse et al. [12] This type of system would be expected to demonstrate the onset of percolation phenomena at low composition; full continuity of the minor phase would be attained at low composition; co-continuity would be maintained over a wide composition range; and the pore size of the blend would change little with increasing minor phase concentration. Increasing the concentration would result in a more dense three-dimensional network of identical pore size. These expectations fit the experimental observations from the results section on every point.

Non-compatible Binary System (Type II)

The non-compatible HDPE/PS binary blend system has a high interfacial tension of about 5.6 mN/m.[5] In such a case, droplet splitting, as opposed to capillary formation, should be a prominent mechanism [30, 31] Even if some capillary breakup does occur, the thread lifetime in this system would be substantially lower than the compatible binary system. It can be reasonably assumed for such a system at low concentration that the droplet frequency > thread frequency during melt mixing.

Direct evidence of the prominence of droplets at low concentration is demonstrated through the same matrix dissolution technique discussed above. Figure 5.17b clearly shows that in the 5 HDPE/95 PS blend a spherical dispersed phase morphology dominates. Fiber formation and continuity development in such a case is then principally developed through droplet-droplet coalescence. Figure 5.15 schematically demonstrates this process. A number of studies have shown the contribution of droplet/droplet coalescence to fiber formation for this interface type.[27, 32] The expected features of such a system would be that percolation phenomena occur at higher composition than in Type I; full continuity would be maintained in a narrower composition range than in Type I; and the pore size of the blend would increase significantly with %minor phase in the usual fashion [8, 33-35] due to droplet - droplet coalescence. These predictions also exactly fit the experimental observations for the Type II system.

Compatible Ternary System (Type III)

The compatibilized ternary system (HDPE/PS/SEBS1) possesses a low static interfacial tension of about 1 mN/m. At first glance one might be tempted to analyze it in the same fashion as the compatible binary blend system. The situations however, are not the same. During the melt mixing of a ternary system possessing an interfacial modifier, an initially interfacially saturated droplet is readily deformed, however, fresh interface is developed during deformation. This situation is schematically illustrated in Figure 5.16. Under dynamic conditions if, for example, a spherical droplet deforms into an extended body with an aspect ratio of 4, that ellipsoid has 4 times more interfacial area than the

equivalent volume sphere. If it is assumed that the time required to saturate the fresh thread interface is >> the thread breakup time, then the compatible ternary system actually more closely resembles the non-compatible binary case (droplet lifetime > thread lifetime) than the compatible binary one.

Direct evidence of the prominence of droplets at low concentration for the Type III interface system is demonstrated once again through the matrix dissolution technique. Figure 5.17c clearly shows that in the 5 HDPE/95 PS/20 SEBS1 blend a spherical dispersed phase morphology dominates. Fiber formation and continuity development in such a case will take place through droplet-droplet interactions. There is one major difference from the Type II case, the Type III droplet possesses interfacial modifier which results in a significant reduction in droplet/droplet coalescence. The effect of added interfacial modifier on coalescence reduction is a well-known phenomenon and has been studied extensively in the past [33-38]. The effect of copolymer on the droplet size has already been confirmed by Cigana et al. [38] in the case of dispersed phase/matrix blend systems. They observed a remarkable suppression of coalescence of the dispersed phase in 80 PS/ 20 EPR blend system with the addition of a tapered diblock copolymer. The volume average diameter of minor phase dropped from 2.7 μm to 0.5 μm.

The expected features for this case would be that percolation phenomena occur at higher composition than Type II due to diminished droplet-droplet coalescence; the region of dual phase continuity should be narrower than Type II due to reduced droplet-droplet coalescence; and a low level of change of pore size with composition is expected due to reduced droplet-droplet coalescence. The overall pore size would be expected to be greater than Type I, but less than Type II. Once again the experimental results are consistent with the expected features. A similar effect of delayed onset of percolation for a Type III system has also been observed by Bourry et al. [4] and was related to the suppression of coalescence in their co-continuous HDPE/PS system in the presence of an interfacial modifier.

5.4.3 Droplet and Thread Lifetimes

It is clear from the above discussion that the formation of stable fibers is critical to the development of continuity. Fiber stability, in turn, is developed through two basic routes, 1) deformation/disintegration phenomena and/or 2) coalescence phenomena. In this paper the observed microstructural features indicate that fiber formation in the Type I system is dominated by deformation/disintegration and demonstrate that fiber formation in the Type II and III systems is dominated by droplet coalescence. It was also shown that the particular approach to achieving continuity has profound consequences on the resulting microstructure. In this study the systems studied were chosen so as to define a clear distinction between the different interface types. The binary compatible blend possessed an interfacial tension about 5 times less than its binary incompatible counterpart. Also, a highly effective interfacial modifier was used for the compatible ternary system (static interfacial tension experiments demonstrate a five-fold decrease in interfacial tension after addition of modifier). In reality, however, when one considers all blends, a broad continuum/spectrum of interface types exists. For example, a variety of binary systems of varying compatibility is possible; incompatible binary systems of widely different interfacial tension are also possible. Also a wide range of interfacial modifiers of varying efficacy is equally a possibility. Other factors which could potentially affect fiber formation during mixing are the type of flow field (an elongational flow field is much more effective in deforming the dispersed phase than shear flow fields) and viscosity ratio. Considering all the potential factors influencing fiber formation in polymer blends, it is clear that a basic parameter classifying the relative balance between fibers and droplets under a given condition would be very useful.

Thread Frequency Ratio

In order to be able to better understand fiber formation in polymer blends, we define a thread frequency ratio (TFR) as:

$$TFR = t.f./(t.f.+d.f.) \qquad (5.7)$$

where t.f. is the thread frequency and d.f. is the droplet frequency. TFR=0 for a blend entirely composed of droplets; TFR=1 for a blend entirely composed of fibers; and TFR=0.5 indicates equal amounts of droplets and fibers. The dependence of TFR with concentration should be quite different for each of the three blend interface systems studied in this paper. In fact by definition all types of polymer blends will demonstrate a TFR = 1 at some given concentration since all blends demonstrate co-continuity. It is possible to trace the generalized dependence of the thread frequency ratio for the three different categories of polymer blend interfaces. This is shown in Figure 5.17. The Type I binary compatible blend will demonstrate a thread frequency ratio of 1 which is independent of concentration (it should be noted that the onset of continuity can still be significantly influenced in the latter case by the extent of deformation or aspect ratio of a given system). The Type II incompatible high interfacial tension blend would have a TFR at low concentrations equal to 0. As concentration increases and coalescence substantially contributes to fiber formation, a transition occurs and the thread frequency ratio begins to tend towards 1. The Type III compatibilized ternary system will experience the transition from a TFR of 0 towards 1 at a higher concentration due to significantly reduced coalescence. In Figure 5.18, the matrix dissolution technique is used to demonstrate the influence of composition on the TFR for the HDPE/PS/SEBS1 system. A gradual increase in the TFR with composition is observed showing the expected trends for a system where co-continuity development is dominated by coalescence phenomena

5.4.4 Microstructures of Diblock vs. Triblock Copolymer in the Compatible Binary Blends

As shown in Figure 5.8, the pore size of HDPE/SEB1 is about half that of HDPE/SEBS1. Table 5.2 indicates that the viscosity ratio between SEBS1 and SEB1 are different. In order to determine if the viscosity ratio is controlling this observed effect on microstructure, blends with a high molecular weight diblock copolymer, SEB2 (M_n = 187,000, containing 26% styrene, referred as SEB2) were prepared and the specific surface area was tested. Table 5.5 lists the specific surface area of the samples. The 50HDPE/50SEB2 blend possesses a surface area of 10.74 m^2/g. It should be noted that in

this case only 80% copolymer was removed (because of the high molecular weight) during extraction and a corrected value of 13.43 m^2/g based on 100% extraction was estimated. This is virtually identical to the surface area value for 50 HDPE/50 SEB1 (13.15m^2/g). The specific surface area of 40 HDPE/60 SEB2 is 13.15 m^2/g. Considering that only 86% copolymer was removed (the same reason mentioned above) during extraction, a corrected value of 15.23.m^2/g based on 100% extraction was estimated. The corrected specific surface area of 40 HDPE/60 SEB2 is identical to the specific surface area of 40 HDPE/60 SEB1 (16.00 m^2/g) as well. Since surface area is related to pore size through volume fraction, these results clearly indicate that the viscosity ratio has little effect on microstructure. This supports previous results on dispersed phase/matrix systems where the role of viscosity ratio on morphology was significantly moderated after addition of an interfacial modifier [34]. Having eliminated the possible influence of viscosity ratio, it appears that the finer structure of the HDPE/SEB1 blend, compared to HDPE/SEBS1 blend, is due primarily to the molecular architecture of the copolymer. An explanation for this effect of architecture on microstructure is the subject of current study.

5.5 Conclusions

In this paper three different categories of blend interfaces are examined systematically in order to isolate the role of the interface in the development of co-continuous morphologies during melt mixing. They are: Type I) compatible binary blends based on HDPE/SEBS1 and HDPE/SEB1; Type II) an incompatible binary system comprised of HDPE/PS; and Type III) compatible ternary systems comprised of HDPE/PS compatibilized by SEBS1 in one case and by SEB1 in another. It is found that the co-continuous morphologies for the Type I compatible binary blend systems exist over a very wide composition range (from 30% copolymer to 68% copolymer) and that the %continuity - composition relationship is identical for both the triblock and diblock binary blends. However, the scale of the morphology is much finer for the blend with diblock copolymer. The usual viscosity ratio models used to predict the region of co-continuity of blends could not describe these systems due to the breadth of the dual phase

continuity region. Nevertheless, it is shown that the viscosity ratio of the low interfacial tension binary blends has no effect on either the composition region of co-continuity or the microstructure of the co-continuous blend.

The Type II, non-compatible HDPE/PS blend, possesses a narrower region of dual phase continuity (from 40% PS to 66% PS) than the Type I compatible binary blends and the Type III, compatible ternary blend system, demonstrates the narrowest region of co-continuity (from 45% PS to 64% PS) of all three. Furthermore, the non-compatible HDPE/PS blend system shows a clear dependence of pore size on phase concentration, while the Type I and Type III interface systems maintain an essentially constant pore size over a wide range of phase concentrations. The wide region of dual phase continuity for the Type I, compatible binary blends, is consistent with an argument based on the formation of highly stable elongated structures during melt mixing. The low interfacial tension of those systems results in very effective deformation of the dispersed phase followed by long breakup times.

Using general arguments based on thread lifetime vs. droplet lifetime during melt processing, a mechanism for the formation of dual phase continuity is proposed. For the Type I compatible binary system with low interfacial tension, the continuity development and microstructural features are consistent with a mechanism dominanted by thread-thread coalescence (thread lifetime>droplet lifetime), while the formation and morphology of the co-continuous Type II non-compatible binary system with high interfacial tension is consistent with a mechanism controlled by droplet-droplet coalescence (droplet lifetime>thread lifetime). In the Type III compatible ternary system, the continuity development and microstructure are controlled by reduced droplet-droplet coalescence. This latter case is considered to be only partially compatibilized due to the generation of fresh interface during the deformation process and hence it can be still be considered that droplet lifetime>thread lifetime. Nevertheless, due to the partial emulsification, the droplet coalescence process is significantly reduced. The relative presence of fibers or droplets during dynamic mixing is confirmed and analysed quantitatively using a matrix dissolution/image analysis technique.

It is clear from the above discussion that the formation of stable fibers is critical to the development of continuity. Fiber stability, in turn, is developed through two basic routes, 1) deformation/disintegration phenomena and/or 2) coalescence phenomena. In this paper the observed microstructural features indicate that fiber formation in the Type I system is dominated by deformation/disintegration followed by thread-thread coalescence and demonstrate that fiber formation in the Type II and III systems is dominated by droplet-droplet coalescence. It was also shown that the particular approach to achieving continuity has profound consequences on the resulting microstructure. A thread frequency ratio (TFR) is proposed as a basic general parameter to classify the relative presence of fibers to droplets during mixing and hence the type of continuity development and microstructure expected for a given system.

5.6 References and notes

(1) Avgeropoulos, G. N; Weissert, F. C.; Biddison, P. H; and Bohm, G. G. A. *Rubber Chem. Technol.* **1976**, 49, 93.

(2) Jordhamo, G. M.; Manson, J. A.; Sperling, L. H. *Polym. Eng. Sci.* **1986**, 26, 517.

(3) Favis, B. D.; Chalifoux, J. P. *Polymer* **1988**, 29, 1761.

(4) Bourry, D.; Favis, B. D. *J. Polym. Sci., Polym. Phys.* **1998**, 36, 1889.

(5) Mekhilef, N.; Favis, B. D.; Carreau, P. J. *J. Polym. Sci., Polym. Phys.* **1997**, 35, 293.

(6) Mekhilef, N.; Verhoogt, H.; *Polymer* **1996**, 37, 4069.

(7) Li, J.; Favis, B. D. *Polymer*. in press.

(8) Lyngaae-Jorgensen, J.; Utracki, L. A. *Makromol. Chem., Makromol., Symp.* **1991**, 48/49, 189.

(9) Paul, D. R.; Barlow, J. W. *J. Macromol. Sci., Rev. Macromol. Chem.* **1980**, C18, 109.

(10) Utracki, L.A. *J. Rheol.* **1991**, 35, 1615.

(11) Metelkin, V. I.; Blekht, V. S. *Colloid J. USSR* **1984**, 46, 425.

(12) Willemse, R. C.; Posthuma de Boer, A.; Van Dam, J.; Gotsis, A. D. *Polymer* **1998**, 39, 5879.

(13) Veenstra, H., van Lent, B. J. J., van Dam, J., Posthuma de Boer, A., Polymer, **1999**, 40, 6661.

(14) Miles, I. S.; Zurek, A. *Polym. Eng. Sci.* **1988**, 28, 796.

(15) Tchoudakov, R.; Breuer, O.; Narkis, M.; Siegmann, A. *Polym. Eng. Sci,* **1996**, 36, 1336.

(16) Levon, K.; Marglina, A.; Patashinsky, A. Z. *Macromolecules* **1993**, 26, 4061.

(17) Gubbles, F.; Jérôme, R.; Teyssié, Ph.; Vanlathem, E.; Deltour, R.; Calderone, A.; Parenté, V.; Brédas, J. L. *Macromolecules* **1994**, 27, 1972.

(18) Verhoogt, H.; van Dam, J.; Posthuma de Boer, A. *Adv. Chem. Ser.* **1994**, 239, 333.

(19) Elemans, P. H. M.; Janssen, J. M. H.; and Meijer, H. E. H. *J. Rheol.* **1990**, 34, 1311.

(20) Chapleau, N.; Favis, B. D.; Carreau, P. J. *J. Polym. Sci, Polym. Phys.* **1998**, 36, 1947.

(21) Lepers, J-C.; Favis, B. D. *J. Polym. Sci, Polym. Phys.* **1999**, 37, 939.

(22) Willis, J. M.; Caldas, V.; Favis, B. D. *J. Mater. Sci.*, **1991**, 26, 4742.

(23) Bourry, D., Master's thesis, École Polytechnique de Montréal, **1995**.

(24) Rayleigh, L. *Proc. London Math. Soc.* **1879**, 10, 4.

(25) Tomotika, S. *Proc. R. Soc.* **1935**, A150, 322.

(26) Saltikov, S. A. *Proceedings of the 2nd International Congress for Stereology*, Helias: New York, **1967**.

(27) Favis, B. D.; Chalifoux, J. P. *Polymer* **1988**, 29, 1761.

(28) Van Oene, H. *J. Colloid Interface Sci.*, **1972**, 40, 448.

(29) Favis, B. D., *Makromol. Chem., Macromol. Symp.* **1992**, 56, 143.

(30) Taylor, G. I. *Proc. R. Soc.London*, **1932**, A138, 41.

(31) Taylor, G. I. *Proc. R. Soc.London*, **1932**, A138, 41.

(32) Elmendorp, J. J.; Van der Vegt, A. K.; *Polym. Eng. Sci.* **1986**, 26, 1332.

(33) Fortelny, I.; Michalkova, D.; Koplikova, J.; Navratilova, E.; Kovar, J. *Angew. Makromol. Chimie* **1990**, 179, 185.

(34) Fayt, R.; Jérôme, R.; Teyssié, Ph. *Makromol. Chem.* **1986**, 187, 837.

(35) Fayt, R.; Jérôme, R.; Teyssié, Ph. *J. Polym. Sci., Polym. Lett.*, **1986**, 24, 25-28.

(36) Fayt, R.; Harrats, C.; Blacher, S.; Jérôme, R.; Teyssié, Ph. *Polym. Mater. Sci. Eng.* **1993**, 69, 178.

(37) Matos, M.; Favis, B. D.; Lomellini, P. *Polymer* **1995**, 36, 3899.

(38) Cigana, P.; Favis, B. D.; Jérôme, R. *J. Polym. Sci., Polym. Phys.* **1996**, 34, 1691.

Figure captions

Figure 5.1 Complex viscosity-frequency/shear rate relationship for SEB1, SEBS1, SEBS2, HDPE and PS at 195°C.

Figure 5.2 Storage modulus-frequency relationship for SEB1, SEBS1, SEBS2, HDPE and PS at 195°C.

Figure 5.3 Breakup process of a SEBS2 triblock copolymer thread imbedded in a HDPE matrix at 195°C, (A) 30 min., (B) 90 min., (C) 120 min., and (D) 180 min.

Figure 5.4 Relative distortion amplitude versus time for SEBS2 triblock copolymer imbedded in a HDPE matrix.

Figure 5.5 Continuity-composition relationship for HDPE/SEB1 and HDPE/SEBS1 blends. The arrow indicates the disintegration point for two blend systems.

Figure 5.6 (a) Schematic illustration of continuity and dual phase continuity development for three different blend systems. I: compatible binary system, II: non-compatible binary blend system and III: compatible ternary system. The arrows stand for the disintegration points for three blend systems during extraction. HDPE/SEBS1 disintegrates at 70% PS (solid arrow), HDPE/PS at 68% PS (thick dash arrow) and HDPE/PS/SEBS1 at 66% PS (fine dash arrow).

Figure 5.6 (b) Expanded view showing the continuity/composition relationship for HDPE/SEBS1, HDPE/PS and HDPE/PS/SEBS1 blends.

Tables

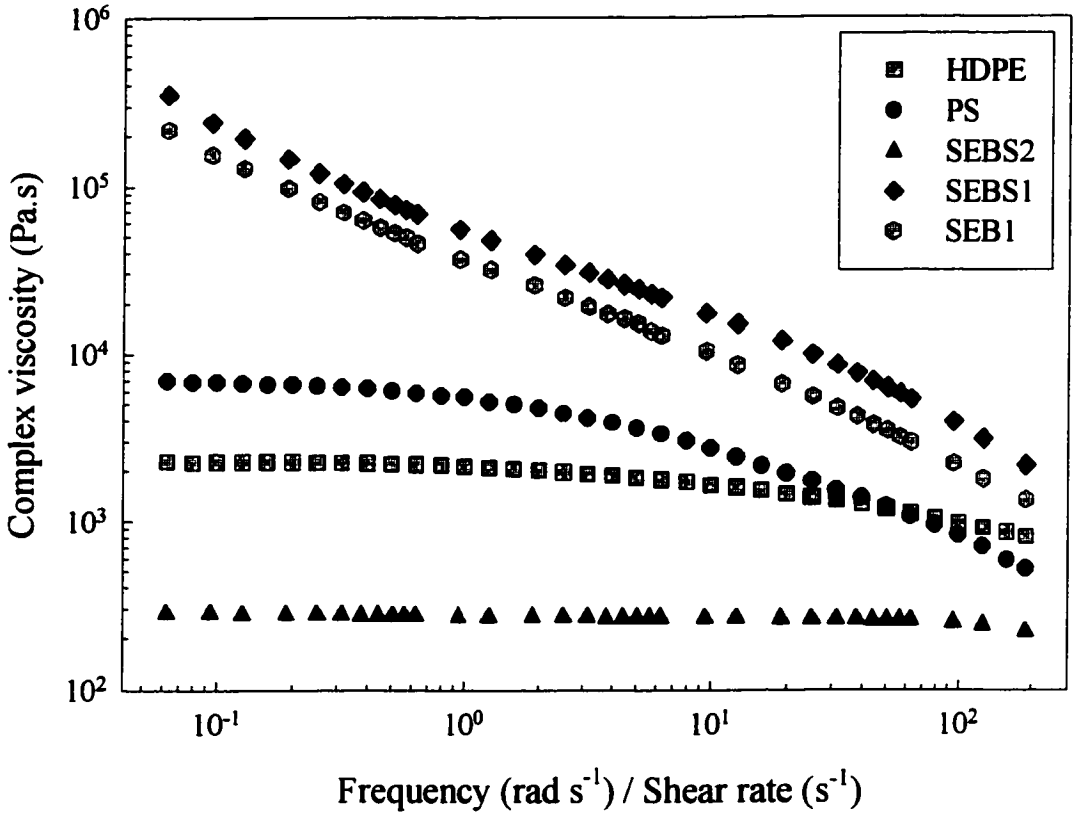

Figure 5.1 Complex viscosity-frequency/shear rate relationship for SEB1, SEBS1, SEBS2, HDPE and PS at 195°C.

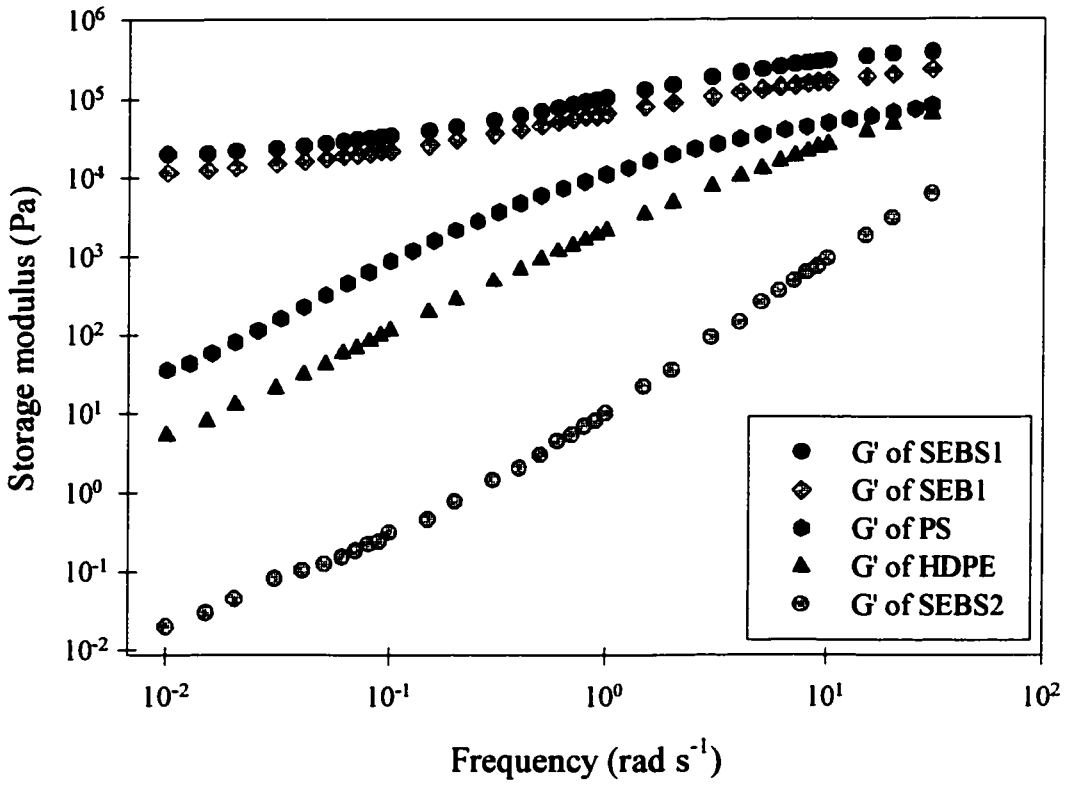

Figure 5.2 Storage modulus-frequency relationship for SEB1, SEBS1, SEBS2, HDPE and PS at 195°C.

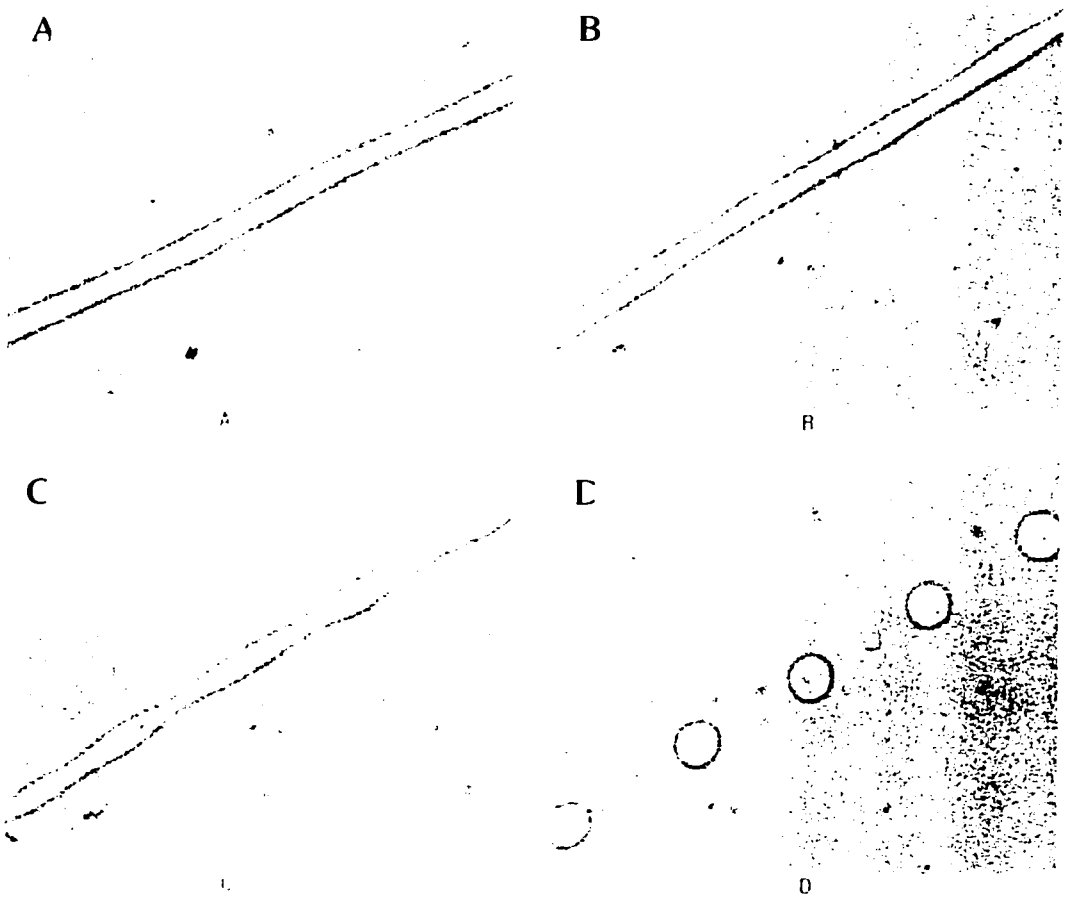

Figure 5.3. Breakup process of a SEBS2 triblock copolymer thread imbedded in a HDPE matrix at 195°C, (A) 30 min., (B) 90 min., (C) 120 min., and (D) 180 min.

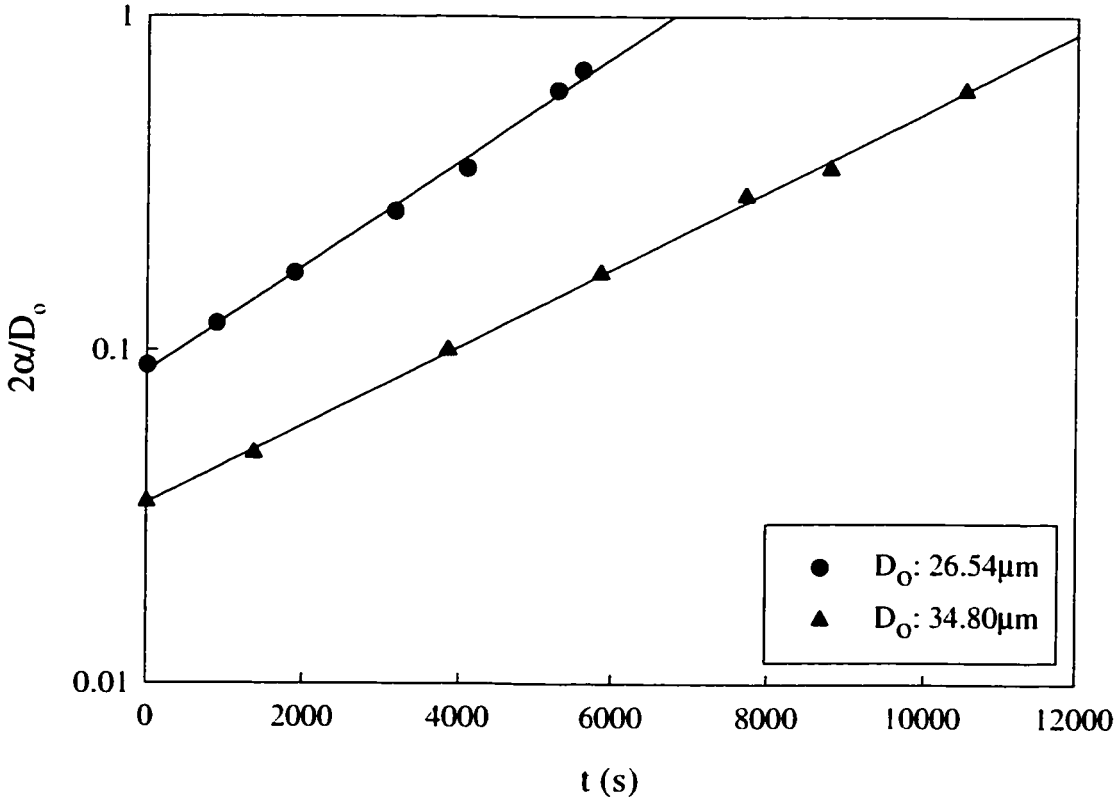

Figure 5.4 Relative distortion amplitude versus time for SEBS2 triblock copolymer imbedded in a HDPE matrix.

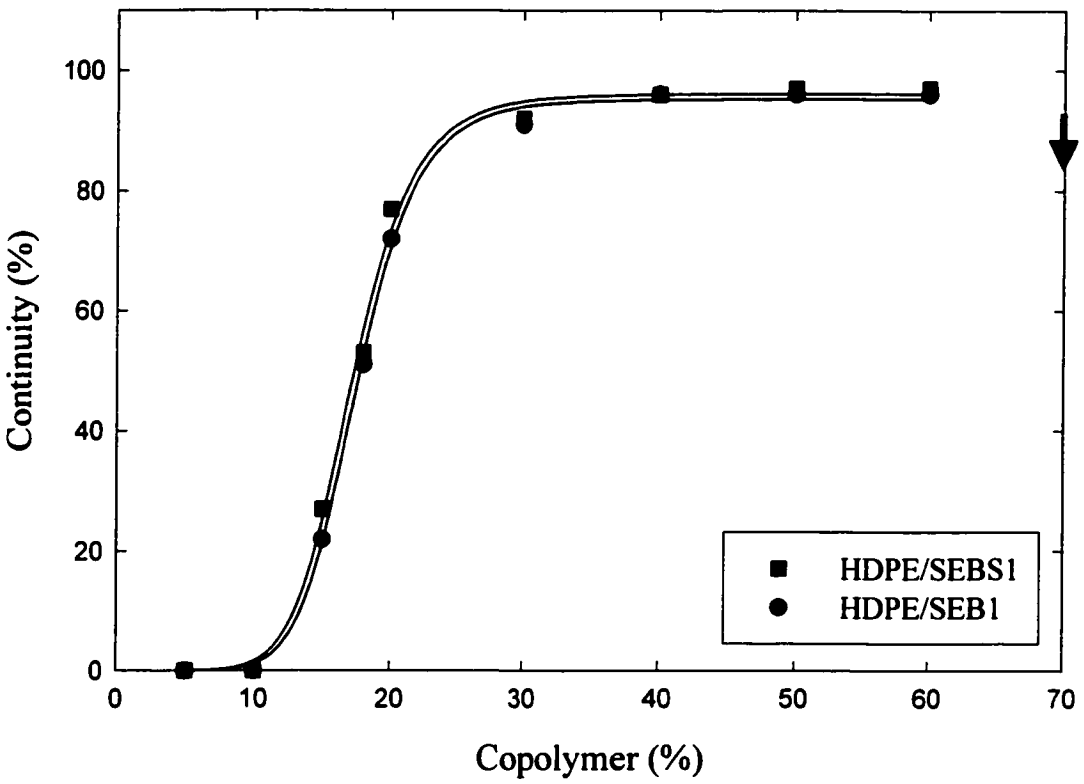

Figure 5.5. Continuity-composition relationship for HDPE/SEB1 and HDPE/SEBS1 blends. The arrow indicates the disintegration point for two blend systems.

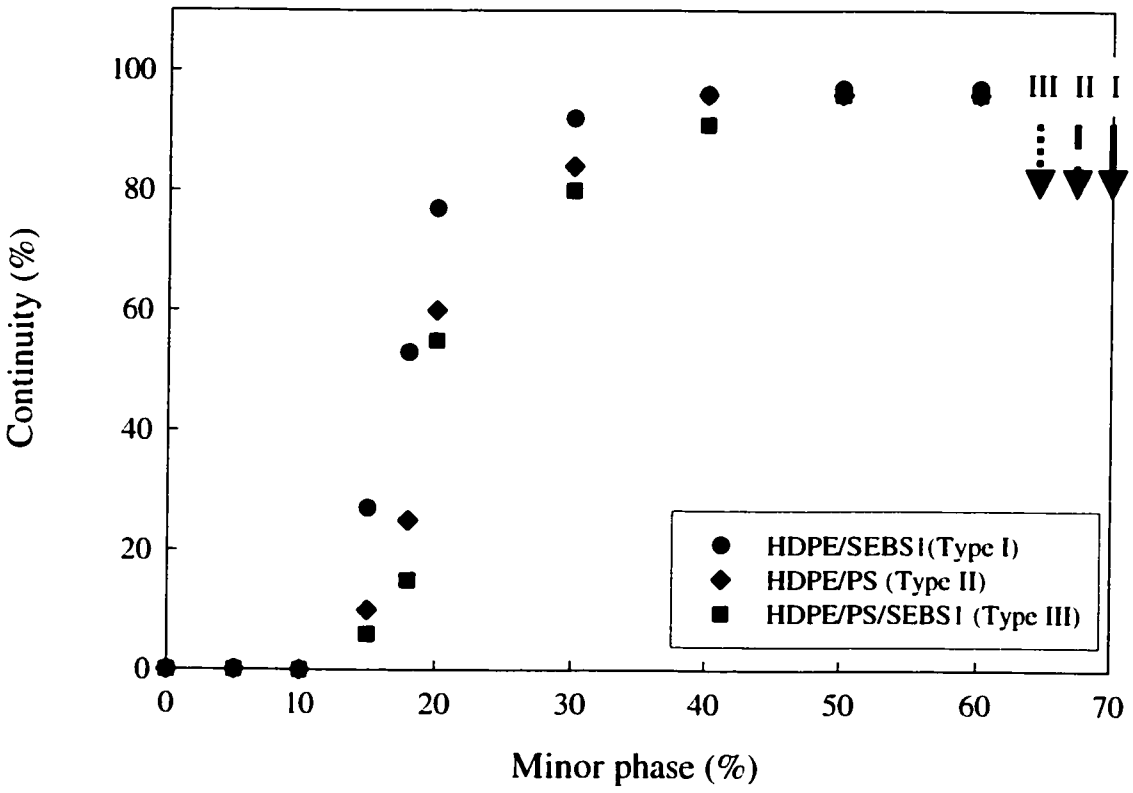

Figure 5.6 (a) Schematic illustration of continuity and dual phase continuity development for three different blend systems. I: compatible binary system, II: non-compatible binary blend system and III: compatible ternary system. The arrows stand for the disintegration points for three blend systems during extraction. HDPE/SEBS1 disintegrates at 70% PS (solid arrow), HDPE/PS at 68% PS (thick dash arrow) and HDPE/PS/SEBS1 at 66% PS (fine dash arrow).

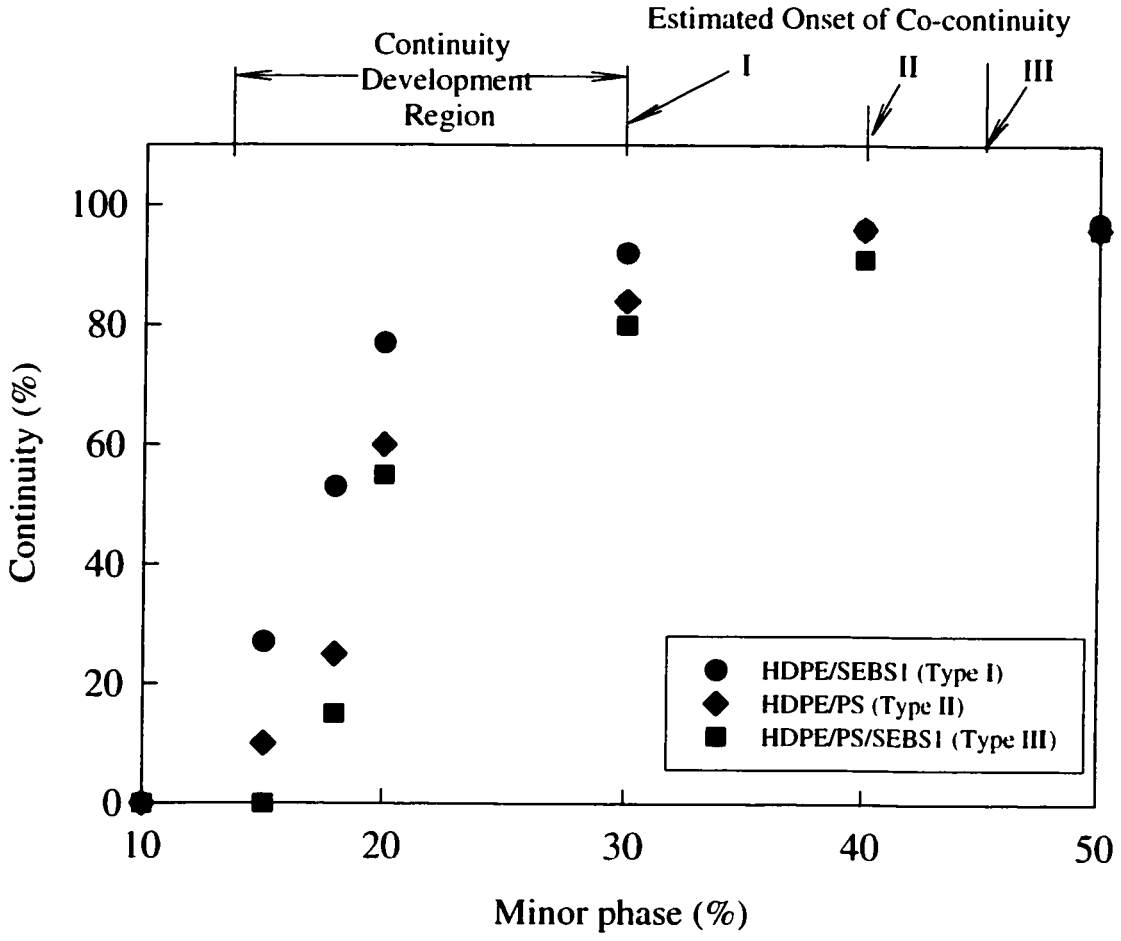

Figure 5.6b Expanded view showing the continuity/composition relationship for HDPE/SEBS1, HDPE/PS and HDPE/PS/SEBS1 blends.

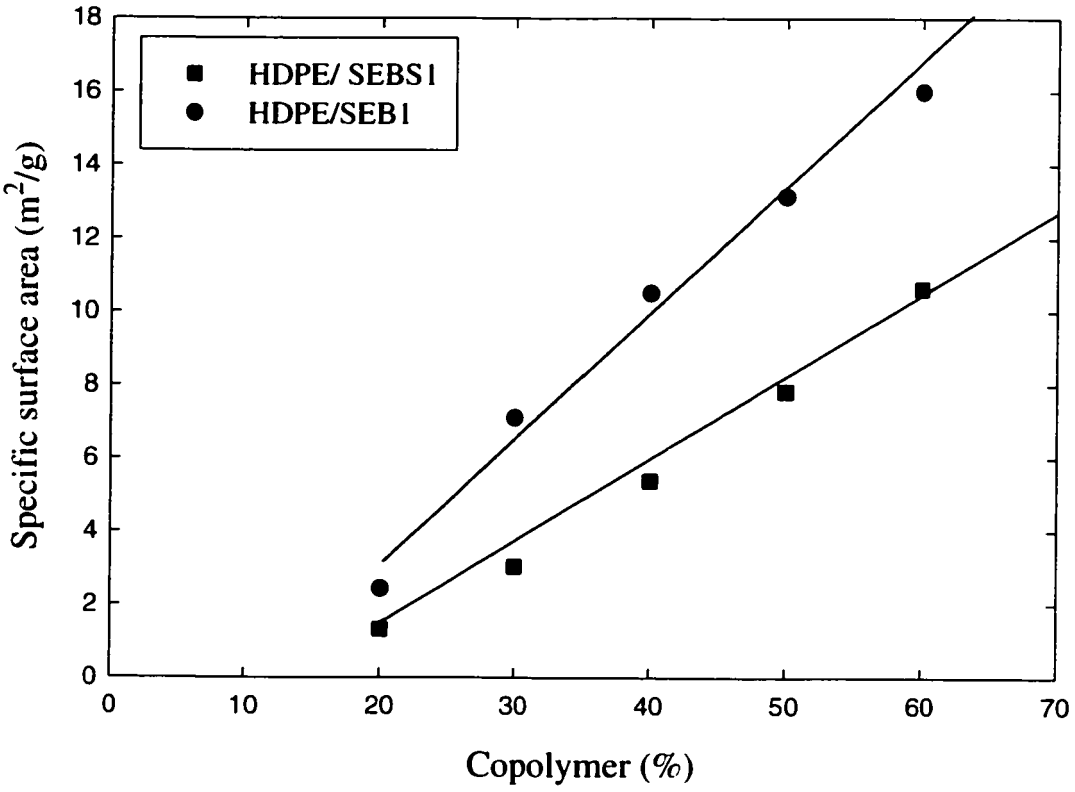

Figure 5.7 Dependence of specific surface area to copolymer amount for extracted HDPE/SEB1 and HDPE/SEBS1 blends.

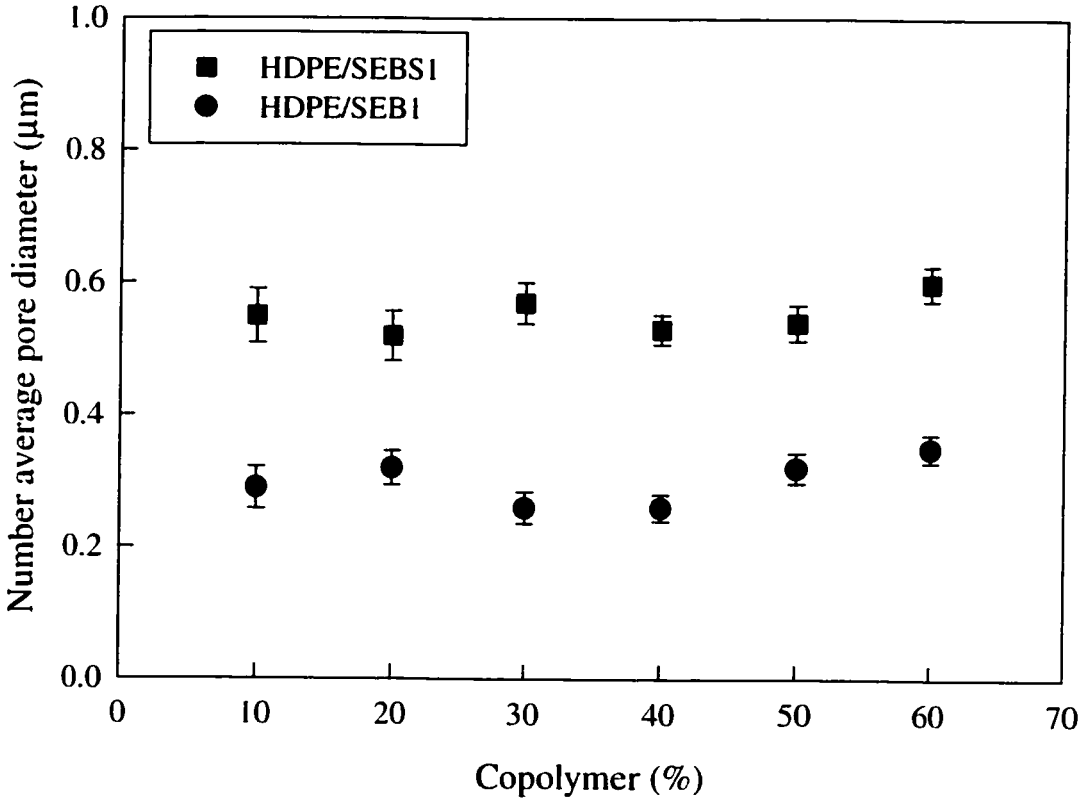

Figure 5.8 Pore size of extracted HDPE/SEB1 and HDPE/SEBS1 blends versus copolymer concentration.

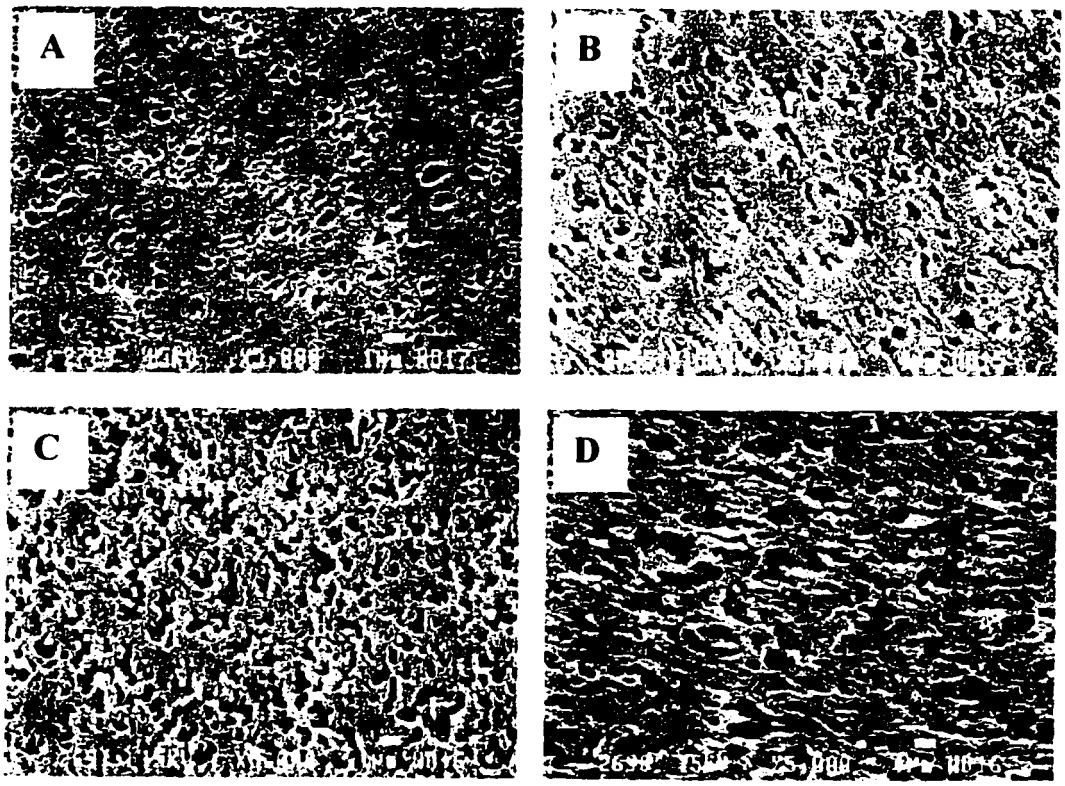

Scale bar: _ 1μm

A. 70 HDPE/30 SEBS1 B. 60 HDPE/40 SEBS1
C. 50 HDPE/50 SEBS1 D. 40 HDPE/60 SEBS1

Figure 5.9 SEM micrographs for HDPE/SEBS1 blends at 195°C.
(A) 70 HDPE/30 SEBS1, (B) 60 HDPE/40 SEBS1,
(C) 50 HDPE/50 SEBS1 and (D) 40 HDPE/60 SEBS1.

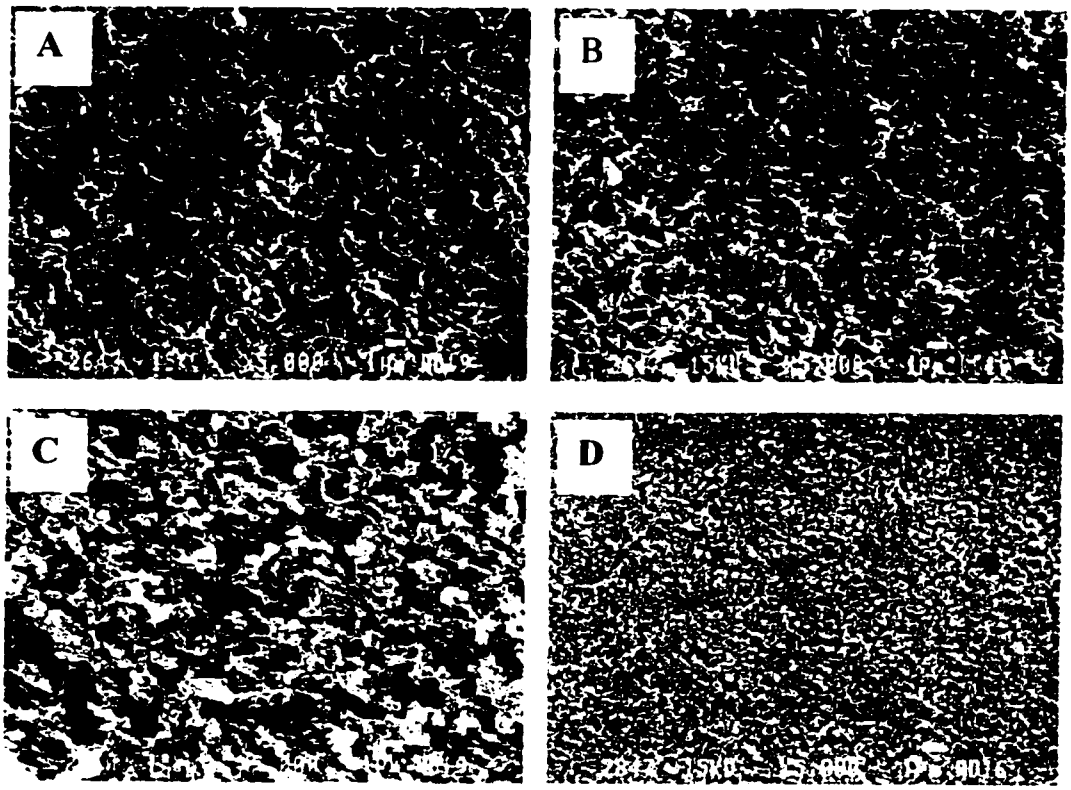

Scale bar: – 1μm

A. 70 HDPE/30 SEB1 B. 60 HDPE/40 SEB1
C. 50 HDPE/50 SEB1 D. 40 HDPE/60 SEB1

Figure 5.10 SEM micrographs for HDPE/SEB1 blends at 195°C. (A) 70 HDPE/30 SEB1, (B) 60 HDPE/40 SEB1, (C) 50 HDPE/50 SEB1 and (D) 40 HDPE/60 SEB1.

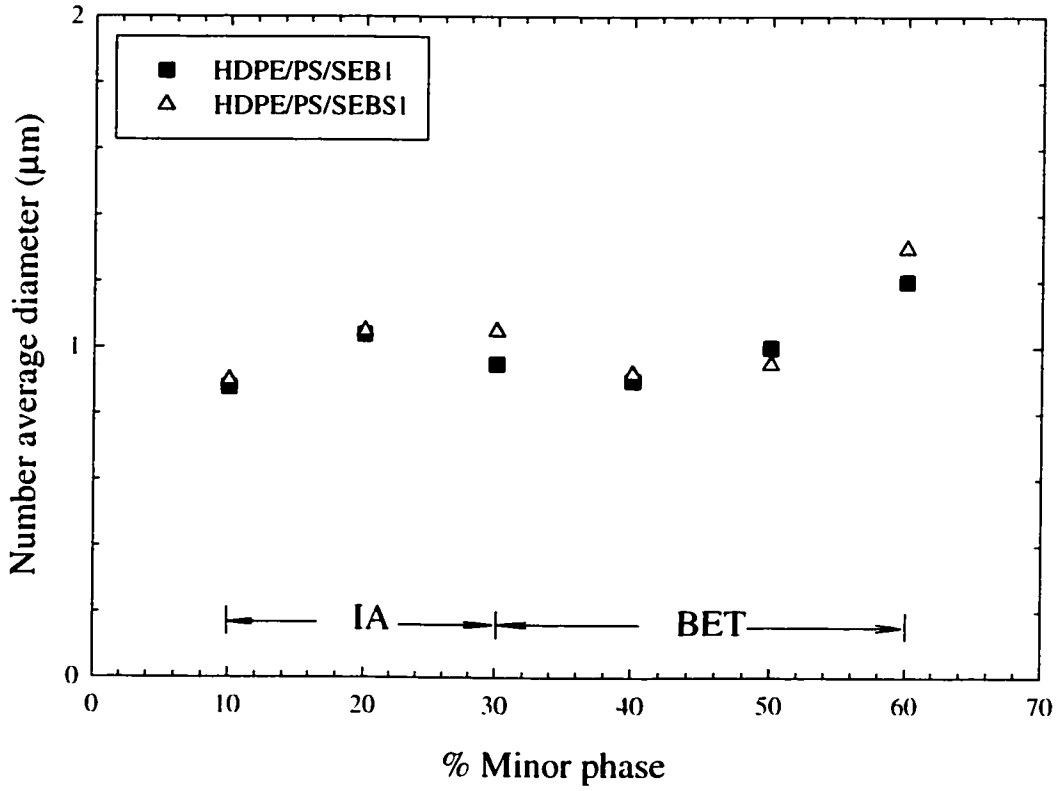

Figure 5.11 Pore size-composition relationship for HDPE/PS/SEBS1 and HDPE/PS/SEB1 blends.

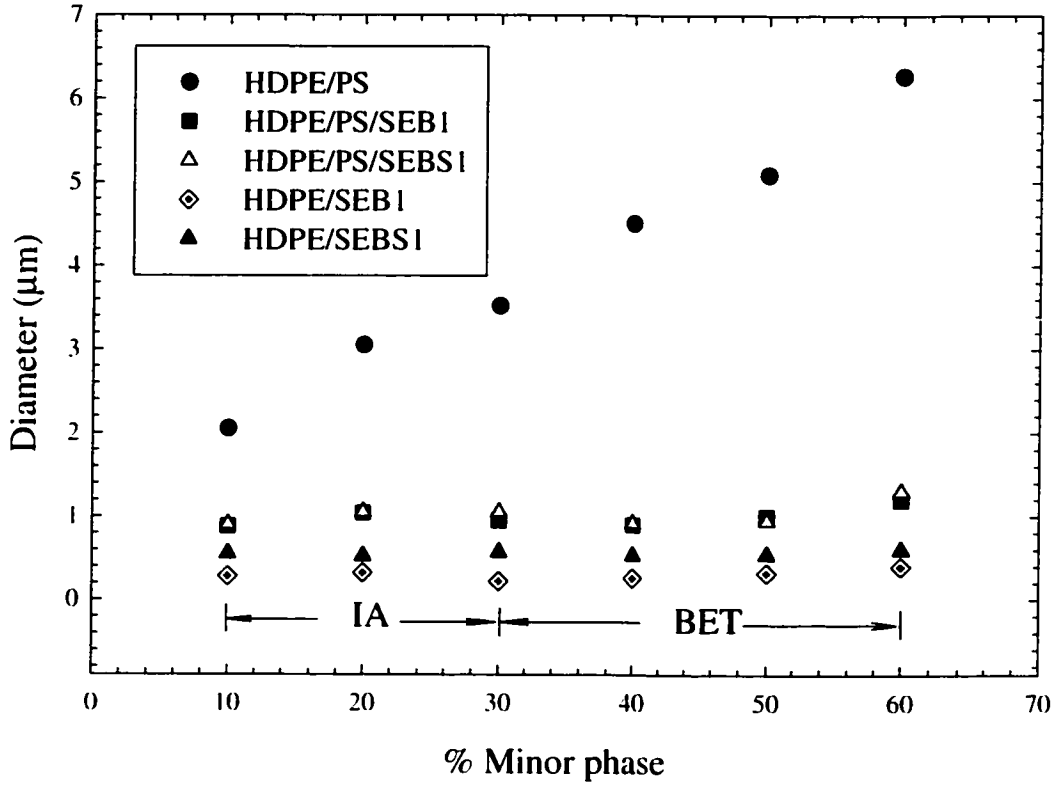

Figure 5.12 Pore size-composition relationship for HDPE/SEB1, HDPE/SEBS1, HDPE/PS, HDPE/PS/SEB1, and HDPE/PS/SEBS1 blends.

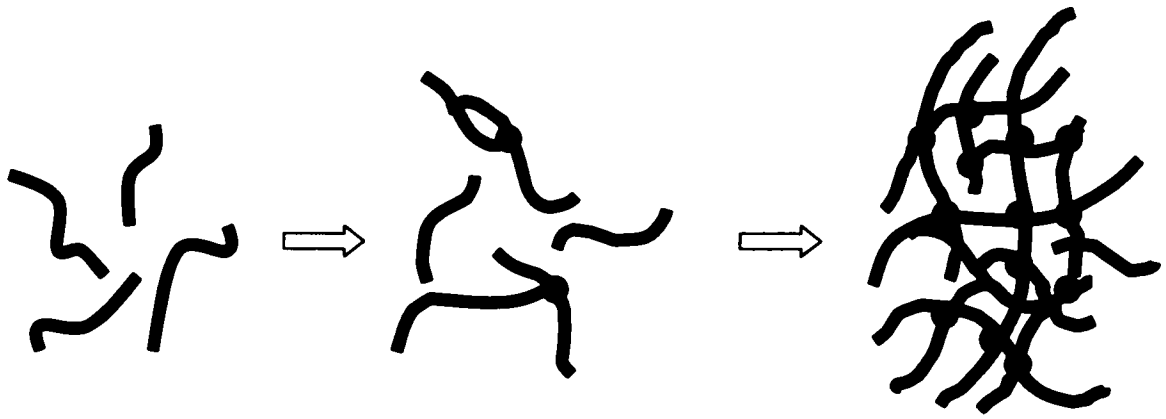

Figure 5.13 Schematic illustration of the development of co-continuity via thread-thread coalescence. This phenomenon occurs when the thread lifetime >> droplet lifetime (at low dispersed phase volume fraction) during melt mixing.

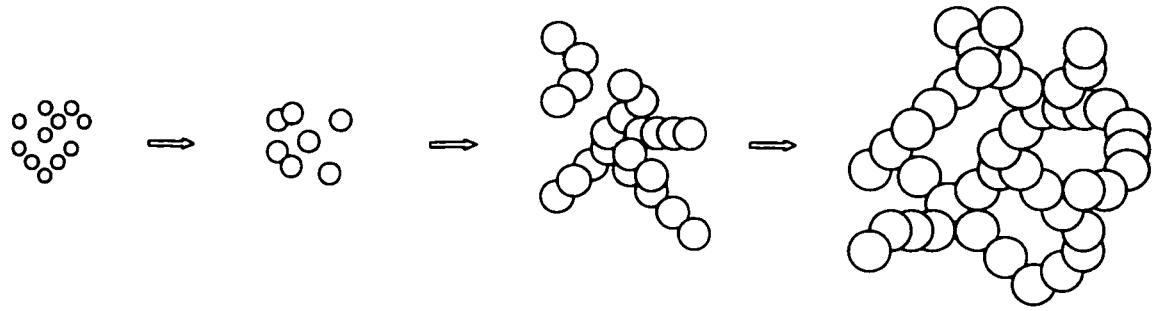

Figure 5. 14. Schematic illustration of development of co-continuity via droplet-droplet coalescence. This phenomenon takes place when the droplet lifetime >> thread lifetime (at low dispersed phase volume fraction) in a non-compatible binary blend system with high interfacial tension.

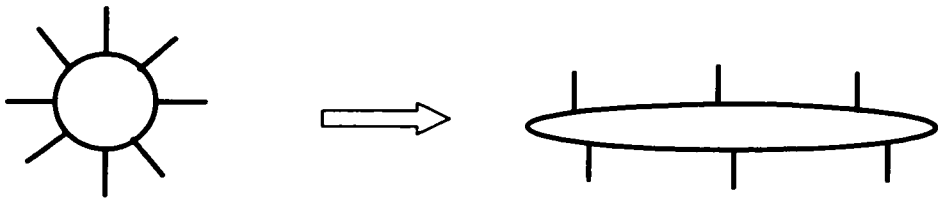

Figure 5.15 Schematic illustration of formation of co-continuity for the compatible ternary system. The saturated droplet saturated with interfacial modifier is deformed, and fresh interface is developed. If the time to emulsify the fresh interface is less than the time for breakup then this system also represents the case of droplet lifetime>thread lifetime (at low dispersed phase volume fraction).

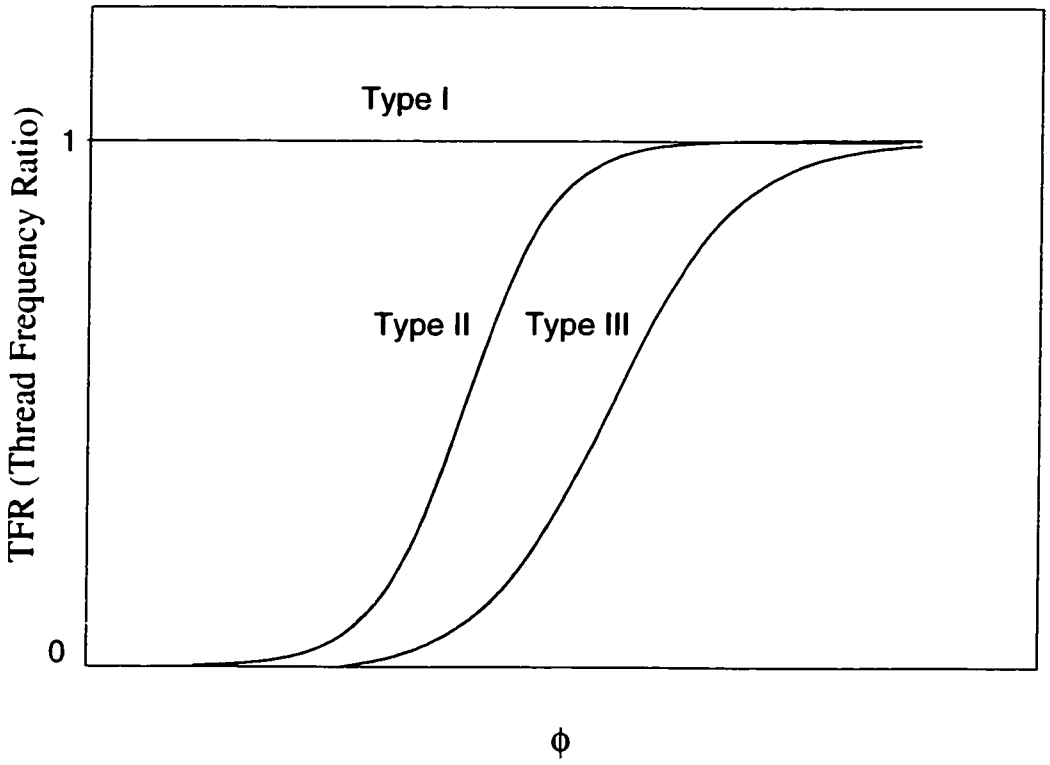

Figure 5.16 Schematic illustration of thread frequency ratio vs volume fraction for the three types of blend interfaces

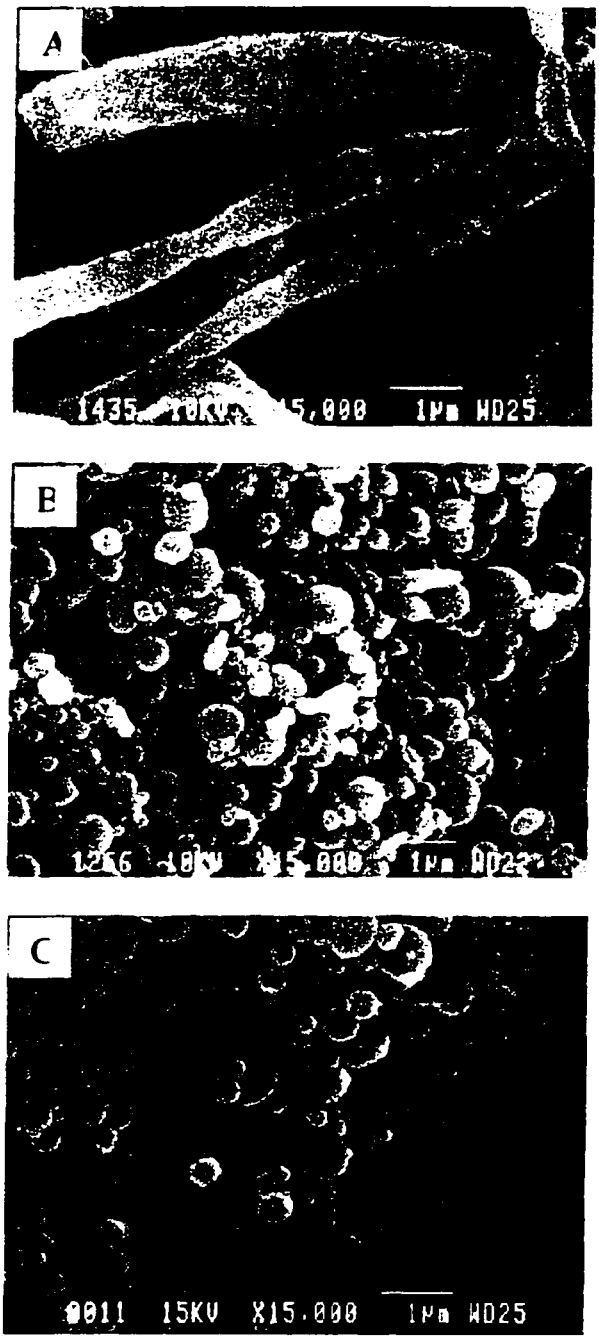

Scale bar: —— 1μm

Figure 17 SEM photomicrographs of the dispersed HDPE phase after the matrix dissolution technique: (a) 5 HDPE/95 SEBS1 (Type I); (b) 5 HDPE/95 PS (Type II); and (c) 5 HDPE/95 PS/20 SEBS1 (Type III).

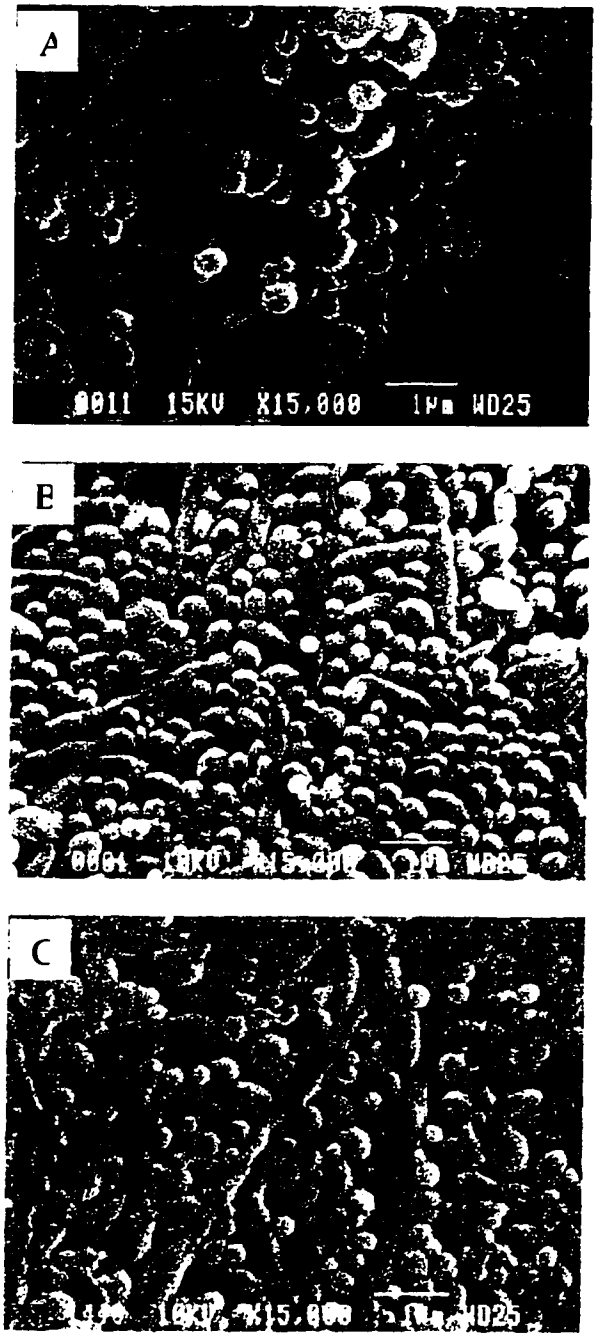

TFR = 0.07

TFR = 0.12

TFR = 0.18

Scale bar: ——— 1μm

Figure 5.18 SEM photomicrographs of the dispersed HDPE phase and the corresponding TFR data after the matrix dissolution technique for a Type III system: (a) 5 HDPE/95 PS/20 SEBS1; (b) 10 HDPE/90 PS/20 SEBS1; and (c) 20 HDPE/80 PS/20 SEBS1.

Table 5.1. Characteristic properties of the materials

	Polystyrene	Polyethylene	SEBS1
M_w	215,000	79,000	---
M_n	100,000	24,000	S=7500 EB=35000 Composition: 30% styrene
Density (20°C) (g/ml)	1.04	0.962	0.910
Density (195°C) (g/ml)	0.974	0.754	0.820
Supplier	Dow	Dow	Shell

	SEBS2	SEB1	SEB2
M_w	---	---	---
M_n	S=3000 EB=39000 Composition: 13% styrene	S=20000 EB=47000 Composition: 30% styrene	S=48620 EB=138380 Composition 26% styrene
Density (20°C) (g/ml)	0.910	0.910	0.910
Density (195°C) (g/ml)	0.820	0.820	0.850
Supplier	Shell	Shell	Shell

Table 5.2. Viscosity and elasticity ratios for all blends studied (50 s^{-1}, T=195°C)

	η^* (Pa.s)	η_d^*/η_m^*	G' (Pa)	G_d'/G_m'
SEBS1	$6.25*10^3$	5.21	$2.77*10^5$	12.53
SEBS2	$2.56*10^2$	0.21	$6.11*10^2$	0.03
SEB1	$3.47*10^3$	2.89	$1.53*10^5$	6.92
SEB2	$5.89*10^3$	4.91	$3.46*10^5$	15.66
PS	$1.28*10^3$	1.06	$3.43*10^4$	1.55
HDPE	$1.20*10^3$		$2.21*10^4$	

Table 5.3. Torque in the Internal Mixer for PS and HDPE

Polymer	rpm	Temperature (°C)	Torque (Nm)
PS	50	195	1.96
HDPE	50	195	1.96

Table 5.4. Influence of viscosity and elasticity on the prediction of the phase inversion point of PS/HDPE

Shear Rate (s^{-1})	$\eta^*_{PS}/\eta^*_{HDPE}$	Predicted Phase Inversion [9] (ϕ_{PS})	G'_{PS}/G'_{HDPE}	Predicted Phase Inversion [4] (ϕ_{PS})
5	2.68	0.72	6.14	0.14
10	1.66	0.62	2.83	0.26
50	1.05	0.51	1.55	0.39
150	0.69	0.41	1.10	0.47
Observed:		0.4 - 0.66		0.4 - 0.66

Table 5.5. Viscosity ratio and specific surface area of HDPE/copolymer blends

Blends	Viscosity ratio at 50 s^{-1}	Specific surface area (m^2/g)
50 HDPE/50 SEB1	2.89	13.15
40HDPE/60 SEB1	2.89	16.00
50 HDPE/50 SEB2	4.91	10.74 (13.43)[a]
40 HDPE/60 SEB2	4.91	13.15 (15.23)[b]

a: corrected value (supposing that 100% of SEB2 is extracted).
b: corrected value (supposing that 100% of SEB2 is extracted).

CHAPTER 6. STRATEGIES TO MEASURE AND OPTIMIZE THE MIGRATION OF THE INTERFACIAL MODIFIER TO THE INTERFACE IN IMMISCIBLE POLYMER BLENDS***

Jianming Li, and Basil D. Favis

Centre de Recherche Appliquée Sur les Polymères (CRASP), Département de Génie Chimique, École Polytechnique de Montréal, P. O. Box 6079 Station Centre-Ville, Montréal, (QC) Canada H3C 3A7

ABSTRACT: A family of emulsification curves has been systematically prepared in order to determine the extent of interfacial modifier migration to the HDPE/PS interface. Through an examination of the evolution of the equilibrium dispersed phase size after interfacial saturation, as well as a comparison of the apparent interfacial area occupied per modifier molecule (A_{app}) (or apparent areal density (Σ_{app})) at the different dispersed phase concentrations, it is possible to detect the onset of micelle formation and to estimate the extent of interfacial coverage. This approach has been applied to polyethylene/polystyrene blends, using a variety of triblock and diblock copolymer interfacial modifiers for that system. It is shown quantitatively that it is the affinity of the block copolymer for the matrix material that dominates migration efficacy to the interface. Asymmetrical block copolymers (30PS:70EB) show a strong tendency to form micelles when HDPE is the matrix. This effect is virtually eliminated when PS is the matrix material or when symmetrical block copolymers (50PS:50EB) are used. In these latter cases all the interfacial modifier finds its way to the interface.

*** submitted for publication in Polymer

Keywords: Emulsification curve; interfacial area per copolymer molecule, micelle formation; interfacial coverage

6.1 Introduction

The addition of an appropriately tailored block copolymer to an incompatible polymer blend can have a profound effect on both the morphology and on the mechanical properties of that blend (1-11). The morphology of the blend is mainly related to the effects of the block copolymer in reducing the interfacial tension (12-14) and suppressing particle – particle coalescence (15-17). This leads to a significant reduction in dispersed phase size (5, 9, 18-21). The efficacy of a copolymer, as an interfacial modifier, for the interface of polymer blend is often characterized by an emulsification curve, which essentially follows the evolution of the dispersed phase size with copolymer composition. The shape of the emulsification curve is highly dependent on interfacial modifier type and on the processing conditions (22). The emulsification curve has been studied for several polymer blend systems (23-25) and it displays a key characteristic, an initial significant drop in the size of the dispersed phase with the addition of copolymer followed by the obtention of an equilibrium value at high concentration of copolymer. A detailed discussion of the fundamentals of the emulsification curve is given in the Results and Discussion Section.

In previous work from this laboratory, Matos et al. (5) studied blends of 90% polystyrene (PS)/10% ethylene-propylene rubber (EPR) compatibilized by commercial triblock copolymers of styrene-ethylene butylene-styrene (SEBS), styrene-butadiene-styrene (SBdS) and a star-shaped copolymer. They noted that the molecular weight of the interfacial agents did not have an effect on the critical concentration for emulsification, nor did it influence the equilibrium particle diameter. They reported that a 30PS:70 ethylene butylene triblock copolymer of 50 , 70, and 174 kg/mole occupied interfacial areas of 13, 27, and 45 nm^2/molecule respectively. They also established that triblock copolymers were more effective as compatibilizers than star-shaped copolymers.

Cigana et al. (7-9) investigated the efficacy of various diblock interfacial modifiers for the polystyrene (PS)/ethylene-propylene rubber (EPR) interface using the emulsification curve. Their results showed that at 90% PS/10%EPR and 80%PS/20% EPR, a diblock copolymer attains a similar critical concentration for interfacial saturation and equilibrium particle size on the emulsification curve. The interfacial area occupied per molecule of diblock modifier of molecular weight 67 kg/mole and composition 30%PS is identical in both cases (5.6 nm^2), despite the fact that 80%PS/20%EPR blend system contains twice as much modifier based on the total blend volume, as the 90%PS/10%EPR blend at the critical concentration. Considering the above interesting phenomenon, they proposed that almost all of the diblock modifier finds its way to the interface during melt blending. At 90%PS/10%EPR they found that a triblock copolymer is a better emulsifier than the diblock (9). However, when the amount of triblock copolymer is doubled in the 80%PS/20% blend, the equilibrium diameter of the dispersed phase increases considerably from 0.35 to 5.5 μm and the apparent interfacial area per molecule decreases from 13 to 5.6 nm^2 (5, 8). This strongly suggested that much of the SEBS in the 80%PS/20%EPR blend was either lost in the form of micelles or was monomolecularly dispersed in one or both of the phases. They concluded that micelle formation below the critical concentration was the key factor for lowering the emulsification efficacy of triblock copolymer. From the above work they suggested that a family of emulsification curves, prepared at different levels of dispersed phase concentration, could be used as a tool to detect the efficacy of an interfacial modifier to migrate to the interface.

Some research work has already considered micelle formation in interfacially modified melt blended systems. Fayt et al. (1) observed the location of block copolymers at the interface of LDPE and PS by a transmission electron microscope (TEM). The block copolymer formed layers with a seemingly regular thickness around the dispersed phase of either PS or LDPE, as well as block copolymer micelles in LDPE phase. Dai et al. (26) investigated the segregation of a poly [(2-vinylpridine)-b-styrene-d_8-b-(2 vinylpridine)] (PVP-dPS-PVP) triblock copolymer and dPS-PVP diblock copolymer to a planar

interface between the PS and PVP by forward recoil spectrometer (FRES). In their experiment, they prepared a series of bilayer samples (one layer is pure PVP and the other layer, PS mixed with various volume fractions of triblock copolymer) and then annealed the samples to allow the block copolymer to segregate to the interface between the PS and PVP homopolymers. They compared the interfacial excess for triblock and diblock copolymer and found that triblock copolymer has a larger critical micelle concentration (CMC) than the diblock copolymer. Polance et al (27). demonstrated that under the influence of a dynamic melt environment, the micelles tend to be significantly smaller than those generated in solution. Jannasch et al. (28) studied the macro-and microphase separation of compatibilizing graft copolymers in melt-mixed PS/polyamide 6 (PA6) blends. In their work the TEM was used to relate the onset of micelle formation to concentrations higher than the critical concentration defined by the emulsification curve.

Cigana et al. (9) carried out a TEM study to analyze micelle formation in the 90%PS/10%EPR blend containing 15%SBdS (based on the dispersed phase). SBdS was chosen because it had been shown to be only a fair emulsifier for that system and should have a tendency therefore to readily demonstrate micelle formation. Furthermore the butadiene part of the block was readily stained using osmium tetroxide. In their work micelle detection was only observed at values equal to or greater than the critical concentration even though the emulsification curve clearly indicated that a significant portion of that modifier was not effectively migrating to the interface. It was concluded that the TEM is limited in its ability to demonstrate the onset of micelle formation. A possible explanation for this effect is that the onset of micelle formation is characterized by a molecular dispersion with a large interparticle distance between micelles. Since the limiting thickness of the TEM is about 100 nm it is likely that these initially formed micelles escape detection.

The objective of this work is to systematically prepare a family of emulsification curves at various levels of the dispersed phase concentration to detect the micelle formation of copolymer below and at the critical concentration level. Since the amount of

added copolymer is calculated based on the quantity of dispersed phase, increasing the dispersed phase concentration also increases the concentration of modifier in the mixing bowl at a given stated level of copolymer. The variation in the observed behaviors will be analyzed to explore the potential of the emulsification curve as a tool to quantify the efficacy of migration of the modifier to the interface. A number of interfacial modifier copolymers of varying architecture and chemical composition will be studied.

6.2 Experimental

6.2.1 Materials

Both the polystyrene (PS) and the high density polyethylene (HDPE) used in this study were obtained from Dow Chemical of Canada. The antioxidant used was Irganox 1010 from Ciba-Geigy. Two types of interfacial agents of well characterized molecular weight and composition were chosen. The first type of modifier consists of two styrene-ethylene-butylene diblock copolymers (SEB) of similar molecular weight and different % styrene, referred to as SEB1 and SEB2, respectively. The second type of modifier consists of two styrene-ethylene-butylene-styrene triblock copolymers (SEBS) of different % styrene: Kraton 1652 and DB1, referred to as SEBS1 and SEBS2, respectively. Some properties of these materials are given in Table 6.1.

6.2.2 Blend Preparation

The materials were blended using a Brabender internal mixer under a nitrogen blanket at 50 rpm. The temperature was set at 195°C and the blending time was 5 min. Prior to blending, all the components were dry mixed and 0.2% of Irganox 1010 was added as an antioxidant. All components were then added into the internal mixer simultaneously (one step mixing). After mixing, the blend was quenched under liquid nitrogen to freeze in the morphology.

The effect of the sequence of addition of interfacial modifier was tested on 10%PS/90%HDPE blends. No difference in the morphology was observed when the copolymer interfacial modifier was initially premixed with the PS phase followed by blending with HDPE.

The copolymer concentration in the blends is expressed in terms of the minor phase volume. Thus, a blend of 10%PS/90%HDPE with 10% added copolymer contains 10 parts PS, 90 parts HDPE and 1 part copolymer (10% of PS content), whereas a blend of 30%PS/70%HDPE with 10% added copolymer contains 30 parts PS, 70 parts HDPE and 3 parts of copolymer (10% of PS content).

6.2.3 Matrix Dissolution

In the cases where PS is the matrix, matrix dissolution was carried out to isolate the dispersed phase for subsequent microscopic observation. The extraction of the PS matrix was performed followed by centrifugation. Initially the sample (about 1gram) was placed into a centrifuge tube filled with 50 ml tetrahydrofuran (THF) at room temperature. The tube containing the sample was then placed on a shaker and shaken for 48 hours. After that, the sample was centrifuged for one hour. The precipitated HDPE was situated at the bottom of the tube and the solution was poured away. To purify the precipitated HDPE, fresh THF solvent was added and the sample was shaken for another 48 hours. This process was repeated three times, which was sufficient to separate the HDPE dispersed phase from PS matrix in the HDPE/PS blend. Finally, all the dispersed phase samples were carefully collected and dried in a vacuum oven at 40°C for 72 hours.

6.2.4 Microtomy and Scanning Electron Microscopy

For the samples with PS as dispersed phase, blends with and without copolymer were microtomed under a jet of liquid nitrogen (-150°C) to create a plane face with a Leica Jung RM 2065 microtome equipped with a glass knife. The samples were then subjected to solvent extraction with a Soxhlet extraction apparatus to remove the dispersed PS phase. This serves to improve the contrast during subsequent microscopic observation. The selective solvent extraction of dispersed PS and copolymer in THF was performed in a Soxhlet extractor for 36 hrs and was then dried in a vacuum oven for 72 hrs at 40°C.

All the samples (with PS and/or with HDPE as dispersed phases) were coated with a gold-palladium alloy. A JEOL 840 scanning electron microscope, operating at 10kV, was used to examine the surfaces.

6.2.5 Image Analysis

A semi-automatic image analyzer used to measure the diameters of the dispersed phase was developed in-house. The operation of this instrument has been described elsewhere (29). SEM photomicrographs were analyzed for each sample to calculate the number average diameter, d_n, and volume average diameter, d_v. Since the microtome does not necessary cut the dispersed phase at the equator and since it is necessary to correct for polydispersity, a correction factor (30) was applied to the diameters determined from SEM micrographs of microtomed surfaces. On average, 200-300 diameters were measured per sample. For the moncopatiblized blends, the uncertainty of the average diameter measurements by this method is about 10%, and for the compatibilized blends, about 5%.

6.3 Results and discussion

6.3.1 General Tendencies of the Emulsification Curve

Figure 6.1a demonstrates a typical idealized emulsification curve such has been studied in this laboratory for several polymer blend systems (4-5, 23-25). The emulsification curve is characterized by an initial significant drop in the size of the dispersed phase with the addition of copolymer followed by the obtention of an equilibrium value (d_{eq}) at a critical concentration of copolymer (C_{crit}). As mentioned earlier, for comparison purposes, it is useful to express the interfacial agent concentration based on the minor phase volume instead of the total volume of the blend. This takes into account the fact that more dispersed phase requires larger quantities of interfacial agent to achieve interfacial saturation, due to the higher total interfacial area. One of the most important features of the emulsification curve is that it can be used to estimate the interfacial area occupied by the interfacial modifier molecule at the interface (A) or its reciprocal the areal density (Σ).

Knowing the equilibrium particle diameter and the critical concentration for emulsification, the interfacial area occupied per molecule may be calculated using the following equation

$$A = \frac{6\varphi_d M}{d_v N_A \varphi_c \rho_c} \qquad (6.1)$$

where, φ_d is the volume fraction of dispersed phase, N_A is Avogadro's number, M is the molecular weight of the copolymer, d_v is the volume average diameter of the dispersed phase and φ_c is the volume fraction of the compatibilizer, and ρ_c is the density of the compatibilizer. The best measure of the diameter is its surface average value, but the volume average diameter is also acceptable since it results in a similar value (5).

An important assumption must be made in the above calculation - one must assume that at the critical concentration, all the interfacial agent added to the system is located at the interface. For this reason, in this study we will refer to the interfacial area occupied per modifier molecule as an apparent area, A_{app}.

6.3.2 Idealized Trends

Based on the above fundamental information, a number of idealized trends can be extrapolated for the emulsification curve. If one studies a family of emulsification curves based on different dispersed phase concentrations (e.g. 1, 5, and 20%) different behaviors related to the efficacy of the interfacial modifier would be expected. In Figures 1b, 1c and 1d we illustrate three basic tendencies:

I) Figure 6.1b represents the family of emulsification curves expected for a system in which all the modifier migrates to the interface and the modifier entirely suppresses dynamic coalescence. In such a case, C_{crit} and d_{eq} are both independent of dispersed phase volume fraction. It follows then that the A_{app} is also independent of volume fraction. In that case A_{app} represents the true interfacial area occupied by the interfacial modifier molecule.

II) Figure 6.1c represents the case where all the modifier migrates to the interface, but the modifier is ineffective at completely suppressing dynamic coalescence. In such a case, the d_{eq} will increase with dispersed phase volume fraction, C_{crit} will decrease with dispersed phase volume fraction and A_{app} will be independent of volume fraction. In this case as well, A_{app} represents a true interfacial area.

III) Figure 6.1d demonstrates the expected trends for a system in which the modifier is not effectively driven to the interface due to micelle formation. In this case d_{eq} will increase with volume fraction of dispersed phase, since micelle formation is concentration dependent. Since the modifier is not migrating effectively to the interface C_{crit} will increase with volume fraction. These changes in d_{eq} and C_{crit} will result in a decrease of A_{app} with volume fraction. In this case obviously A_{app} does not represent the true interfacial area occupied per modifier molecule since the system is only partially emulsified.

6.3.3 Family of Emulsification Curves for PS Dispersed in HDPE

The surfaces prepared by microtoming and followed by minor phase dissolution for 10% PS/90%HDPE blends in the absence of and with compatibilizer are shown in Figures 6.2a and 6.2b as observed by SEM. It can immediately be seen that the presence of interfacial modifier in the blends results in a decrease in the diameters of the dispersed phase.

The effect of the interfacial modifier on the morphology of the HDPE/PS blends at various PS concentrations (1, 2, 5, 10, 20, 30%) is illustrated in Figures 6.3a and 6.3b. Note that we report C_{crit} here as the midpoint of an estimated range. Figures 6.3a and 6.3b clearly indicate an increase in d_{eq} with dispersed phase volume fraction as well as a tendency for C_{crit} to increase. The volume average diameter as well as the A_{app} at the critical concentration is given in Table 6.2 for each minor phase concentration. From 1% to 30% dispersed phase, one observes an increase in the critical concentration from 12.5% to 15% and an increase in the d_{eq} from 0.58 to 1.41μm.

Figure 6.4 illustrates the estimated A_{app} values at C_{crit} as a function of dispersed phase volume fraction. There is obviously a decrease in the interfacial area occupied per molecule with increasing minor phase concentration. SEBS1 in 99%HDPE/1%PS and 98%HDPE/2%PS possesses the same A_{app} values (8.4 nm^2). A sharp decrease of A_{app} occurs at 95%HDPE/5%PS (5.4nm^2), and after that this value almost keeps more or less a constant in the systems of 90%HDPE/10%PS (3.1nm^2), 80%HDPE/20%PS (3.1nm^2), 70%HDPE/30%PS (2.9nm^2) and 50%HDPE/50%PS (2.7nm^2). This phenomenon will be

discussed in terms of interfacial coverage later. SEM observation and gravimetric analysis demonstrate that the sample of 70%HDPE/30%PS is partially co-continuous and 50%HDPE/50%PS blend is fully co-continuous. The A_{app} of 50%HDPE/50%PS was obtained using the surface area value obtained by BET technique (21) and the A_{app} of the other samples were obtained by image analysis. To verify if the A_{app} obtained from two different methods is consistent, the A_{app} of 70%HDPE/30%PS obtained by BET was compared with that of same sample obtained by image analysis. Interestingly enough, the data from two the different methods are basically identical.

Based on the previous discussion, the above results indicate a system with an interfacial modifier that demonstrates significant micelle formation (Trend III behavior, Figure 6.1d). Since the above study uses an SEBS triblock interfacial modifier with a 30%PS:70%EB composition, it would be very useful to test the performance of that same modifier for the same blend system but with PS as the matrix.

6.3.4 Emulsification Curve for HDPE Dispersed in PS

In the previous section excellent visualization of the dispersed phase morphology on the SEM was made possible by pre-extracting the PS dispersed phase (Figures 6.2a and 6.2b). Since it is not possible to dissolve HDPE without dissolving PS, in this part the dispersed phase size is estimated using a matrix dissolution approach as outlined in the Experimental Section. The morphologies of the dispersed HDPE (from 10%HDPE/90%PS blend) in absence of and with compatibilizer after matrix dissolution are shown in Figures 6.5a and 6.5b as observed by SEM. A significant particle size reduction is observed by the addition of 12.5%SEBS1. Figure 6.6 illustrates the emulsification curve of 90%PS/10%HDPE. The results show that the critical concentration for 90%PS/10%HDPE is 12.5% SEBS1 (based on the dispersed phase). The equilibrium diameter of dispersed HDPE in the 90%PS/10%HDPE blend is 0.71μm at 12.5% SEBS1 (based on the dispersed HDPE phase) with an A_{app} of 6.9nm^2/molecule. For comparison purposes, the 90%HDPE/10%PS emulsification curve is also shown. It is clear that the SEBS1 modifier is much more effective at reducing the particle size when PS is the matrix. The reduction in particle size is 3.1 ($d_{v(0\%)}/d_{eq}$) as compared to 2.1

($d_{v(0.9)}/d_{eq}$) for the HDPE matrix system. These results indicate quantitatively that the chemical composition of the block copolymer plays a critical role in determining micelle formation for these systems.

Figure 6.4 also illustrates the A_{app} data of the system with PS as matrix at three different concentrations of dispersed phase. Note that it was not possible to reliably apply the matrix dissolution technique at 1 and 2% minor phase concentrations. A value of about 7nm^2/molecule for 5, 10 and 20% dispersed HDPE phase is obtained. The A_{app} value is essentially independent of dispersed phase concentration (see Table 6.3). The A_{app} data obtained from the PS matrix system is very close to those of 99%HDPE/1%PS and 98%HDPE/2%PS (about 8.4 nm^2/molecule), especially when one considers that a different technique was used to examine the morphology. The close relationship between the A_{app} values at 1%PS/99%HDPE and 2%PS/98%HDPE with the concentration independent values for A_{app} with 5%HDPE/95%PS, 10%HDPE/90%PS and 20%HDPE/80%PS strongly suggests that no micelle formation occurs under those conditions and that essentially all the modifier is migrating to the interface. Micelle formation in such systems which are highly effective at repulsing the interfacial modifier to the interface would only be observed at values exceeding C_{crit}. In other words micelle formation would only be observed after interfacial saturation.

Fayt et al. (1) investigated an LDPE/PS blend system compatibilized by HPB-b-PIP-b-styrene block copolymer (M_n: 65,000-15,000-50,000) via TEM observation. They noted qualitatively that in their 80%LDPE/20%PS blend system, a part of HPB-b-PIP-b-PS block copolymer was dispersed in the LDPE phase but not in the PS phase. It is obvious that the current phenomenon is consistent with their observation. The affinity between HDPE and SEBS1 is significant due to the 70% EB block in SEBS1. This behavior leads to difficulties in migrating the modifier to the interface.

6.3.5 Interfacial Coverage

In the previous section it was established that all the modifier migrates to the interface (for concentrations at or below C_{crit}) for 1, 2% PS in HDPE and for all the PS in

HDPE blends studied. Based on this result it should then be possible to estimate interfacial coverage for these systems in the following way:

$$\% \text{ Interfacial coverage} = (A_{appi\%}/A_{1\%}) \times 100 \qquad (6.2)$$

where, $A_{appi\%}$ is the apparent interfacial area occupied per copolymer molecule at C_{crit} and a dispersed phase concentration of i%, $A_{1\%}$ is the interfacial area occupied per copolymer molecule at 1% dispersed phase.

Figure 6.7 shows the interfacial coverage versus %minor phase for the HDPE/PS blends compatibilized by SEBS1. For the system compatibilized by SEBS1 triblock copolymer, the interfacial coverage for 99%HDPE/1%PS and 98%HDPE/2%PS is the same with a value of 100%. Then it decreases with increasing dispersed phase concentration, from 64% for the 95%HDPE/5%PS to 32% for the 50%HDPE/50%PS. As mentioned earlier, if there were no micelle formation, all the copolymer would have migrated to the interface and the interfacial area occupied per molecule would not change with the concentration of the minor phase, resulting in a saturated interface with constant interfacial coverage at a value of 100%. The relationship between the interfacial coverage and dispersed phase concentration can be categorized into three regions:

(1) Region I. All Modifier Migrates to the Interface

At 1% and 2% dispersed phase the amount of copolymer in the mixture is relatively low since the amount is based on the dispersed phase concentration. Under these conditions all the copolymer molecules find their way to the interface between the dispersed phase and matrix. The copolymer molecules do not form micelles at modifier concentration less than or equal to the critical concentration. Interfacial coverage is 100%.

(2) Region II. Onset of Micelle Formation

With the addition of more minor phase the amount of the copolymer increases as well. The sharp decrease of the interfacial coverage indicates that only a portion of copolymer migrates to the interface, while the rest is trapped in the matrix forming

micelles. The interfacial coverage diminishes from 100% to 38% and this zone can be considered as the onset region of micelle formation.

(3) Region III. Quasi Equilibrium between Micelle Formation and Partially Saturated Interface

At minor phase concentration in excess of 10% a quasi equilibrium between micelle formation and partially saturated interface is established at the critical concentration of modifier. An almost constant interfacial coverage (about 30%) versus %minor phase is obtained in this region.

6.3.6 Influence of the Copolymer Architecture and Chemical Composition on Its Migration to the Interface

6.3.6.1 Copolymer vs. Triblock Copolymer

Direct comparisons of diblock and triblock copolymer efficacy were made on systems comprising 90%HDPE/10%PS and 80%HDPE/20%PS, modified by both SEBS1 (triblock) and SEB1 (diblock) interfacial agents. The emulsification curves for the two blend systems are shown in Figures 6.8a and 6.8b. The critical concentrations for the triblock copolymers have already been shown in Figures 6.3a and 6.3b as well as in Table 6.2. For the diblock copolymer the C_{crit} is somewhat more difficult to determine and hence is shown as a range in Figures 6.8a and 6.8b and the midpoint value is used in the calculations for the interfacial area. The estimated the d_{eq}, $d_{v(0\%)}/d_{eq}$ values, the midpoint critical concentration and the interfacial area occupied per molecule for the diblock curves shown in Figures 6.8a and 6.8b are all reported in Table 6.4. It is clear from the $d_{v(0\%)}/d_{eq}$ values (1.7 for 90%HDPE/10%PS, and 1.9 for 80%HDPE/20%PS) that the diblock copolymer is less effective at reducing the particle size than the triblock (2.1 for 90%HDPE/10%PS, and 2.8 for 80%HDPE/20%PS). This is consistent with the previous investigation (9) on PS/EPR blend compatibilized by triblock and diblock copolymer, respectively.

The estimated apparent interfacial areas for the diblock copolymer at 10 and 20 percent PS dispersed phase are 4.2 and 3.5nm^2/molecule. The interfacial area for the diblock copolymer at 1% dispersed phase was found to be 6.0 nm^2/molecule. At 1%

dispersed phase, presumeably in the absence of any micelle effects, the diblock demonstrates a lower interfacial area (6.0nm^2/molecule) than the corresponding triblock copolymer (8.4nm^2/molecule). This is reasonably expected since the diblock possesses one joint while the triblock possesses two joints and must loop in and out of the interface. These results support previous observations by Cigana et al. (9). However, the difference in interfacial area occupied per molecule between diblock and triblock in this study are less pronounced than in the previous one.

By treating the above apparent interfacial areas according to equation (2.2), the interfacial coverage for the diblock copolymer can also be reported in Figure 6.9. The evolution of interfacial coverage with dispersed phase concentration can now be directly compared for both diblock and triblock copolymers. Although the diblock also demonstrates significant difficulties in migrating to the interface, it appears to be somewhat less susceptible to micelle formation than the triblock copolymer for the blends with HDPE as the matrix. If we recall the observation that the diblock copolymer was a less effective emulsifier overall than the triblock copolymer (Figures 6.8a and 6.8b), this suggests that the poorer capacity of the diblock copolymer to emulsify is likely related to less suppression of dynamic coalescence. The triblock copolymer loops in and out of the interface as opposed to the diblock which possesses only one joint. These results support previous observations from this laboratory (9). The above results raise a series of other questions. Is it the looping or the density of joints across the interface that affects dynamic coalescence? This could be studied by a variation in the molecular weight of the interfacial modifier. Matos et al.(5) demonstrated that an equivalent d_{eq} was obtained for a series of SEBS modifiers of widely different molecular weights for an EPR dispersed in PS system. Those results coupled with these strongly indicate that it is the looping effect of the triblock more than the absolute number of interfacial joints that influence dynamic coalescence. Another possible explanation could be that the diblock is less effective at reducing interfacial tension than the triblock copolymer. This latter possibility is not very likely since Leibler (31) has shown theoretically that diblocks were slightly more effective than triblocks at reducing the interfacial tension in a ternary blend.

6.3.6.2 Effect of the Chemical Composition of the Triblock Copolymer

In order to investigate the effect of chemical composition of the triblock copolymer on compatibilization, blends of 90%HDPE/10%PS modified by SEBS1and SEBS2 respectively were prepared. The SEBS1 and SEBS2 are styrene-ethylene butylene-styrene triblock copolymers (50kg/mol, 30% styrene for SEBS1 and 88 kg/mol, 50% styrene for SEBS2). Figure 6.10 illustrates these data. An equilibrium dispersed phase size (d_{eq}) of 1.29 μm is obtained for 90%HDPE/10%PS/15%SEBS1, and 0.71 μm for the 90%HDPE/10%PS/15%SEBS2, (see Table 4). The d_{eq} obtained in the latter case is virtually identical to the 1 and 2% dispersed PS phase systems reported in Figure 3a. From the above results, it is demonstrated that triblock micelle formation can be virtually eliminated through the use of a triblock copolymer with a symmetrical 50:50 composition. It appears clear, in light of these results, that the principle driving force to micelle formation as demonstrated in Figures 6.9 and 6.10 is the asymmetrical structure of interfacial agent, and hence the affinity of the asymmetical interfacial modifier to the HDPE matrix.

6.3.6.3 Effect of the Chemical Composition of the Diblock Copolymer

Figure 6.11 demonstrates the emulsification effect of 90%HDPE/10%PS modified by SEB1 (67 kg/mol and 30% styrene) and SEB2 (63 kg/mol and 53% styrene) diblock copolymers, respectively. At this dispersed phase composition SEB2 reduces the particle size more significantly than SEB1 ($d_{v(0\%)}/d_{eq}$ is 2.7 vs 1.7).The equilibrium diameter obtained for the blend compatibilized by SEB2 has a value of 1.0μm as compared to 1.54 μm with SEB1 (Table 4). If we assume a similar C_{crit} for the system 90%HDPE/10%PS/SEB2 an A_{app} of 6.2 nm^2/molecule is obtained as compared to an A_{app} of 3.5nm^2 for SEB1. The above results indicate that the diblock with the balanced composition clearly emulsifies the blend more effectively than that with a lower styrene weight fraction.

Leibler (3) suggested that to form a thermodynamically stable droplet phase in a strongly incompatible blend system, a very symmetrical copolymer should be used. Diblock copolymers with an equal block composition (symmetrical) would be more

effective interfacial agents than asymmetrical copolymers. This is due to the fact that for such a symmetrical diblock copolymer, the spontaneous curvature is low and it would be subjected to a less severe entropic penalty at a plane interface than in a spherical micelle (the interface of a spherical particle with a diameter of a few tenths of a micron is essentially plane on a molecular scale); the asymmetrical diblock, on the other hand, would "prefer" the spherical micelle configuration. Thus, according to Leibler, the more symmetrical a diblock copolymer, the more efficient it would be in emulsifying a polymer blend. Although this effect can play a part in determining micelle formation this study clearly illustrates the dominant role of the affinity of the modifier for the matrix phase in micelle formation.

6.4 Conclusions

In this study it is shown that a family of emulsification curves, prepared at a variety of dispersed phase concentrations, can be used as a powerful tool to estimate the efficacy of interfacial modifier migration to the interface in an immiscible polymer blend. Through an examination of the evolution of the equilibrium dispersed phase size after interfacial saturation, as well as a comparison of the apparent interfacial area occupied per modifier molecule (A_{app}) (or apparent areal density (Σ_{app})) at the different dispersed phase concentrations, it is possible to detect the onset of micelle formation. An approach to estimate the extent of interfacial coverage based on these data is also presented. This approach was applied to polyethylene/polystyrene blends. When polystyrene is dispersed in polyethylene it is shown that an asymmetric 70EB:30PS SEBS triblock block copolymer demonstrates an onset of micelle formation at 5% of dispersed phase. Three regions are identified: I) a region where all modifier migrates to the interface (1 and 2% dispersed phase); II) an onset region of micelle formation (5-10% dispersed phase) and III) a region of quasi-equilibrium between micelle formation and a partially saturated interface (>20% dispersed phase). When the reverse system of polyethylene dispersed in polystyrene is studied, it is shown, using the same approach, that all the modifier migrates to the interface over a wide range of dispersed phase concentrations. This

clearly underlines the dominant role of the affinity of the EB block in the asymmetric copolymer for HDPE in determining micelle formation. Use of an asymmetric diblock copolymer for the PS dispersed in HDPE blend also demonstrates significant micelle formation, although the phenomenon is less pronounced than the triblock case. Micelle formation in the PS dispersed in HDPE system can be virtually eliminated through the use of a symmetric (50:50) triblock or diblock copolymer.

6.5 References

1. Fayt, R.; Jérôme, R.; Teyssié, Ph. *Makromol. Chem.*, 1986, 187, 837.
2. Ouhadi, R.; Fayt, R.; Jérôme, R.; Teyssié, Ph. *Polym. Commun.*, 1986, 27, 212.
3. Leibler, L. *Makromol. Chem. Makromol. Symp.*, 1988, 16, 1.
4. Favis, B. D. *Polymer*, 1994, 35, 1552.
5. Matos, M.; Favis, B. *Polymer*, 1995, 36, 3899.
6. Israels, R.; Jasnow, D.; Balazs, L.; Guo, L.; Krausch, G.; Sokolov, J.; Rafailovich, M. *J. Chem. Phys.*, 1995, 102, 8149.
7. Cigana, P.; Favis, B. D.; Jérôme, R., *J. Polym. Sci., Polym. Phys.*, 1996, 34, 1691.
8. Cigana, P.; Favis, B. D.; Albert, C., Vu-Khanh, T., *Macromolecules*, 1997, 30, 4163.
9. Cigana, P. and Favis, B. D., *Polymer*, 1998, 39, 3373.
10. Chen, C., White, J. L., *Polym. Eng. Sci.*, 1993, 33, 923.
11. Bourry, D., Favis, B. D., *J. Polym. Sci., Polym. Phys.*, 1998, 36, 1889.
12. Paul, D. R., Bucknall, C. B., editors, *Polymer Blends*, Vol. 1. 2000, Wiley-Interscience, New York.
13. Elemans, P. H. M., Janssen, J. M. H., Meijer, H. E. H., *J. Rheol*, 1990, 34, 1311.
14. Ramic, A. J., Stehlin, J. C., Hudson, S. D., Jamieson, A. M., Manas-Zloczower, I., *Macromolecules*, 2000, 33, 371.
15. Sundararaj, U., Macosko, C. W., *Macromolecules*, 1995, 28, 2647.

16. BeckTan, N. C., Tai, S-K, Briber, R. N., *Polymer*, 1996, 37, 3509.

17. Milner, S. T., Xi, H. W., *J. Rheol.*, 1996, 40, 663.

18. Patterson, H. T., Hu, H. K., Grindstaff, T. H., *J. Polym. Sci., Polym. Lett.*, 1971, 34, 31.

19. Fayt, R., Jérôme, R., and Teyssié, Ph., *J. Polym. Sci., Polym. Phys.*, 1982, 20, 2209.

20. Mekhilef, N., Favis, B. D., and Carreau, P. J., *J. Polym. Sci., Polym. Phys.*, 1997,35, 293.

21. Li, J., and Favis, B. D., *Polymer*, 2001, 42, 5047.

22. Djakovic, L., Dokic, P., Radivojevic, P., Sefer, I., and Sovilj, V., *Colloid and Polym. Sci.*, 1987,265, 993.

23. Willis, J. M., and Favis, B. D., *Polym. Eng. Sci.*, 1988, 28, 1416.

24. Lepers, J-C., Favis, B. D., and Lacroix, C., *J. Polym. Sci., Polym. Phys.*, 1999, 37, 939.

25. Liang, H., Favis, B. D., Yu, Y. S., and Eisenberg, A., *Macromolecules*, 1999, 32, 1637.

26. Dai, K. H., Washiyama, J., and Kramer, E., *Macromolecules*, 1994, 27, 4544.

27. Polance, R., Nichols, K. L., and Jayarman, K., *Polymer*, 1994, 35, 5051.

28. Jannasch, P., Hassander, H., and Wesslen, B., *J. Polym. Sci., Polym. Phys.*, 1996, 34, 1289.

29. Favis, B. D., Willis, J. M., *J. Polym. Sci., Polym. Phys.*, 1990, 28, 2259.

30. Saltikov, S. A., *Proc. 2nd Int. Cong. For Stereology*, Helias: New York, 1967.

31. Leibler, L., *Macromolecules*, 1982, 15, 1283.

Figure captions

Figure 6.1 General conceptual tendencies of emulsification curves. (a) general features of an emulsification curve; (b) family of emulsification curves expected for a system in which all the modifier migrates to the interface and the modifier entirely suppresses dynamic coalescence; (c) family of emulsification curves expected for the case where all the modifier migrates to the interface, but the modifier is ineffective at completely suppressing dynamic coalescence; and (d) family of emulsification curves expected for a system in which the modifier is not effectively driven to the interface due to micelle formation.

Figure 6.2 SEM of 90%HDPE/10%PS blends in the absence of and with compatibilizer: (a). 0% of SEBS1; (b) 15% of SEBS1.

Figure 6.3 A family of experimentally determined emulsification curves for the HDPE/PS blends at various dispersed phase concentrations. (a) emulsification curves for 99%HDPE/1%PS, 98%HDPE/2%PS and 95%HDPE/5%PS blends; (b) emulsification curves for 90%HDPE/10%PS, 80%HDPE/20%PS and 70%HDPE/30%PS blends.

Figure 6.4 A_{app} versus dispersed phase concentration for blends with both HDPE and PS as matrix.

Figure 6.5 SEM of 10%HDPE/90%PS blends in the absence of and with compatibilizer after matrix dissolution: (a). 0% of SEBS1; (b) 12.5% of SEBS1.

Figure 6.6 Emulsification curves for 90%HDPE/10%PS and 90%PS/10%HDPE blends modified by SEBS1 triblock copolymer. The arrows indicate the critical concentration for interfacial saturation of the blend systems.

Figure 6.7 Interfacial coverage versus the dispersed phase concentration for PS dispersed in HDPE with SEBS1 as the interfacial modifier. Three distinct regions are observed in this system. Region I) all of the copolymer goes to the interface; region II) onset of micelle formation in the system; and region III) a quasi equilibrium between micelle formation and a partially saturated interface.

Tables

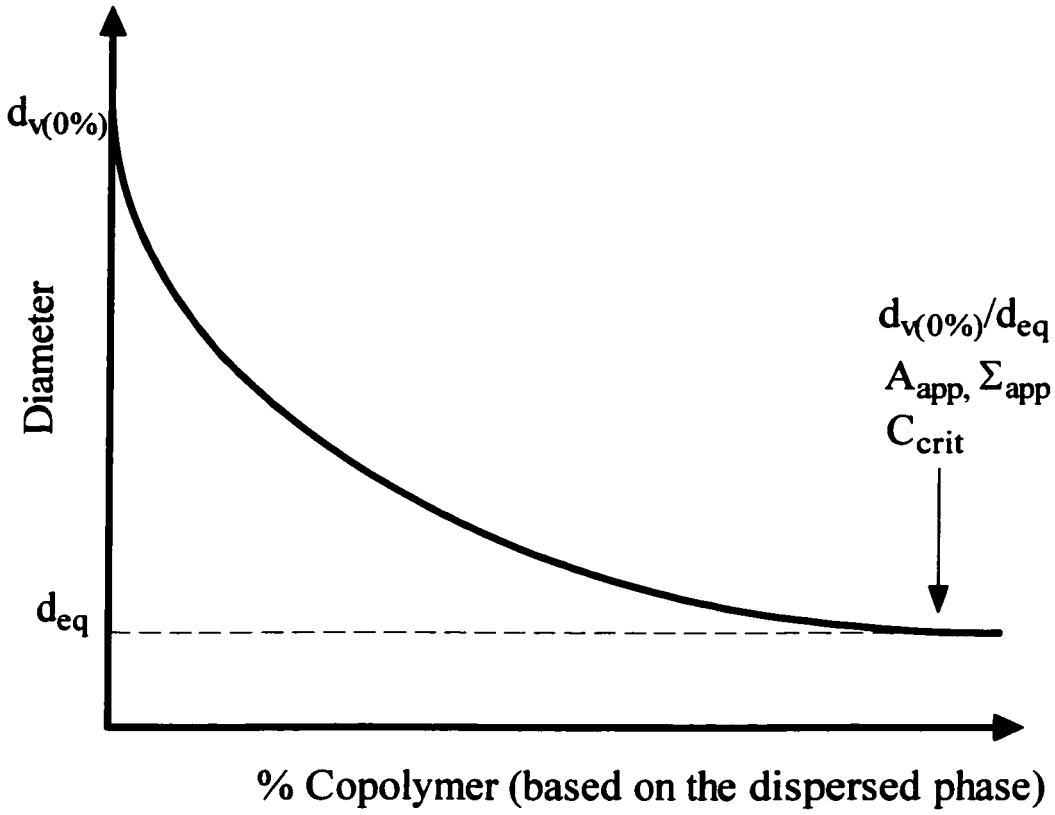

Figure 6.1a General features of an emulsification curve

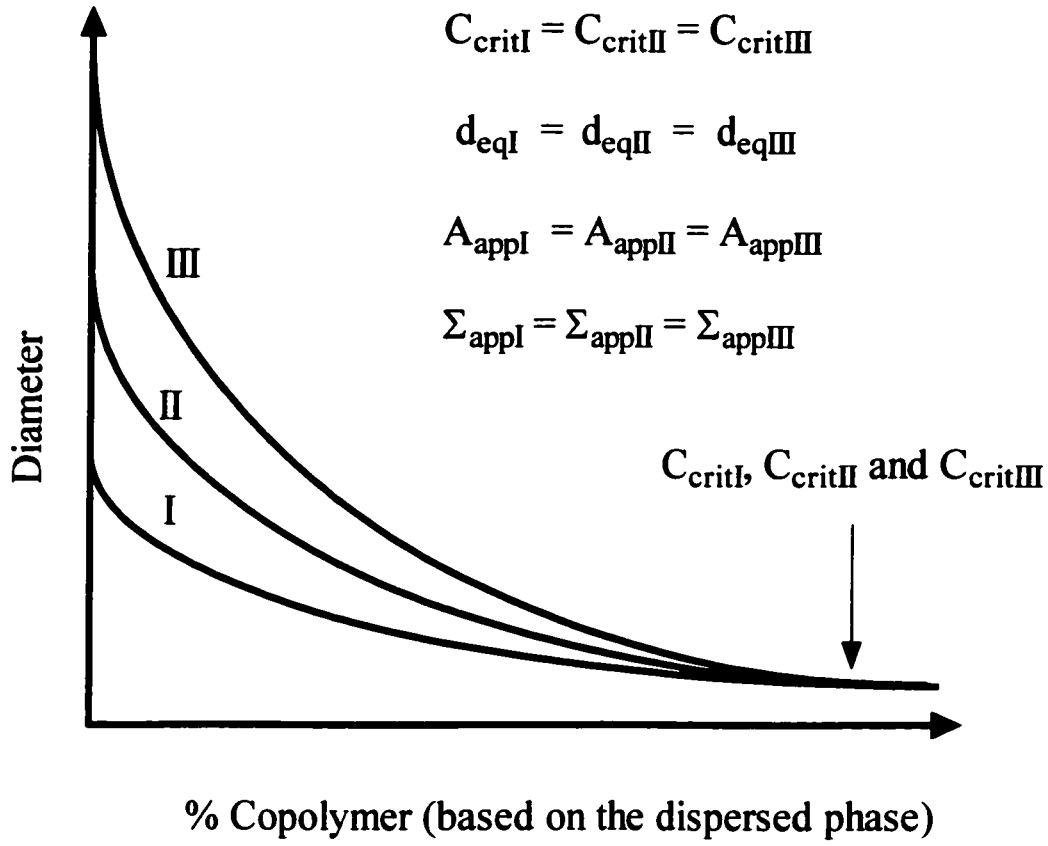

Figure 6.1b. Family of emulsification curves expected for a system in which all the modifier migrates to the interface and the modifier entirely suppresses dynamic coalescence.

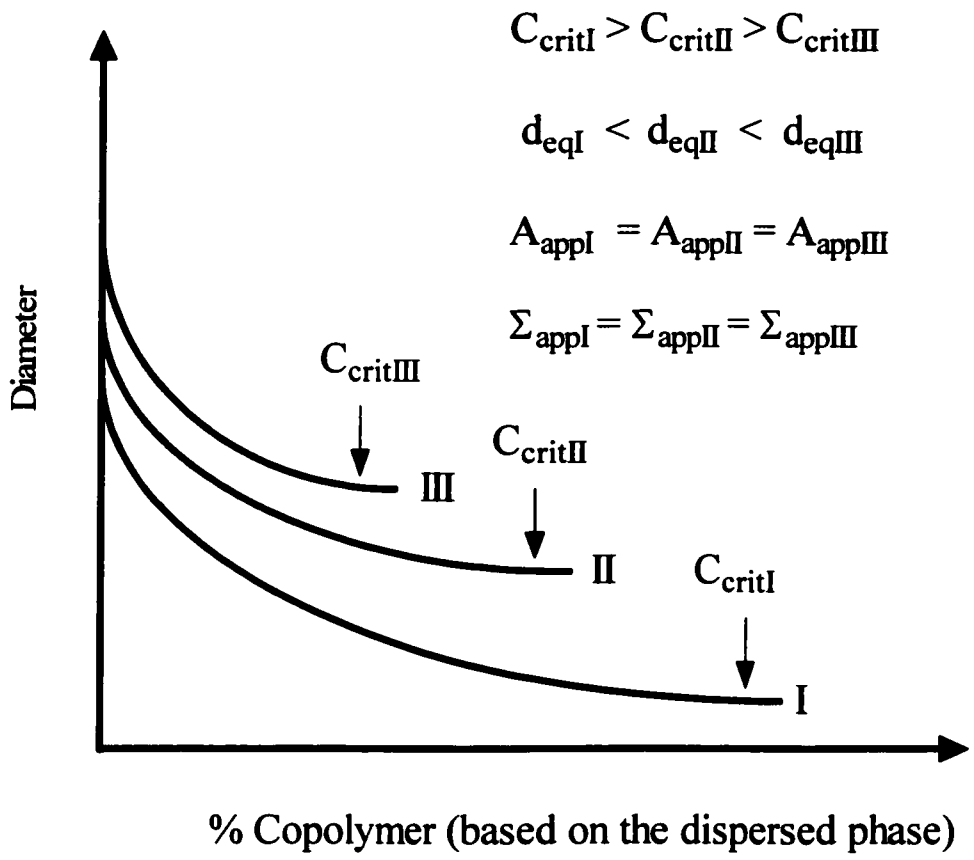

Figure 6.1c. Family of emulsification curves expected for the case where all the modifier migrates to the interface, but the modifier is ineffective at completely suppressing dynamic coalescence.

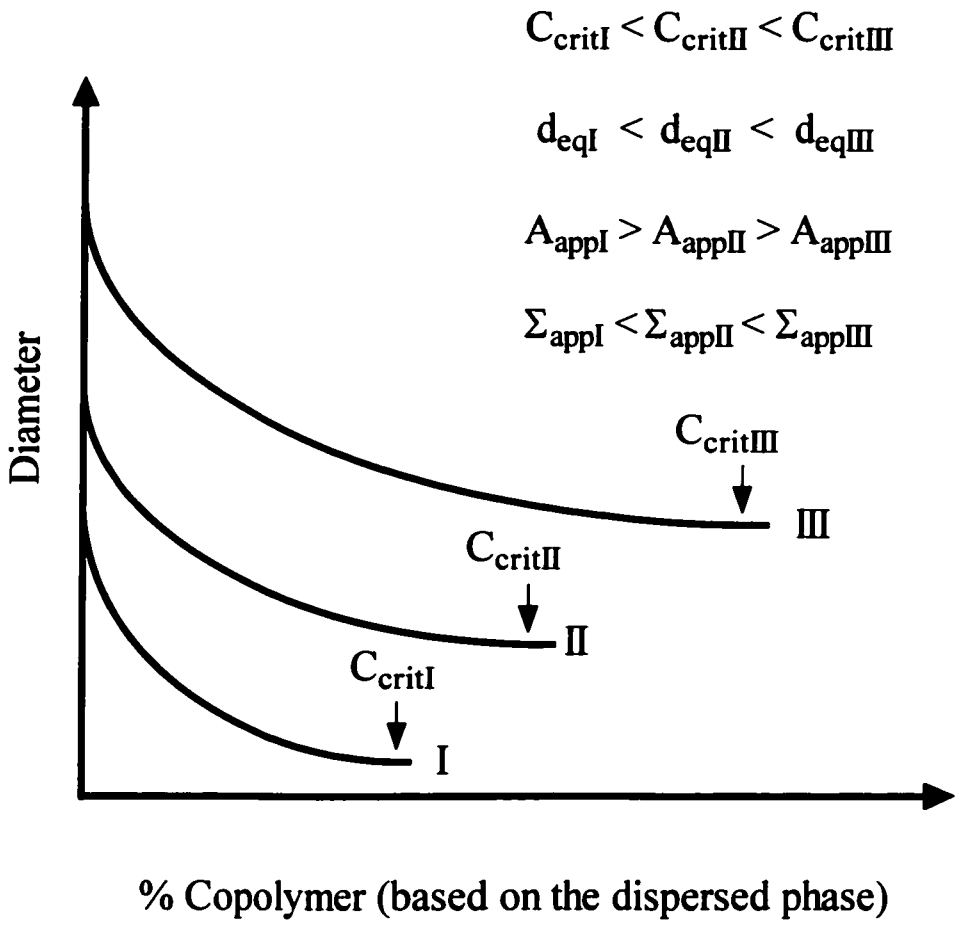

Figure 6.1d. Family of emulsification curves expected for a system in which the modifier is not effectively driven to the interface due to micelle formation.

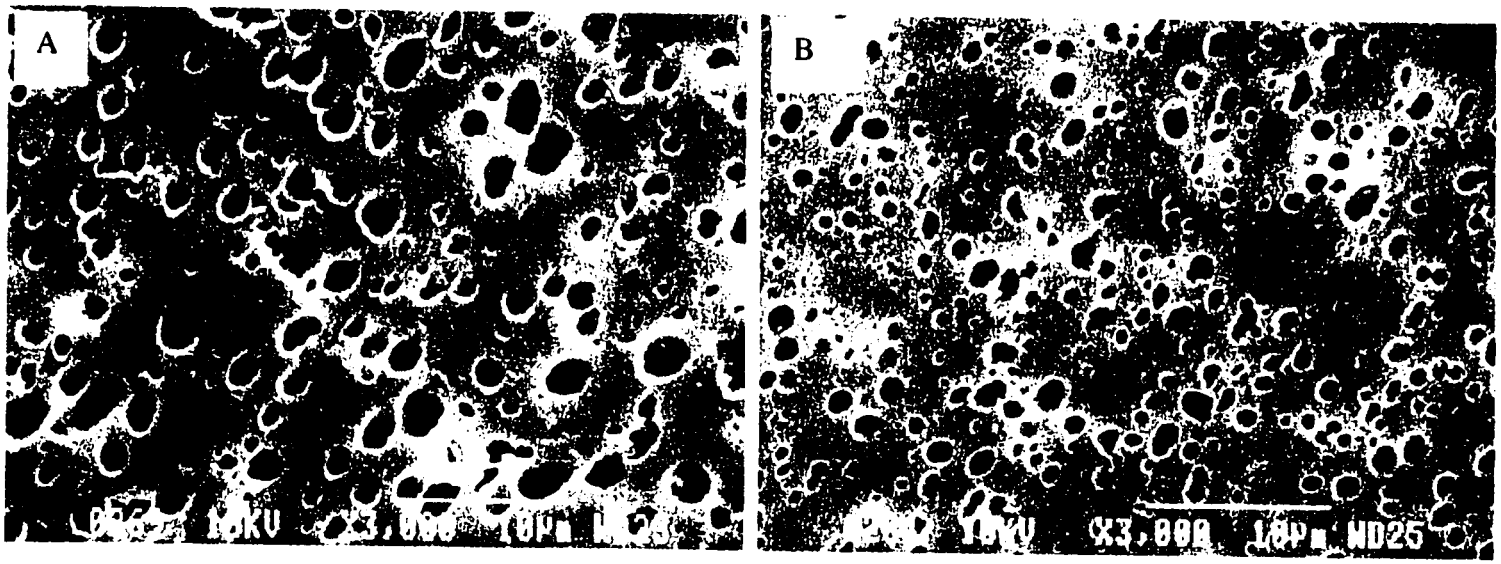

Scale bar: ———— 10 μm

Figure 6. 2. SEM of 90%HDPE/10%PS blends without and with compatibilizer: (a). 0% of SEBS1; (b) 15% of SEBS1.

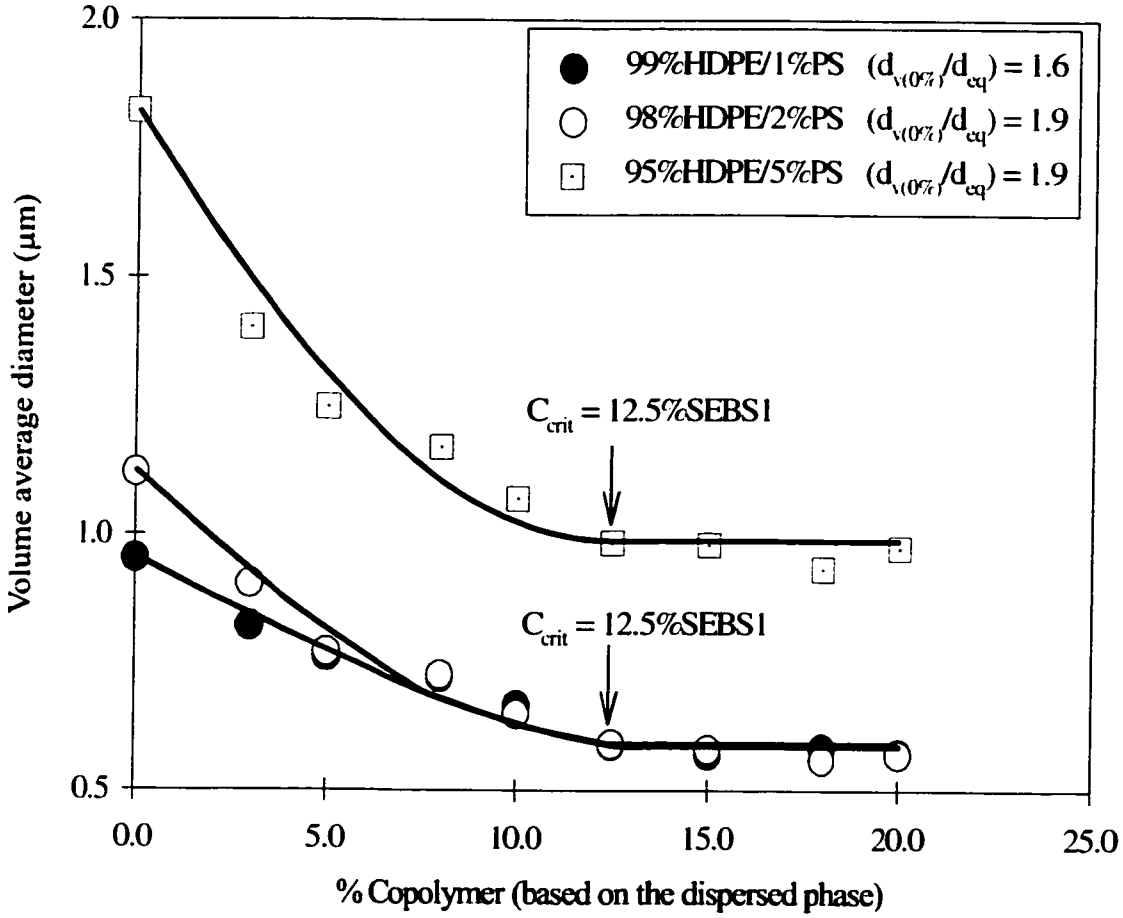

Figure 6.3a. A family of emulsification curves for 99%HDPE/1%PS, 98%HDPE/2%PS and 95%HDPE/5%PS blends.

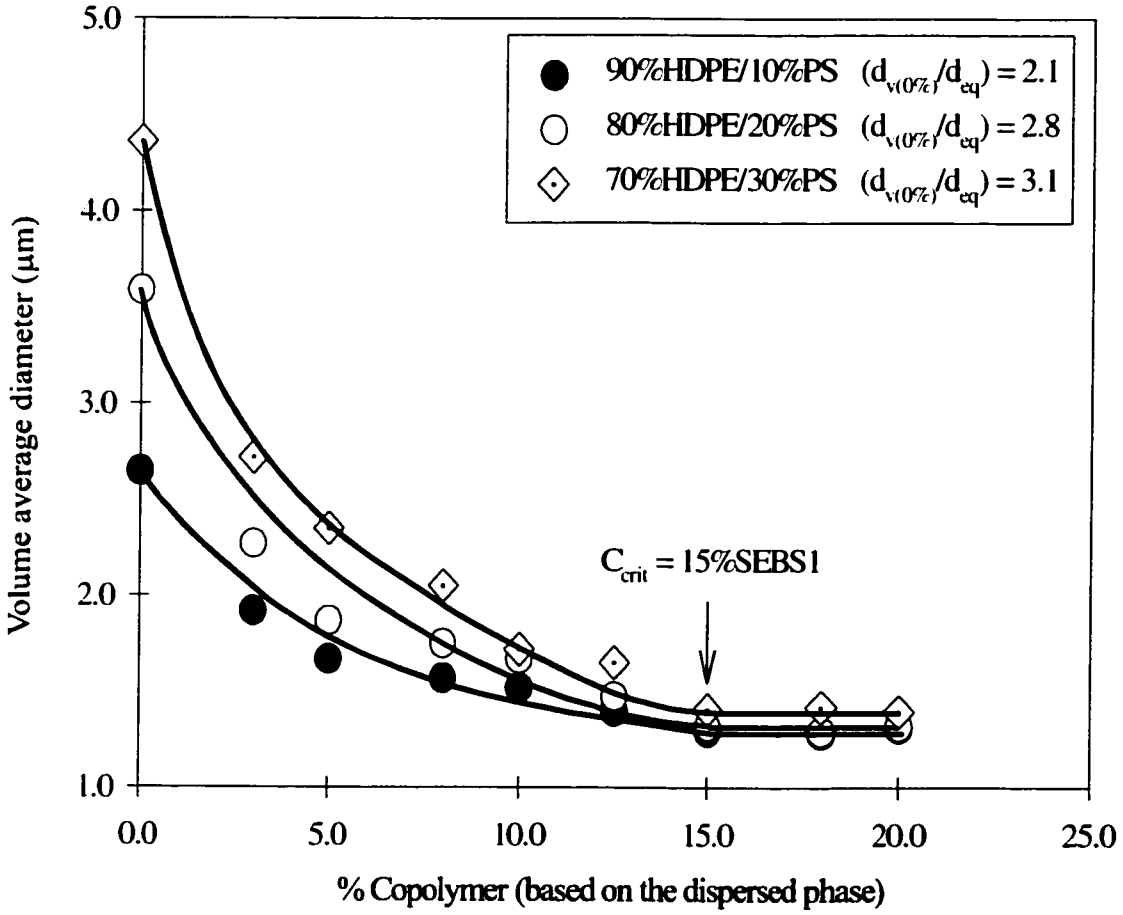

Figure 6.3b. A family of experimentally determined emulsification curves for 90%HDPE/10%PS, 80%HDPE/20%PS and 70%HDPE/30%PS.

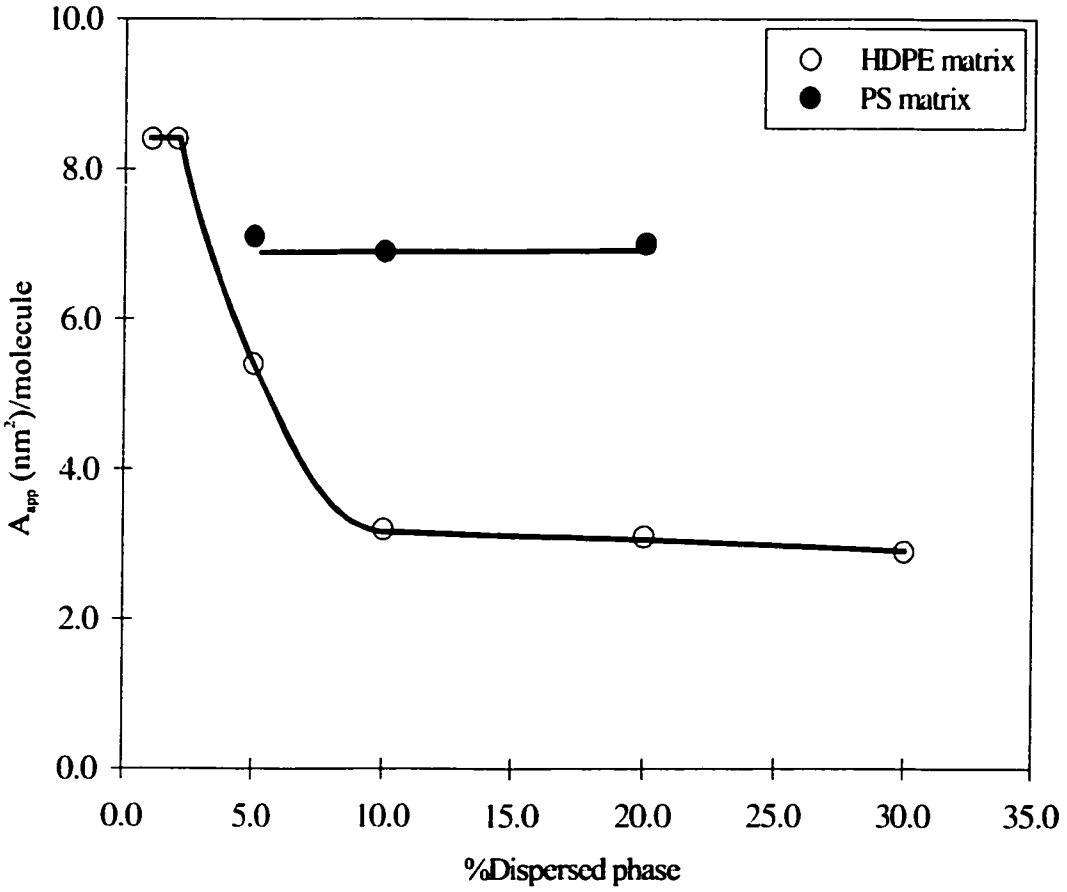

Figure 6.4. A_{app} versus dispersed phase concentration for blends with both HDPE and PS as matrix.

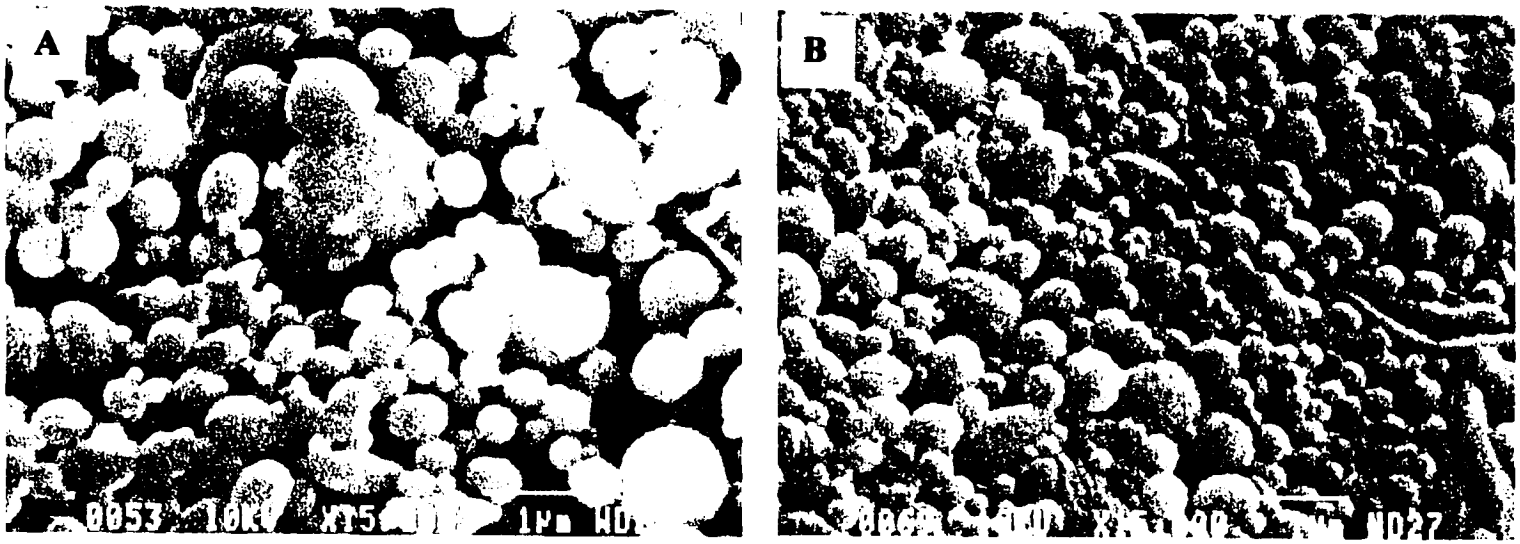

Scale bar: ——— 1μm

Figure 6.5. SEM of 10%HDPE/90%PS blends in the absence of and with compatibilizer after matrix Dissolution: (a). 0% of SEBS1; (b) 12.5% of SEBS1.

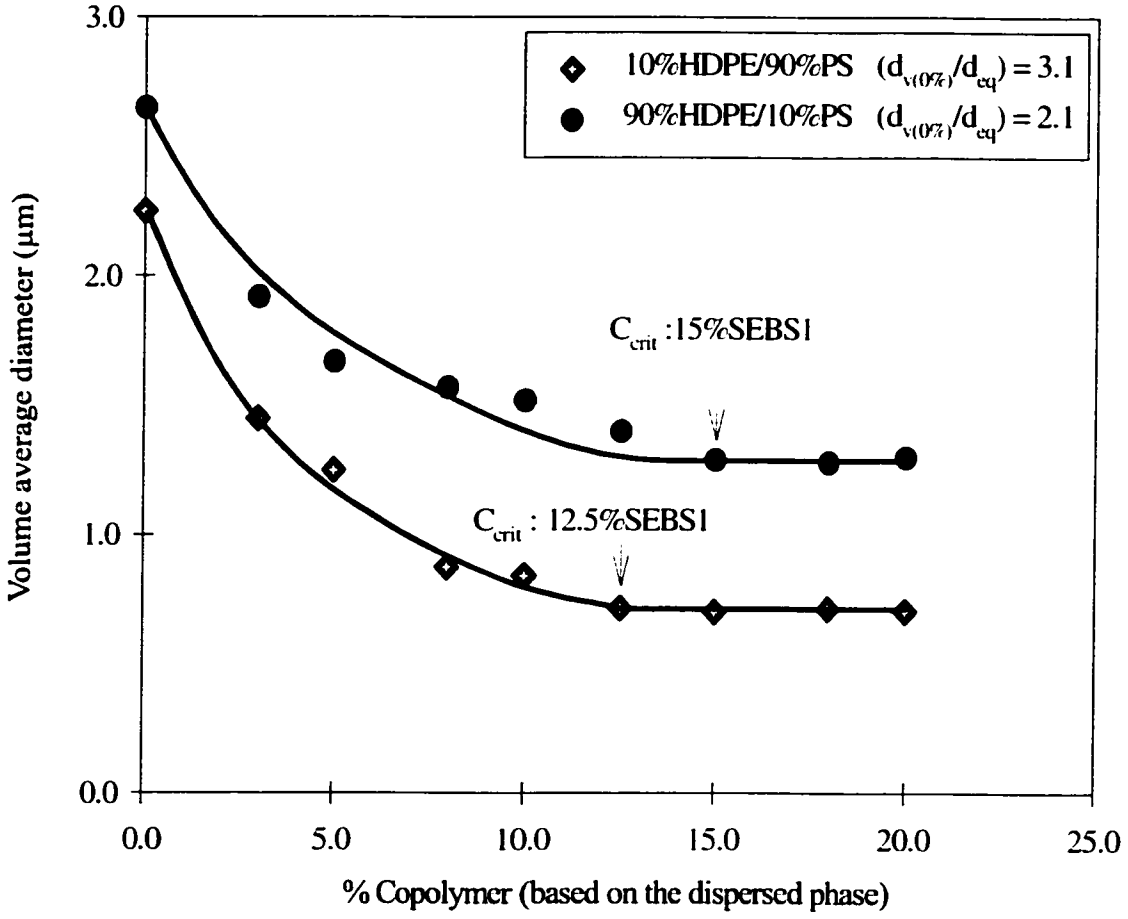

Figure 6.6.. Emulsification curves for 90%HDPE/10%PS and 90%PS/10%HDPE blends modified by SEBS1 triblock copolymer. The arrows indicate the critical concentration for interfacial saturation of the blend systems.

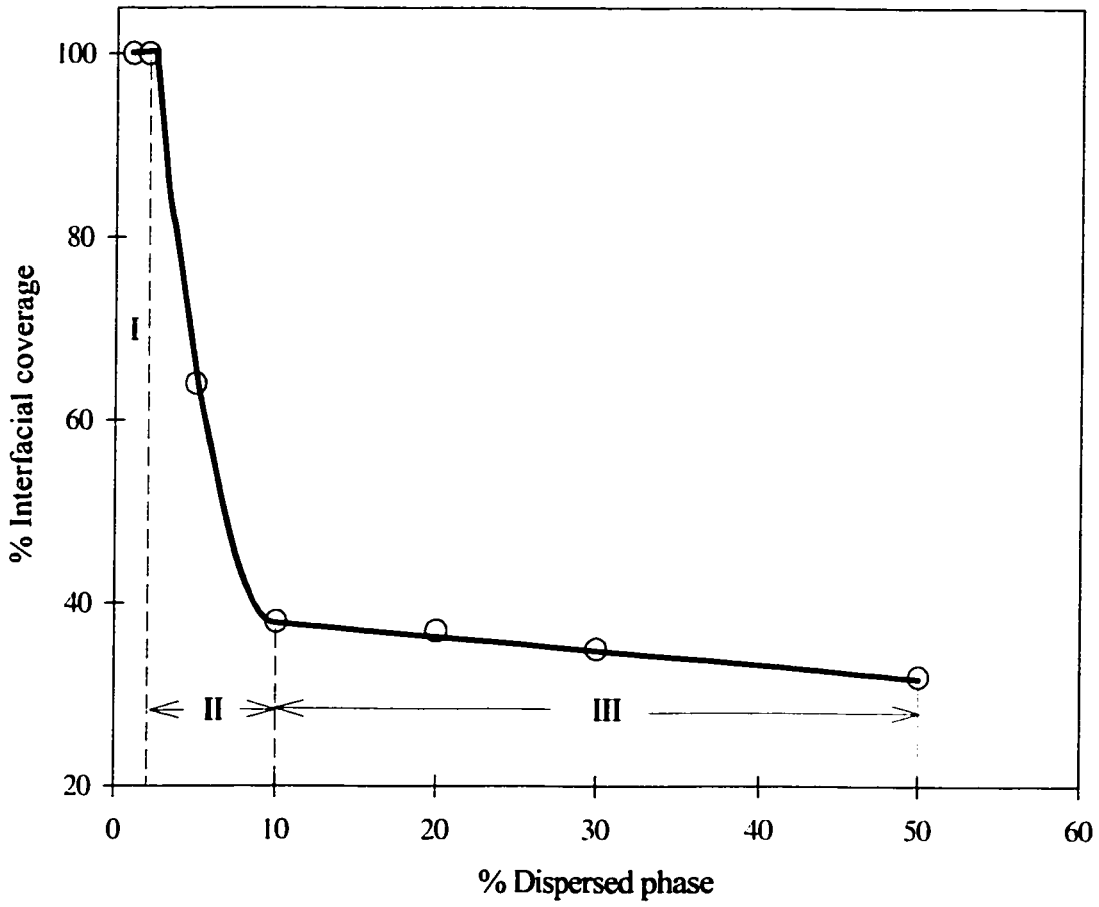

Figure 6.7. Interfacial coverage versus the dispersed phase concentration for PS dispersed in HDPE with SEBS1 as the interfacial modifier. Three distinct regions are observed in this system. Region I) all of the copolymer goes to the interface; region II) onset of micelle formation in the system; and region III) a quasi equilibrium between micelle formation and a partially saturated interface.

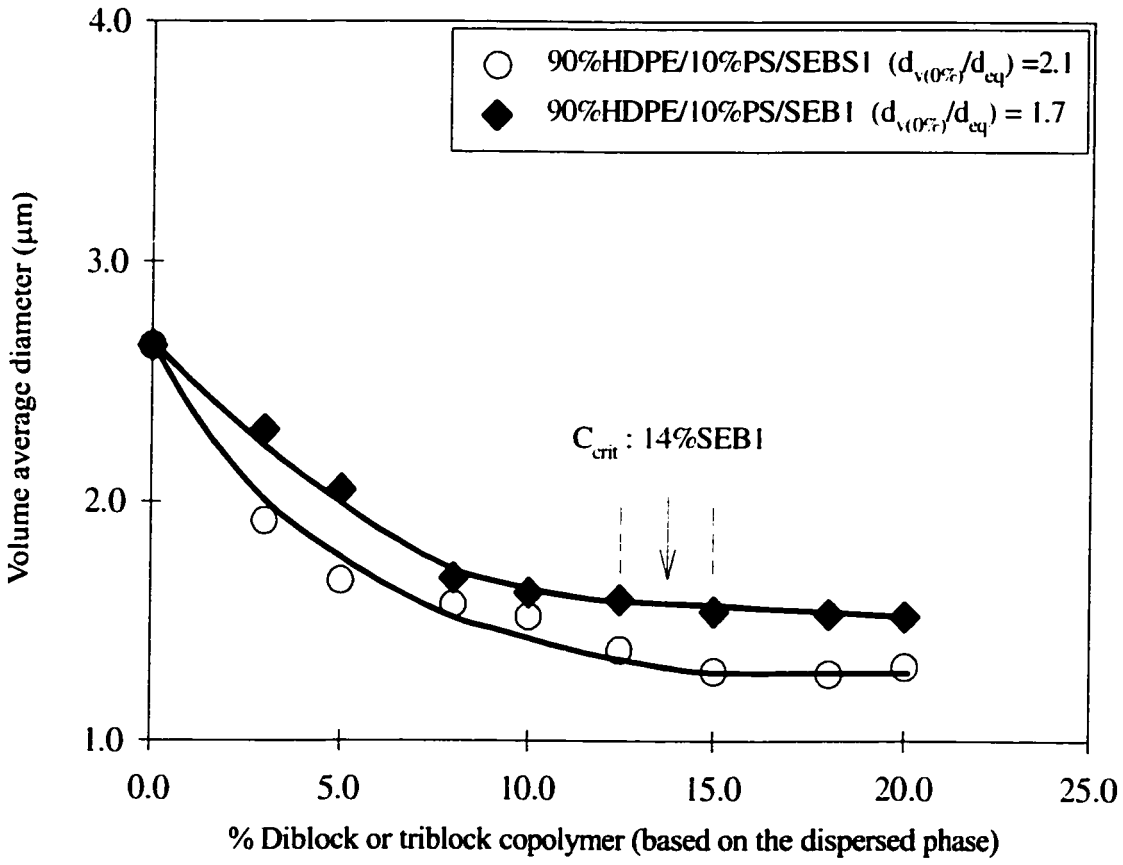

Figure 6.8a. The influence of the architecture of the copolymer (diblock vs triblock) on the emulsification of 90%HDPE/10%PS blend.

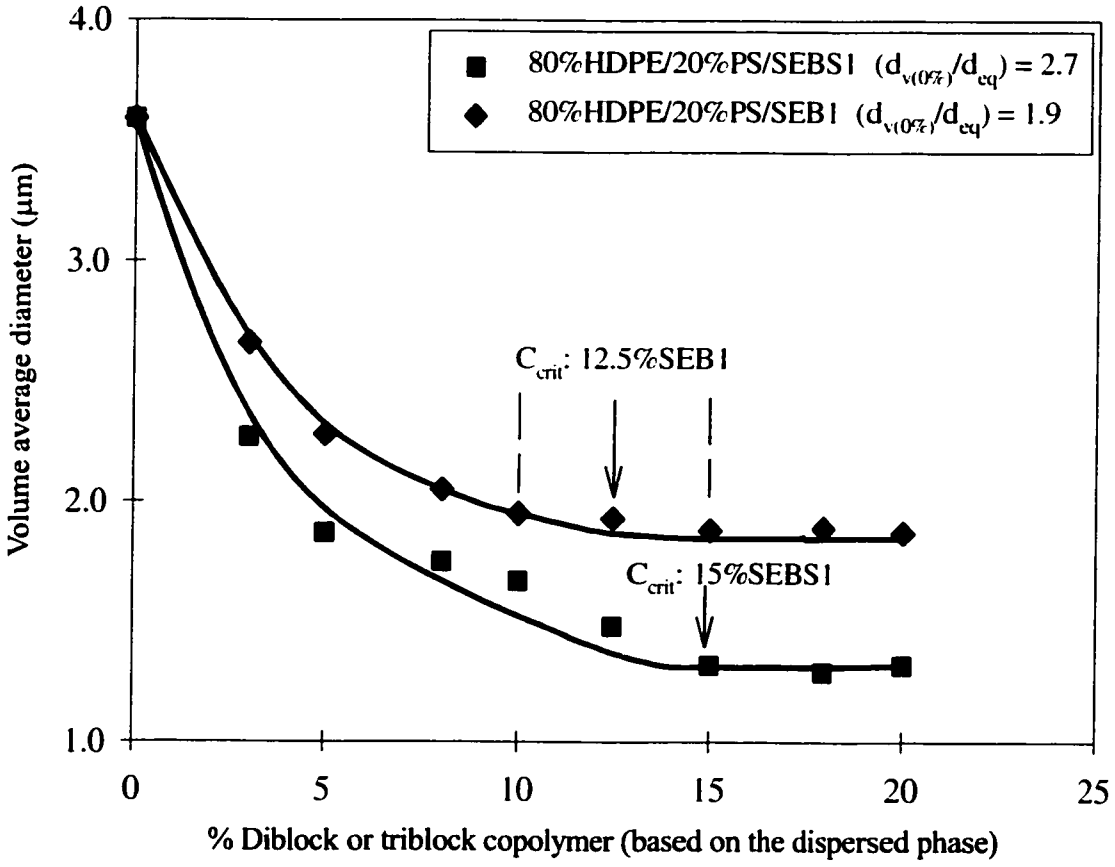

Figure 6.8b. The influence of the copolymer architecture (diblock vs triblock) on the emulsification of 80%HDPE/20%PS blend system.

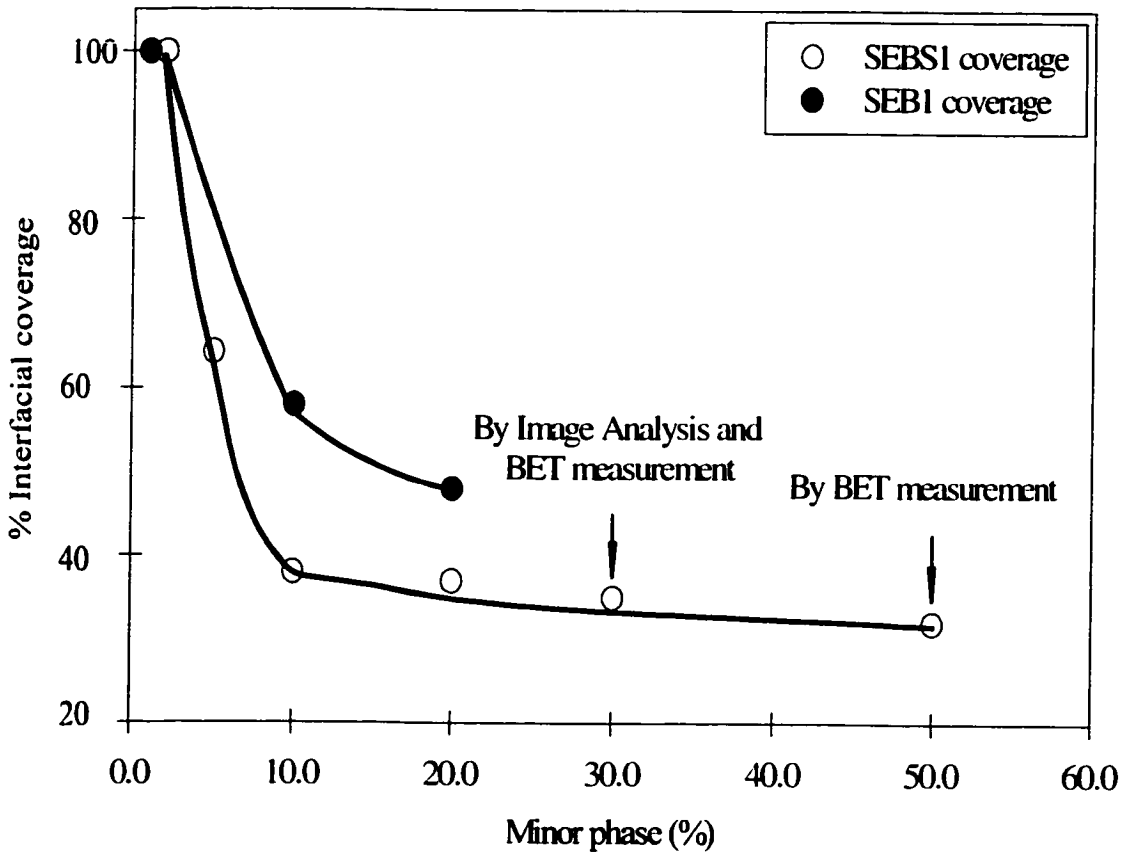

Figure 6.9. Interfacial coverage versus the dispersed phase concentration for blends compatibilized by diblock and triblock copolymer.

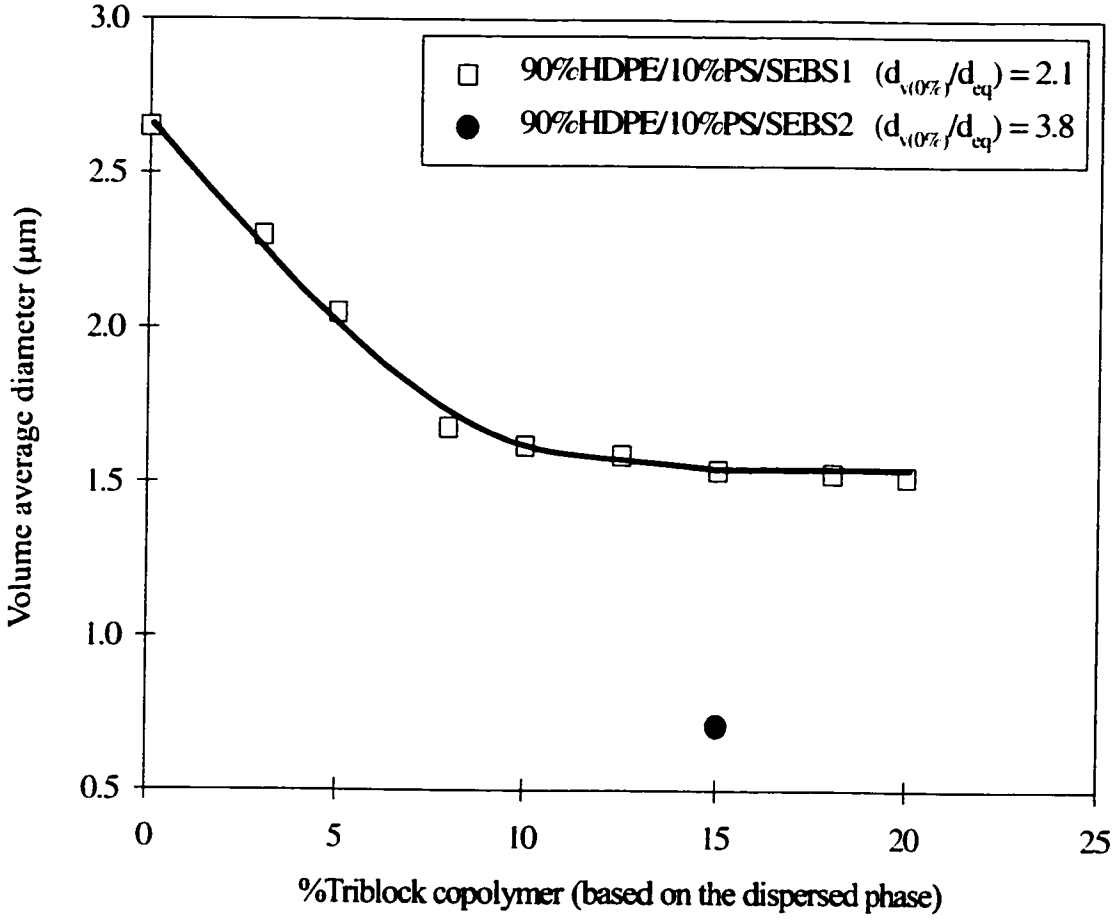

Figure 6.10. The influence of the chemical composition of triblock copolymer on the emulsification of HDPE/PS blends.

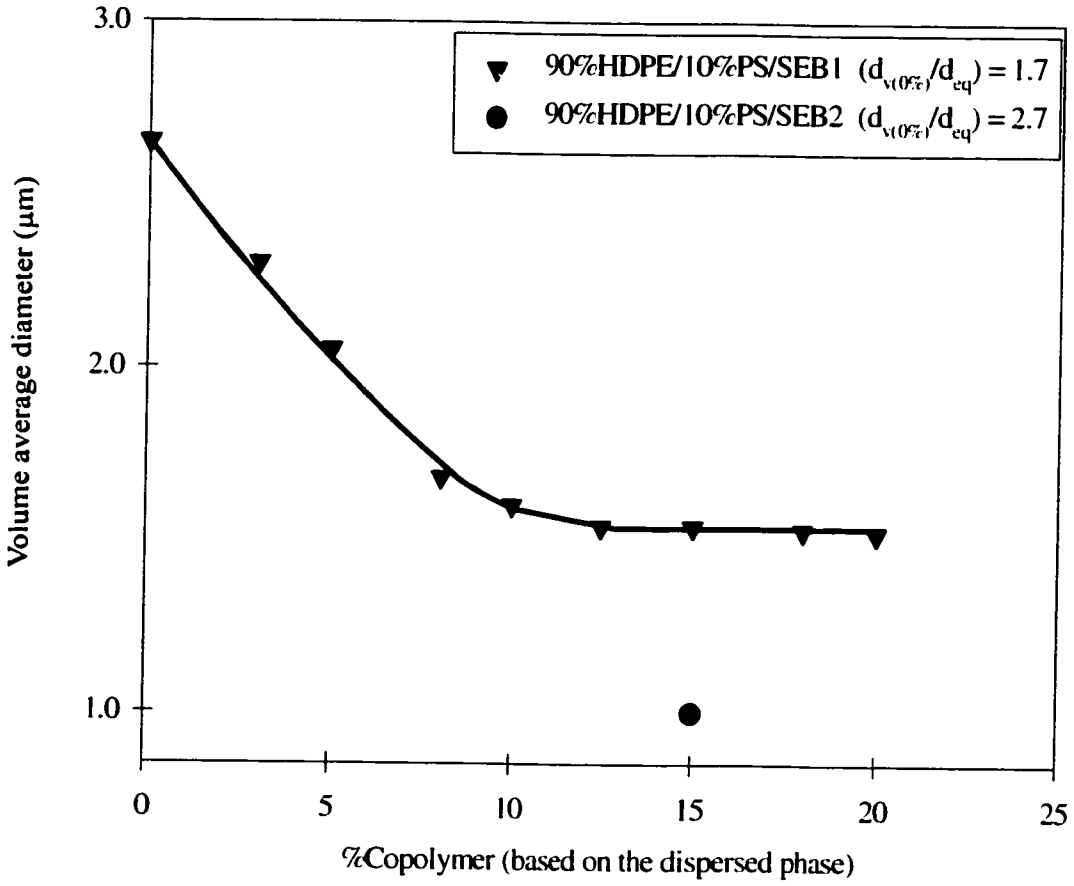

Figure 6.11. The influence of the chemical composition of diblock copolymer on the emulsification of HDPE/PS blends.

Table 6.1 Characteristic properties of materials

	PS	HDPE	SEBS1
M_w	215,000	79,000	
M_n	100,000	24,000	S=7500 EB=35000 Composition: 30% styrene
Density (20°C) (g/ml)	1.04	0.962	0.910
Supplier	Dow	Dow	Shell

	SEB1	SEBS2	SEB2
M_w		---	---
M_n	S=20000 EB=47000 Composition: 30% styrene	S=22000 EB=44000 Composition: 50% styrene	S=33390 EB=29610 Composition: 53% styrene
Density (20°C) (g/ml)	0.910	0.910	0.910
Supplier	Shell	Home made	Home made

Table 6.2 Equilibrium volume average diameter (d_{eq}), apparent interfacial area occupied per copolymer molecule (A_{app}) and apparent areal density (Σ_{app}) for the compatibilized HDPE/PS blends at the critical concentration (HDPE as matrix)

Blends	C_{crit} (%)	d_{eq} (μm)	$d_{v(0.5)}/d_{eq}$	A_{app} (nm^2/molecule)	Σ_{app} (molecule/nm^2)
99%HDPE/1%PS	12.5	0.58	1.6	8.4	0.12
98%HDPE/2%PS	12.5	0.58	1.9	8.4	0.12
95%HDPE/5%PS	12.5	0.98	1.9	5.4	0.19
90%HDPE/10%PS	15.0	1.29	2.1	3.2	0.31
80%HDPE/20%PS	15.0	1.31	2.8	3.1	0.32
70%HDPE/30%PS	15.0	1.41	3.1	2.9	0.34

Table 6.3 Equilibrium volume average diameter (d_{eq}), apparent interfacial area occupied per copolymer molecule (A_{app}) and apparent areal density (Σ_{app}) for the compatibilized HDPE/PS blends at the critical concentration (PS as matrix)

Blends	C_{crit} (%SEBS1)	d_{eq} (μm)	$dv_{(0.5)}/d_{eq}$	A_{app} (nm^2/molecule)	Σ_{app} (molecule/nm^2)
95%PS/5%HDPE	12.5	0.68	2.2	7.1	0.14
90%PS/10%HDPE	12.5	0.70	3.1	6.9	0.14
80%PS/20%HDPE	12.5	0.69	4.2	7.0	0.14

Table 6.4 Influence of the copolymer architecture and chemical composition on emulsification for the 90%HDPE/10%PS and 80%HDPE/20%PS blends

Blends	C_{crit} (%)	d_{eq} (μm)	$d_{v(0\%)}/d_{eq}$	A_{app}(nm^2/molecule)	Σ_{app} (molecule/nm^2)
90%HDPE/10%PS/SEBS1	15.0	1.29	2.1	3.2	0.31
90%HDPE/10%PS/SEB1	14.0	1.54	1.7	4.2	0.24
80%HDPE/20%PS/SEBS1	15.0	1.31	2.8	3.1	0.32
80%HDPE/20%PS/SEB1	12.5	1.88	1.9	3.5	0.29
90%HDPE/10%PS/SEBS2	15.0	0.71	3.8	10.0	0.1
90%HDPE/10%PS/SEB2	15.0	1.00	2.7	5.2	0.19

CHAPTER 7. SCIENTIFIC CONTRIBUTIONS

Contribution I Co-continuous polymer blends possess very complex morphological structures. The lack of adequate characterization technique has been a hindrance to the effective exploitation and study of co-continuous morphology in polymer blends. The BET nitrogen adsorption technique has been introduced for the characterization of the co-continuous structure of polymer blends for the first time. Rapidity and accuracy make this technique a powerful approach to the characterization of co-continuous polymer blends.

Contribution II With a proper characterization technique, the role of the type of polymer-polymer interface on morphology in co-continuous polymer blends has been investigated. A new conceptual mechanism for the formation of dual phase continuity has been proposed. A new parameter, TFR (thread frequency ratio), has been introduced to classify the relative importance of fibers and droplets in the development of the co-continuous and the formation of microstructure during melt mixing.

Contribution III A family of emulsification curves, prepared at variety of dispersed phase conditions, has been used as an effective tool to estimate the efficacy of interfacial modifier migration to the interface. It is proposed as technique to detect the onset of micelle formation. Micelle formation in the PS dispersed in HDPE system can be virtually eliminated through the use of a symmetric (50:50) triblock or diblock copolymer.

CHAPTER 8 CONCLUSIONS AND RECOMMENDATIONS

Conclusions:

- BET nitrogen adsorption technique is found to be an effective route to analyze the microstructure of co-continuous polymer blends.

- Tracking of surface area via the BET technique provides a powerful quantitative tool to analyzing the efficacy of interfacial modifiers at emulsifying co-continuous morphologies.

- The blend interface type plays a crucial role in the development of co-continuity and microstructure features. The three different categories of blend interfaces are: compatible binary blends based on HDPE/SEBS and HDPE/SEB (Type I), incompatible binary system comprised of HDPE/PS (Type II), and compatible ternary system comprised of HDPE/PS compatibilized by SEBS in one case and by SEB in another.

- A mechanism for the formation of dual phase continuity based on droplet and fiber lifetime during melt mixing has been proposed. For the Type I compatible system continuity development and microstructural features are dominated by thread-thread coalescence. In the Type II incompatible system continuity development and microstructural features are controlled by droplet-droplet coalescence. In the Type III compatibilized ternary system continuity and microstructural features are controlled by reduced droplet-droplet coalescence. Generation of fresh interface during droplet deformation results in a system that is only partially emulsified.

- A thread frequency ratio (TFR) is proposed as basic general parameter to classify the relative presence of fibers to droplets during melt mixing and hence the type of continuity development for a given system.

- A family of emulsification curves, prepared at a variety of dispersed phase concentrations, can be used as a powerful tool to estimate the efficacy of interfacial modifier migration to the interface in an immiscible polymer blend.

- Micelle formation in the PS dispersed in HDPE system can be virtually eliminated through the use of a symmetric (50:50) triblock or diblock copolymer.

RECOMMENDATIONS

- With the knowledge of a judicious control of a variety of parameters, future work should focus on the generation and stabilization of co-continuous blends with nano-structural morphology.

- A relationship needs to be established between the molecular architecture, chemical composition, molecular weight, etc. of copolymer interfacial modifiers and their efficacy on the modifying the morphology of co-continuous polymer blends.

- Relationship between morphology and mechanical properties of co-continuous blends, noncompatibilized and compatibilized, should be explored. Testing temperature could cover the range from room temperature to above glass transition temperature.

- Previous work in this laboratory has shown that the elasticity of the polymer phase has a strong influence on the development of dual phase continuity. Future work should consider the development of a comprehensive model incorporating both elastic and viscous effects.

CHAPTER 9 REFERENCES

Akiyama, S., INOUE, T and NISHI, T. (1979). *Polymer Blends- Compatibility and Interface*, CMC. press, Tokyo.

ALLEN, G. (1985). *Polymer*, **26**, 1248.

ANASTASIADIS, S. H., GANCARZ, I and KOBERSTEIN, J.T. (1989). Compatibilizing effect of triblock copolymers: added to the polymer/polymer interface. *Macromolecules*, **22**, 1449-1453.

ARENDS, C. B. (1992). Percolation in injection molded polymer blends. *Polym. Eng. Sci.*, **32**, 841-844.

AVGEROPOULOS, G. N., WEISSERT, F. C., BIDDISON, P. H. and BÖHM, G. C. A. (1975). *Rubber Chemistry and Technology*, **49**, 93.

BARTHÈS-BIESEL, D., and. ACRIVOS, A. A. (1973). *J. Fluid Mech.*, **61**, 1.

BENTLEY, B. J. and LEAL, L.G. (1986). *J. Fluid Mech.*, **167**, 219.

BOULLOUX, A., ERNST, B., LOBBRECHT, A. and MULLER, R. (1997). *Polymer*, **38**, 4775.

BOURRY, D., and FAVIS, B. D. (1998). Cocontinuity and phase inversion in HDPE/PS blends: influence of interfacial modification and elasticity. *J. Polym. Sci. Polym. Phys.*, **36**, 1889-1899.

BOUSMINA, M., and MULLER, R. (1993). *J. Rheol.*, **37**, 663.

CHAPPELAER, D. C. (1964). Interfacial tension between molten polymers, Polymer Preprints, 32, 99-108.

CHIN, H. B., and HAN, C. D. (1979). *J. Rheol.*, **23**, 557.

CHO, K., JEON, H. K., PARK, C. E., KIM, J. and KIM, K. U. (1996). *Polymer*, **37**, 1117.

COOK, W. D., ZHANG, T., MOAD, G., VAN DEIPEN, G., CSER, F., FOX, B. and O'SHEA, M. (1996). *J. Appl. Polym. Sci.*, **62**,1699.

COULALOGLOU, C. A. and TAVLARIDES, L. L. (1977). *Chem. Eng. Sci.*, **32**, 1289.

COX, R. G. (1969). The deformation of a drop in a general time-dependent flow. *J. Fluid Mech.*, **37**, 601-623.

DAVID, B., KOZLOWISKI, M. and. TADMOR, Z. (1993). *Polym. Eng. Sci.*, **33**, 227.

DE BRUIJN R. A. (1989). PhD thesis, Eindhoven University of Technology, The Netherlands.

DE ROOVER, B., DEVAUX, J. and LEGRAS, R. (1997). PamXD,5/PP-g-MA blend. II.rheology and phase inversion location. *J. Polym. Sci., Polym. Chem.*, **35**, 917-925.

DJAKOVIC, L., DOKIC, P., RADIVJEVIC, P., SEFER, I. AND SOVILJ, V. (1987). Action of emulsifiers during homogenisation of oil/water emulsions. *Colloid and Polym. Sci.*, **265**, 993-1000.

EINSTEIN, A. (1911). *Ann. Physik.*, **19**, 289 (1906), *Ibid.*, **34**, 591.

ELMENDORP, J. J. and VAN DER VEGT, A. K. (1986). A study on polymer blending microrheology: part IV: The influence of coalescence on blend morphology origination. *Polym. Eng. Sci.*, **26**, 1332-1338.

ELEMANS, P. H.,. JANSSEN, J. M. and MEIJER,H. E. H. (1990). The measurement of interfacial modifier in polymer/polymer systems: The breaking thread method. *J. Rheol.*, **34**, 1311-1326.

FAVIS, B .D. (1992). *Makromol. chem. Macromol. symp.*, **56**, 143.

FAVIS, B. D. (1990). The effect of processing parameters on the morphology of an immiscible binary blends. *J. Appl. Polym. Sci.*, **39**, 285-300.

FAVIS, B. D., and Chalifoux, J. P. (1988). Influence of composition on the morphology of polypropylene/polycarbonate blends. *Polymer*, **29**, 1761-1767.

FAVIS, B. D., and Willis, J. M. (1990). *J. Polym. Sci., Polym. Phys. Ed.*, **28**, 2259.

FAVIS, B. D. (1994). Phase size/interface relationships in polymer blends: the emulsification curve. *Polymer*, **35**, 1552-1555.

FAVIS, B. D., CIGANA, P., MATOS, M., and TREMBLY, A. (1997). Factors influencing the efficacy of an interfacial modifier for the interface in an immiscible polymer blend. *The Canadian Journal of Chemical. Engineering*, **75**, 273-280.

FAVIS, B. D., SARAZIN. P. and Li, J. (2001). *Provis US Patent*.

FAYT, R., JÉRÔME, R. and TESSIÉ, PH. (1989). Molecular design of multicomponent polymer systems. XIV. Control of the mechanical properties of polyethylene/polystyrene

blends by block copolymer. *J. Polym. Sci., Polym. Phys.*, **27**, 775-793.

FAYT, R., JÉRÔME, R. and TESSIÉ, PH., Characterization and control of control at interface in emulsified incompatible blends. *Polym. Eng. Sci.*, **27**, 328-334.

FAYT, R., JÉRÔME, R. and TESSIÉ, PH. (1986). Molecular desigh of multicomponet polymer systems. XIII. Control of morphology of polyethylene/polystyrene blends by block copolymers. *Makromol. Chem.*, **187**, 837-852.

FAYT, R., JÉRÔME R. and TESSIÉ, PH. (1986). Molecular design of multicomponent polymer systems. XII. Direct observation of the location of a block copolymer in low density polyethylene/polystyrene blends. *J. Polym. Sci., Polym. Lett.*, **24**, 25-28.

FLORY, P. J. (1941). *J. Am. Chem. Soc.*, **63**, 3083.

FLUMERFELT, R. W. (1972). Drop breackup in simple shear fields of viscoelastic fluids. *Ind. Eng. Chem. Fundam.*, **11**, 312-318.

FLUMERFELT, R. W. (1980). *J. Colloid Interface Sci.*, **76**, 330.

FORTELNY, I. and KOVAR, J. (1989). *Eur. Polym. J.*, **25**, 317.

FORTELNY, I. and KOVAR. (1992). Effect of the composition and properties of components on the phase structure of polymer blends. J., *Eur. Polym. J.*, **28**, 85-90.

FORTELNY, I., CERNA, Z., BINKO, J., KOVAR, J. (1993). *J. Appl. Polym. Sci.*, **48**, 1731.

GAUTHIER, F., GOLDSMITH, H. L. and MASON, S. G. (1971). *Rheol. Acta*, **10**, 344.

GERGEN, W. P. and DAVISON, S. (1977). *U.S. Patent* 4,041,103.

GHODGAONKAR, P. G. and SUNDARARAJ, U. (1996). *Polym. Eng. Sci.*, **36**, 1656.

GODDARD, J. D. and. MILLER, C. (1967). *J. Fluid Mech.*, **28**, 657.

GRACE, H. P. (1982). *Eng. Found. Res. Conference Mixing 3rd*. N. H. Andover (1971), republished as Dispersion Phenomena in High Viscosity Immiscible Fluid Systems and Application of Static Mixers as Dispersion Devices in Such Systems, *Chem. Eng. Commun.*, **14**, 225-277.

GRAEBLING, D. and MULLER, R. (1990). *J. Rheol.*, **34**, 193.

GUBBELS, F., JÉRÔME R., et al. (1994). *Macromolecules*, **27**, 1972.

HAN, C. D. and FUNATSU, K. (1978). *J. Rheol.*, **22**, 113.

HAMMERSLEY, J. M. (1957). *Proc. Cambridge Philos. Soc.*, **53**, 642.

HOURSTON, D. J. and SHÄFER, F-U. (1996). *Polymer*, 37, 3521.

HO, R. M., WU, C. H. and SU, A. C. (1990). *Polym. Eng. Sci.*, **30**, 511.

HSU, W. Y. and WU, S. (1993). Percolation behaviour in morphology and modulus of polymer blends. *Polym. Eng. Sci.*, 33, 293-302.

HU, W., KOBERSTEIN, J. T., LINGELSER, J. P. and GALLOT, Y. (1995). Interfacial tension reduction in polystyrene/poly(dimethylsiloxane) blends by the addition of poly(styrene-b-dimethylsiloxane). *Macromolecules*, **28**, 5209.

JEELANI, S. A.K. and HEARTLAND, S. (1991). *Chem. Eng. Sci.*, **46**, 1807.

JORDHAMO, G. M., MANSON, J. A. and SPERLING, L. H. (1986). Phase continuity and inversion in polymer blends and simultaneous interpenetrating networks. *Polym. Eng. Sci.*, **26**, 517-524.

KIRKPATRICK, S.(1973). *Rev. Mod. Phys.*, **45**, 574.

KAMAL, M. R., LAI-FOOK, R. and DEMARQUETTE, N. R. (1994). *Polym. Eng. Sci.*, **34**, 1834.

LAMB, H. (1932). *Hydrodynamics*, 6th ed., Dover Press, New York.

LEE, J. K. and HAN, C. D. (1999). *Polymer*, **40**, 2521.

LEPERS, J-C., FAVIS, B. D. and TABAR, R. J. (1997). The relative role of coalescence and interfacial tension in controlling dispersed phase size reduction during the compatibilization of polyethylene terephthalate/polypropyrene blends. *J. Polym. Sci., Polym. Phys.*, **35**, 2271-2280.

LEVITT, L. and MACOSKO, C. W. (1996). *Polym. Eng. Sci.*, **36**, 1647.

LEVON, K., MARGLINA, A. and PATASHINSKY, A. Z. (1993). *Macromolecules*, **26**, 4061.

LIANG, H., and FAVIS, B. D. (1997). Surface modification strategies for multicomponent polymer systems. 2 Study of the interfacial tension and morphology of linear-low density polyethylene/poly(vinyl chloride) blends. *J. Ind. Eng. Chem. Research*, **36**, 1211-1217.

LUCIANI, A., CHAMPAGNE, M. F. and UTRACKI, L. A. (1996). *Polym. Networks Blends*, **6**, 51.

LYNGAAE-JORGENSEN, J. and UTRACKI, L. A. (1991). Dual phase continuity in polymer blends. *Makromol. ChemiMacromol. symp.*, **48/49**, 189-209.

MARGOLINA, A. and WU, S. (1988). Percolation model for brittle-tough transition in nylon/rubber blends. *Polymer*, **29**, 2170-2173.

MARGOLINA, A. (1990). *Polym. Commun.*, **31**, 95.

MATOS, M., and FAVIS, B. D. and LOMELLINI, P. (1995). Interfacial modification of polymer blends: the emulsification curve. Part I: influence of molecular weight and chemical composition of the interfacial modifier. *Polymer*, **36**, 3899-3907.

MAXWELL, B. and JASSO, G. L. (1983) *Polym. Eng. Sci.*, **23**, 614.

MCKNIGHT, W. J., LENZ, R. W., MUSTO, P. V. and SOMANI, R. J. (1985). Binary alloys of nylon 6 and ethylene-methacrylic acid copolymers: morphological, thermal and mechanical analysis. *Polym. Eng. Sci.*, **25**, 1124-1134.

MEKHILEF, N., FAVIS, B. D. and CARREAU, P. J. (1997). Morphological stability, interfacial tension and dual phase continuity in polystyrene/polyethylene blend. *J. Polym. Sci., Polym. Phys.*, **35**, 293-308.

MEHTA, A. and ISAYEV, A. I. (1991). *Polym. Eng. Sci.*, **31**, 971.

MEIJER, H. E. H., LEMSTRA, P. J.and ELEMANS, P. H. M. (1988). *Makromol. Chem., Makromol. Symp.*, 16, 113.

MILES, I. S. and ZUREK, A. (1988). Preparation, structure, and properties of two phase co-continuous polymer blends. *Polym. Eng. Sci.*, **28**, 796-805.

MURALIDHAR, R. and RAMKRISHNA, D. (1988). *6th Eur. Conf. Mixing*, 213.

NOBILE, M. R., AMENDOLA, E. and NICOLAIS, L. (1989). *Polym. Eng. Sci.*, **29**, 244.

OLABISHI, L., ROBESON, M. and SHAW, M.T. (1979). *Polymer-Polymer Miscibility*, Academic Press, New York.

OLDROYD, J. G. (1955). *Proc.* Roy. Soc., London, **A232**, 567.

PALIERNE, J. F. (1990). *Rheol. Acta*, **29**, 204.

PATTERSON, H. T., HU, K. H. and GRINDSTAFF, T. H. (1971). Measurement of interfacial and surface tensions in polymer systems. *J. Polym. Sci., Part C* **34**, 31-43.

PAUL, D. P. and BARLOW, J. W. (1980). *J. Makromol. Sci. Rev. Macromol. Chem.*, **C18**, 109.

PAUL, D. P. and BUCKNALL, C. B. (2000) *Polymer Blends*, Vols. 1 and 2, Wiley-Interscience, New York.

PLOCHOCKI, A. P., DALI, S. S. and ANDREWS, R. D. (1990) *Polym. Eng. Sci.*, **30**, 741.

RAMKRISHNA, D.(1985). *Rev. Chem. Eng.*, **3**, 49.

RAY, I., and KHASTGIR, D. (1993). Correlation between morphology with dynamic

mechanical, thermal, physicomechanical properties and electrical conductivity for EVA-LDPE blends. *Polymer*, **34**, 2030-2037.

RAYLEIGH, J. W. S. (1879). *Proc. London Math. Soc.*, **10**, 4.

ROE, R. J. (1969). *J. Coll. Interf. Sci.*, **31**, 228.

ROLAND, C. M. and BÖHM, G. G. A. (1984). *Polym. Sci., Polym. Phys.*, **22**, 79.

ROSCOE, R. (1967). *J. Fluid Mech.*, **28**, 273.

RUMSCHEIDT, F. D. and MASON, S. G. (1961). *J. Colloid. Sci.*, **16**, 238.

SAKELLARIOU, P., EASLMOND, G. C. and MILES, I. S. (1989). Interfacial activity of polycarbonate/polystyrene graft copolymers in polycarbonate/polystyrene blends. *Polymer*, **34**, 3037-3047.

SCHOLZ, P., FROELICH, D. and MULLER, R. (1989). *J. Rheol.*, **33**, 481.

SCHUGENS, CH., MARQUET, V., GRANDFILS, C., JEROME R. and TEYSSIE, PH.(1996). *Polymer*, **37**, 1027.

SERPE, G., JARRIN, J. and DAWANS, F. (1990). *Polym. Eng. Sci.*, **30**, 553.

SMOLUCHOWSKI, M. (1916). *Physik. Z.*, **17**, 557.

SMOLUCHOWSKI, M. (1917). *Z. Physik. Chem.*, **92**, 129.

STEINMANN, S., GRONSKI, W. and FRIEDRICH, C. (2001). Co-continuous polymer

blends: influence of viscosity and elasticity ratios of the constituent polymers on phase inversion. *Polymer*, **42**, 6619-6629.

STAUFFER, D. (1979). *Scaling theory of percolation clusters, Physics Report*, **54**, 1.

STONE, H. A., BENTLEY, B. J. and LEAL, L. G. (1986). An experimental study of transient effects in the breakup of viscous drops. *J. Fluid Mech.*, **173**, 131-158.

SUNDARARAJ, U. and MACOSKO, C. W. (1995). Drop breakup and coalescence in polymer blends: the effects of concentration and compatibilization. *Macromolecules*, **28**, 2647-2657.

TAYLOR, G. I. (1932). The viscosity of a fluid containing small drops of another fluid. *Proc. Roy. Soc.*, **A, 138**, 41-48.

TAYLOR, G. I. (1934). The formation of emulsions on definable fields of flow. *Proc. Roy. Soc.*, **A, 146,** 501-523.

TCHOUDAKOV, R., BREUER, O., NARKIS, M. and. SIEGMANN, A. (1996). *Polym. Eng. Sci.*, **36**, 1336.

TJONG, S. C., LIU, S. L. and LI, K. R. (1996). *J. Mater. Sci.*, **31**, 479.

TOKITA, N. (1977). Analysis of morphology formation in elastomer blends. *Rubber Chem. Technol.*, **50**, 292-300.

TOMOTIKA, S. (1935). On the stability of cylindrical thread of a viscous liquid surrounded by another viscous fluid. *Proc. Roy. Soc. London*, **A, 150**, 322-337.

THORNTON, B. A., VILLASENOR, B. G. and MAXWELL, B.(1980). *J. Appl. Polym. Sci.*, **25**, 653.

UTRACKI, L. A. (1989). *Polymer Alloys and Blends*, Hanser Publishers, New York, P180.

UTRACKI, L. A. (1991). On the viscosity-concentration dependence of immiscible polymer blends. *Journal of Rheology*. **35**, 1615-1637.

VAN OENE, H. (1972). Modes of dispersion of viscoelastic fluids in flow. J. Colloid Interface Sci., 40, 448-467.

WATKINS, V. H. and HOBBS, S.Y. (1993). Determination of interfacial tensions between BPA polycarbonate and styrene-acrylonitrile copolymers from capillary thread instability measurements. *Polymer*. **34**, 3955-3959.

WHITMOER, M. D. and NOOLANDI, J. (1985). Theory of micelle formation in block copolymer/homopolymer blends. *Macromolecules*, 18, 657-665.

WILLEMS, R. C., POSTHUMS DE BOER, A., VAN DAM, J. and GOTSIS, A. D. (1999). *Polymer*, **39**, 5879.

WILLIS, J. M. and FAVIS, B. D. (1988). Processing-morphology relationships of compatibilized polyolefin/polyamide blends. *Polym. Eng. Sci.*, **28**, 1416-1426.

WILLIS, J. M., FAVIS, B. D. and LUNT, J. (1990). Reactive processing of polystyrene-co-maleic anhydride/elastomer blends: processing-morphology-property relationships. *Polym. Eng. Sci.*, **30**, 1073-1084.

WU. S. (1987). Formation of dispersed phase in incompatible polymer blends: interfacial and rheological effects. *Polym. Eng. Sci.*, **27**, 335-343.

VAN DE VEN, T. G. M. (1989). *Colloidal Hydrodynamics*, Academic Press, New York.

VAN GISBERGEN, J. (1991). PhD Thesis, Eindhoven University of Technology, Eindhoven, The Netherlands.

VAN OENE, H. (1972). *J. Coll. Interf. Sci.*, **28**, 1453.

VAN OENE, H. (1978). *J. Coll. Interf. Sci.*, **40**, 448.

VEESTRA, H., VERKOOIJEN, P. C. J., VAN LENT, B. J. J.,VAN DAM, J., POSTHUMA DE BOER, A. and NIJHOF, A. H. J. (2000). *Polymer*, **41**, 1817.

VEESTRA, H., NORD, B., VAN DAM, J. and POSTHUMA DE BOER, A. (1999). *Polymer*, **40**, 5223.

YORSHIDA, M., MA, J. J., MIN, K., WHITE, J. L. and QUIRK, R. P. (1990). *Polym. Eng. Sci.*, **30**, 30.

XIE, H. Q., XU, J.and ZHOU, S. (1991). *Polymer* **32**, 95.

ZIFF, Z. M. (1986). *Macromolecules*, **19**, 2513.

ANNEX

This work is an initial exploratory study on reactive compatibilization on polyamide/polystyrene blend system.

POLYAMIDE (PA)/POLYSTYRENE (PS) AND POLYAMIDE (PA)/POLYSTYRENE (PS)/MALEATED STYRENE-BUTYLENE-STYRENE (SEBS-g-MA) BLENDS

Abstract: Blends of polyamide (PA)/polystyrene (PS) with and in absence of compatibilizer were investigated over the entire range of compositions in steps of 10%PA. It was observed that PA/PS blends displayed large domain size when PA and PS were the dispersed phase, respectively. The co-continuous region for the non-compatibilized blend appears in the PA composition from 45% to 55% with relatively rough morphological structures. The morphological features and interfacial situation was observed by scanning electron microscopy (SEM). Improved compatibilization of blends of PA/PS was achieved by addition of a maleated styrene- butylene-styrene (SEBS-g-MA) which is miscible in the PS phase and has a functional group which is capable of reacting with the amine end group in the polyamide phase. The graft copolymer formed, by reaction between SEBS-g-MA and polyamide-6 during melt mixing, strongly lowers the interfacial tension between the two polymers (from 9.6 to 3.0mN/m), and reduces the coalescence of the dispersed phase and coarsening of the co-continuous structure, thus leading to a much fine dispersed phase size and co-continuous structures. The effect of compatibilizer content on domain size of dispersed phase was determined by emulsification curves at a fixed ratio of PA to PS (90%PA/10%PS and 10%PA/90%PS). A value of about 10 parts of interfacial modifier based on the dispersed phase is obtained as the interface is saturated. Meanwhile, the co-continuous regions of the compatibilized and noncompatibilized system are found to be identical, ranging from 45 to 55 % PA.

Introduction

Reactive compatibilization of immiscible blends is a useful strategy to develop new material with a desirable combination of properties. Reactive compatibilization involves an in situ reaction of functionalized components during processing to form block or graft copolymers at the interfaces between the phases (1-12). Polyamide is an attractive class of engineering materials due to their excellent strength and stiffness, low friction, chemical and wear resistance. However, polyamide is moisture sensitive. Polystyrene is insensitive to moisture, excellent electrical insulation and durable to various weathering conditions. But PS is poor in solvent resistant. Hence, PA/PS blends are expected to complement each disadvantage while maintaining the good properties of each other. However, PA and PS are thermodynamically immiscible in whole temperature and in whole composition ranges. Fortunately, the inherent chemical functionality of polyamide makes them an attractive candidate for modification. Compatibility problems are often overcome by using a suitable compatibilizing agent. Such compatibilizing agent can physically miscible with one phase of the blend but has chemical functionality to react with another phase. This situation is expected to lead to an efficient reduction in the dispersed phase domain size through a reduction in interfacial tension (13-14) and an increased resistance to coalescence through steric stabilization (15-17) at the interface. In this study, an attempt is to incorporate a functionalized triblock copolymer as a reactive compatibilizer into blends of PA6 and PS, to evaluate the extent of emulsification that occurs during melt mixing and to examine the influence of the compatibilization on the dual phase continuity.

Experimental

Materials

The polymers used in this study were polyamide in pallet form from BASF company, polystyrene in pallet form from Dow Chemical. These two polymers were dried at 80°C overnight in a vacuum oven to remove adsorbed water before processing. The SEBS functionalized with 2wt% MA onto the hydrocarbon chains, designated as SEBS-g-MA,

is Kraton FG 1901, supplied by Shell USA. Some properties obtained for these polymers are given in Table 1

Rheological Analysis

Rheological characterization of the different homopolymer was carried out using a Rheometric Scientific constant stress rheometer for PA, PS and SEBS-g-MA. The experiment was performed in parallel-plate geometry with a gap of about 1.4mm under a nitrogen atmosphere at a temperature of 250°C and in the range of 0.01-30Hz frequency. These data are listed in Table 2.

Interfacial tension measurement

This technique which is based on the observation of capillary instability development has been widely used to determine the interfacial tension of the polymer blends. It consists of inserting a thread of one polymer between two films of another polymer. Threads of PA were produced by drawing out the molten PA pellets on a hot plate while carefully controlling the heating temperature. A PS film with a thickness of around 0.3mm was obtained by compressing PS pellets at 250°C for 3 min. The SEBS-g-MA can neither be mixed with PA thread (the retraction force in the thread could not be removed even though the thread annealed at 100°C for 24 hr before testing) nor can be mixed with PS film (the film turned into opaque). The thread containing SEBS-g-MA was obtained by putting SEBS-g-MA thread into a SEBS-g-MA saturated THF solution for 8 hrs and then the PA thread was dried in a vacuum oven at the temperature 50°C for 8 hrs. Before testing the threads of PA were annealed for 24 hrs at 90°C to permit stress relaxation. The total sandwich sample was put between a glass slide and a cover slip. Then it was heated to a temperature in a Mettler hot stage model FP 82-HT equipped with a FP central processor. The direct observation of the evolution of the thread shape was carried out on a Nikon optical transmission microscope. The whole process was recorded on a VHS video recorder. The measurement of evolution of the distortion amplitude of the thread over time as well as the wavelength was obtained by Visilog 4.1.3 image analysis software. Usually two or three distortions were monitored. Five tests were necessary for each PA and PS pair. The typical error in the interfacial tension measurement was about

±10%. Details concerning the theoretical backgrounds can be found in previous works (13,18-19).

Blending

Mixtures of PA and PS, with and in absence of SEBS-g-MA were melt blended in a Brabender mixing chamber using blade type rollers. A complete composition range was prepared from100% PS to 100%PA in steps of 10% (weight). A typical blending experiment consisted of the following steps. The temperature of mixing chamber was initially set at 250°C, while the blades were turning at 50 r.p.m. In most case, 25 grams of the various polymers were dry blended together and introduced simultaneously to the Brabender mixing chamber. To limit oxidation during mixing, 0.2% Irganox B225 was added to each blend. Once all of the resin was added the blend was allowed to mix for 8 min under the constant flow of dry nitrogen. At the end of 8 min, the melt was rapidly dropped into a bath of liquid nitrogen to freeze in the morphology. The time required to feed the entire charge into the mixer was around 25 s. it should be noted that all concentrations are reported as weight fraction.

Solvent extraction

Selective solvent extraction of PS was performed in a Soxhlet extraction apparatus with tetrahydrofuran (THF) for 36 hrs. Extraction of PA was carried out at room temperature for about one week. Initially, the PA sample (about1 gram) was placed into a tube filled with100ml formic acid. The tube containing the PA sample was then shaken on a shaker for 48 hrs. Then the solution was poured away, fresh solvent was added and the sample was shaken again. This process was repeated three times, which was sufficient to attain a constant weight. Gravimetric method was used to determine the extent of co-continuity of PS (the same equation was used for PA) using the following equation:

$$\%continuity = \frac{(weight\ PS_{initial} - weight\ PS_{final})}{weigh\ PS_{initial}} \times 100 \qquad (1)$$

Scanning electron microscopy

Prior to SEM observation the samples were microtomed by a Reichert Jung Supercut microtome equipped with a glass knife to get plane surfaces for each specimen. For the non-compatibilized blends, the samples were microtomed at the room temperature. For the compatibilized blends, before microtoming, each sample was frozen in liquid nitrogen. While cutting, the surface of the sample was held at approximately -130°C to reduce the degree of surface deformation.

The microtomed samples were then treated with a suitable solvent to dissolve the minor phase present at the surface of the specimen. For the polyamide minor phase, this procedure consisted of soaking the specimen in formic acid in room temperature for four days. To dissolve the polystyrene minor phase the specimens were extracted in a soxhlet extractor with tetrahydrofuran (THF) for 36hrs. The extracted samples were dried in a vacuum oven for 48 hrs. The microtomed samples were coated with gold and palladium, and observed under a Jeol 840 scanning electron microscope operated at a working voltage of 10kV.

Image analysis

The semi-automatic image analyzer was used to measure the diameters of dispersed phase. The operation of this instrument has been described elsewhere (20). For each sample, approximately 150 - 200 diameter measurements were obtained from the SEM photomicrographs of the microtomed surfaces. Since the microtome does not happen to cut the dispersed phase at the equator and since it is necessary to correct for polydispersity, a correction factor (21) was applied to the diameters determined from SEM micrographs of microtomed surfaces. Number average diameters, d_n, and volume average diameters, d_v, were obtained. The typical error for the measurement of d_n and d_v is about ±10%

BET measurement

In order to characterize co-continuous blend morphology, A flowsorb BET instrument was used to measure the surface area and pore size of the extracted samples. When the nitrogen gas adsorbed on the surface of the sample monolayer adsorption is assumed. We

further assume that (1) the geometric shape of the pore is an interconnected cylinder; (2) the total volume of the pore is equal to that of extracted phase, and (3) the total surface area is that of the pore wall. Knowing the total amount of the nitrogen gas absorbed and cross section of the nitrogen molecule the total surface area can be estimated. With the above assumption and surface area measured the pore diameter, d, can be calculated using following equation,

$$d = \frac{4V}{S} \qquad (2)$$

where, V is the volume of extracted phase and S, the surface area of the sample. Prior to testing, a given amount of nitrogen gas was introduced to the instrument through a septum to calibrate the system. Sample testing was conducted at liquid nitrogen temperature (about -166°C). Further details of this technique are given in previous work (22).

Results and discussion

Rheology

Figure 1 shows the complex viscosity as a function of frequency/shear rate for PA, PS and SEBS-g-MA. The blends in this study were prepared at 50 rpm which is equivalent to the shear rate about $50s^{-1}$. The viscosity of SEBS-g-MA appears to be the highest among the three in the whole range of shear rates. PA and PS appear a plateau in low shear rate region while SEBS-g-MA does not.

Emulsification effect

The compatibilizing efficiency of the SEBS-g-MA graft copolymer in 90%PS/10%PA blends has been examined by evaluating PA domain sizes from emulsification curve. The volume average and number average diameter of PA domains are plotted in Figure 2 versus the added amount of SEBS-g-MA. The non-compatibilized 90%PS/10%PA shows a large size of dispersed phase (3.7μm in d_v and 1.9μm in d_n). Adding SEBS-g-MA to the blends significantly reduces the domain sizes at increasing compatibilizer concentration. The ternary blend containing a low compatibilizer content (3% SEBS-g-MA) show an

average d_v of 2.5μm and dn of 1.6μm. For the blends with higher amount of modifier (8% SEBS-g-MA), The average d_v and d_n decrease to about 2.3 μm and 1.5 μm, respectively. The minimum PA domain size (1.7μm in d_v and 1.3μm in d_n) is achieved at a critical copolymer concentration of about 10%SEBS-g-MA (based on the dispersed PA phase). Above the critical concentration, the domain size remains almost constant. For comparison purposes, Figure 3 illustrates the emulsification curve of 90%PA/10%PS. The results show that the critical concentration for 90%PA/10%PS is 10% SEBS-g-MA (based on the dispersed PS phase). The equilibrium diameter of dispersed PS in the 90%PA/10%PS blend is 1.5μm in d_v and 1.0μm in d_n, respectively. It is evident from Table 2 that the viscosity ratio for above blend systems is different (4.3 for PA dispersed in PS and 0.23 for PS dispersed in PA). The similar equilibrium diameter for the two systems indicates that interfacial modification appear to be the dominant factor for controlling the dispersed phase seize. Even the phase seize versus viscosity ratio dependence is less pronounced for a compatibilized blend system (23).

Co-continuity

1.Non-compatible system

Figure 4 illustrates the relationship between degree of continuity and composition of blend. The degree of continuity of the dispersed phase was determined using solvent dissolution. Formic acid can dissolve PA easily without any influence on PS, while THF can dissolve PS easily without any influence on PA. The blend containing 30%PS shows only 7% continuity after THF extraction. When the PS composition is increased to 40%, the level of continuity achieves 92%. A fully continuous structure is obtained at about 45%PS. The blend containing 60% PS was no longer self-supporting after the PS phase had been extracted, meaning that the PA was dispersed in the PS matrix. The 55%PS/45%PA blend did not fall apart upon extraction and the remaining structure is still in an integrate form upon solvent evaporation. When PA is extracted by formic acid the continuity of PA is 23% at20% PA and this increases to 85% at 40%PA. A fully continuous structure is obtained at about 50%PA after solvent extraction. The blend

containing 60%PA falls apart upon dissolution with formic acid. The 55%PA/45%PS blend did not fall apart upon extraction and the remaining structure has no indication of disintegration upon solvent evaporation. Formic acid solvent extraction further confirms that the region of dual phase continuity occurs in a concentration region approximately from 45% to 55%PS

2. Compatibilized system

Figure 5 illustrates the relationship between degree of continuity and composition for the compatible PA/PS blend system after solvent extraction. No continuity was observed up to about 30% PS. However, the degree of continuity of the sample arrives to 90% for the 40%PS/60%PA/20%SEBS-g-MA blend. Full continuity occurs at 45% PS. The sample has no indication of disintegration for the 55%PS/45%PA/20%SEBS-g-MA blend after extraction. However, the extracted sample does disintegrate for the 60%PS/40%PA/20%SEBS after extracting by THF. As the same reason mentioned before, at this composition the original continuous PA phase turns into discontinuous phase while the PS phase remains its continuous state. When PA is extracted by formic acid, there is no continuity for the 10%PA/90%PS/20%SEBS-g-MA blend. A level of 20% continuity is observed at 20%PA. The continuity increases to 83% at 40%PA and a fully continuous structure is obtained at about 45%PA. The sample appears in an integrate form for the 55%PA/45%/20%SEBS-g-MA blend after formic acid solvent extraction. The extracted structure disintegrates at 60%PA. The above observations indicate that the region of dual phase continuity is achieved in a PA composition of 45-55%. It is interesting to note that compatibilized and noncompatibilized blend systems show an identical co-continuous region.

Interfacial tension

The interfacial tension of uncompatibilized PA/PS was determined by thread breaking method and illustrated in Figure 6. From the slope of the straight line the interfacial tension obtained is 9.6 mN/m. Xing et al. (24) used same technique to measure the interfacial tension for PA/PS system at 230°C, a value of 8.4 mN/m was obtained.

Considering the error scale (± 15 %) for this technique, the above data can be regarded as identical.

For the compatibilized PA/PS blend, as described in the Experiment Section the PA thread containing SEBS-g-MA by melt mixing was not suitable for the testing due to the retraction stress, which could not be removed without deforming the thread. Therefore the PA thread was treated with a SEBS-g-MA saturated THF solution. It is believed that the surface of PA is completely surrounded by SEBS-g-MA molecules. The SEBS-g-MA reacted with PA during the test, which significantly reduced interfacial tension between PA and PS. A equilibrium value of 3.0 mN/m was obtained for the compatibilized PA/PS system (see Figure 7). The significant reduction of interfacial tension indicates that a graft copolymer is formed in situ through reaction of anhydride with the terminal amine groups of PA, thus:

SEBS-g-MA + H_2N-PA ⟶ SEBS-g-PA

This will be further discussed in *Morphology* part.

Morphology

1.Non-compatibilized system

Figure 8 shows scanning electron microscope photographs for non-compatibilized PA/PS blends. When PA composition less than 50% the dark areas correspond to extracted PA phase, and when PA is above 50% the dark areas correspond to extracted PS phase. For 10%PA/90PS, the dispersed PA phase forms discrete round spheres with a volume average particle diameter of 3.5μm. The particle size is increased significantly with increasing dispersed PA volume fraction (4.1μm in d_v for 20%PA/80%PS and 6.7μm in d_v for 30%PA/70%PS). This indicates a significant coalescence of the PA domains and the generation of a co-continuous structure at 45% PA. A narrow composition range of co-continuity has been observed (from 45%PA to 55%PA). When the system enters co-continuous region, the interfacial area and thus interfacial energy attains a maximum value. The spontaneous reduction of interfacial energy during melt processing is responsible for the rough morphological structure of the non-compatibilized PA/PS system. When the volume of PA is in excess of 60%, a droplet-type morphology

composed by a PS domain, surrounded by a PA matrix, is eventually formed. The PS domain size becomes smaller and smaller with decreasing PS volume fraction.

2. Compatibilized system

Figure. 9 shows that the morphology of compatibilized PA/PS blend system. A droplet/matrix morphology appears in 10%PA/90%PS/20%SEBS-g-MA, surrounded by the PS matrix. The domain size of PA (about less than 2μm in d_v) appears to be much smaller than that of non-compatibilized counterpart and changes little with increasing the PA volume fraction. The formation of graft copolymers at the PA/PS interface during melt processing results in a reduction in interfacial tension and stabilization against drop coalescence which are the causes for the reduction of particle size. As indicated by formic solvent extraction, the full co-continuity occurs at 45%PA/55%PS and the co-continuous structure maintains up to 55%PA. A droplets/matrix and thread/matrix morphology is observed when the system arrives to 60%PA. It is clear that this composition has already surpassed phase inversion point. Therefore, the phase inversion should be in the range of 55-60%PA.

The mechanism of formation of co-continuous morphology

1. Non-compatibilized PA/PS blend system

From above observation it is strongly suggested that the continuity development of the dispersed phase for the noncompatibilized blend system is basically through droplet-droplet coalescence. The same situation can be applied to the system in which the dispersed PS phase is in the PA matrix.

2. Compatible PA/PS blend system

The compatibilized PA/PS blend system shows the same % continuity/compositon relationship as the non-compatibilized PA/PS. This phenomenon seems to be contradictory to the previous study (25) in this laboratory. In that study, it was found that the partial continuity of dispersed PS phase in HDPE/PS blend compatibilized by SEBS triblock copolymer starts at a higher concentration than its incompatible counterpart due to reduced droplet-droplet coalescence. It should be noted that in current study the amount of SEBS-g-MA used is twice as much as required for the interfacial saturation.

The droplet will be deformed under the shear stress during melt blending and the deformed body will generate fresh interface. However, the copolymer in the mixer is sufficient enough to saturate the fresh interface. Under such condition the deformed body will be stabilized. Nevertheless, there is no indication of widening the region of co-continuity because the deformed dispersed phase will lead onset of co-continuity to a lower minor phase concentration. Figure 10 shows the droplets and thread-like dispersed PA phases in 30 %PA/70%PS/20%SEBS-G-MA blend. Therefore the mechanism of co-continuity development in this study could be more complicated.

Conclusions

The reaction between SEBS-g-MA and PA forms a graft copolymer in-situ, which locates at the interface between PA and PS. A three fold reduction of interfacial tension of the system has been observed. The reduction of coalescence is significant in the high concentration of dispersed phase.

The amount of copolymer in excess stabilizes the deformed body, resulting in a situation where droplets and threads co-exist. However, the region of co-continuity has not been changed by addition of interfacial modifier (from 45-55%PA).

References:

1. Baker, W. E., *Saleem. Polym. Eng. Sci.*, **27**: 1634 (1987).
2. Butta, E., Levita, G., Machetti, A., Lazzeri, A., *Polym. Eng. Sci.*, **26**: 63 (1986).
3. Chen, C. C., Fontan, E., Min, K., White, J. L., *Polym. Eng. Sci.*, **28**: 69 (1988).
4. Willis, J. M., Favis, B. D., *Polym. Eng. Sci.*, **30**: 17 (1990).
5. Molnar, A., Eisenberg, A., *Polymer*, **32**: 370 (1991).
6. De Roover, B., Devaux, J., Legras, R., *J. Polym. Sci., Polym. Chem.*, **35**: 917 (1997).
7. Cimmino, S., Coppola, F., D'orazio, L., Graco, R., Maglio, G., Malinconico, M., Mancarella, C., Martuscilli, E., Ragosta, G., *Polymer*, **27**: 1874 (1986).

8. Macknight, W. J., Lenz, R. W., Musto, P. V., Somani, R. *J.. Polym. Eng. Sci.*, **25**: 1124 (1985).
9. Braun, D., Illing, W., *Angew. Makromol. Chem.* **154**: 179 (1987).
10. Fairley, G., Prud'homme, R. E., *Polym. Eng. Sci.*, **27**: 1465 (1987).
11. Fayt, R, Teyssie, Ph., *J. Polym. Sci., Polym. Lett. Edn.*; **27**: 481 (1989).
12. Caldas, V., Brown, G. R., Willis, J. M., *Macromolecules*, **23**: 338 (1990).
13. Elemans, P. H. M., Janssen, J. M. H., Meijer, H. E. H., *J. Rheol.*; **34**: 1311 (1990).
14. Leibler, L., *Makromol. Chem. Makromol. Symp.*; **16**: 1 (1988).
15. Sundararaj, U., Macosko, C. W., *Macromolecules*, **28**: 2647 (1995).
16. BeckTan, N. C., Tai, S.-K., Briber, R. N., *Polymer*, **37**: 3509 (1996).
17. Milner, S. T., Xi, H. W., *J. Rheol.*, **40**: 663 (1996).
18. Tomotika, S., *Proc.R. Soc. London*, Ser. **A** 1935; **A**150: 322.
19. Liang, H., Favis, B. D., *Ind. Eng. Chem. Res.*, **36**: 1211 (1997).
20. Favis, B. D., Chalifoux, J. P., *Polym. Eng. Sci.*, **27**: 1591 (1987).
21. Saltikov, S. A., *Proceedings of the 2nd International Congress for Stereology*, Helias: New York, 1967.
22. Li, J., Favis, B. D., *Polymer*, **42**: 5047 (2001).
23. Willis, J. M., Caldas, V., Favis, B. D., *J. Mater. Sci.*, **26**, 4742 (1991).
24. Xing, P., Bousmina, M., Rodrigue, D., Kamal, M.R., *Macromolecules*, **33**: 8020 (2000).
25. Li, J., Ma, P, Favis, B. D., *Macromolecules*, (accepted).

Figure captions

1. Complex viscosity-frequency/shear rate relationship for PA, PS and SEBS-g-MA at 250°C.
2. Emulsification curve for 10%PA/90%PS blend modified by SEBS-g-MA copolymer.
3. Emulsification curve for 90%PA/10%PS blend modified by SEBS-g-MA copolymer.
4. Continuity-composition relationship for non-compatibilized PA/PS blends.
5. Continuity-composition relationship for compatibilized PA/PS blends.
6. Relative distortion amplitude versus time for PA thread imbedded in a PS matrix.
7. Relative distortion amplitude versus time for PA thread containing SEBS-g-MA copolymer imbedded in a PS matrix.
8. SEM micrographs for non-compatibilized PA/PS at 250°C.
9. SEM micrographs for compatibilized PA/PS at 250°C.
10. SEM micrograph for a 30%PA/70%PS/20%SEBS-g-MA blend at 250°C

Tables

Table 1. Characteristic properties of materials

Table 2. The rheological behavior of PA, PS and SEBS-g-MA (rpm=50, $\dot{\gamma}$=50 S^{-1}, T=250°C)

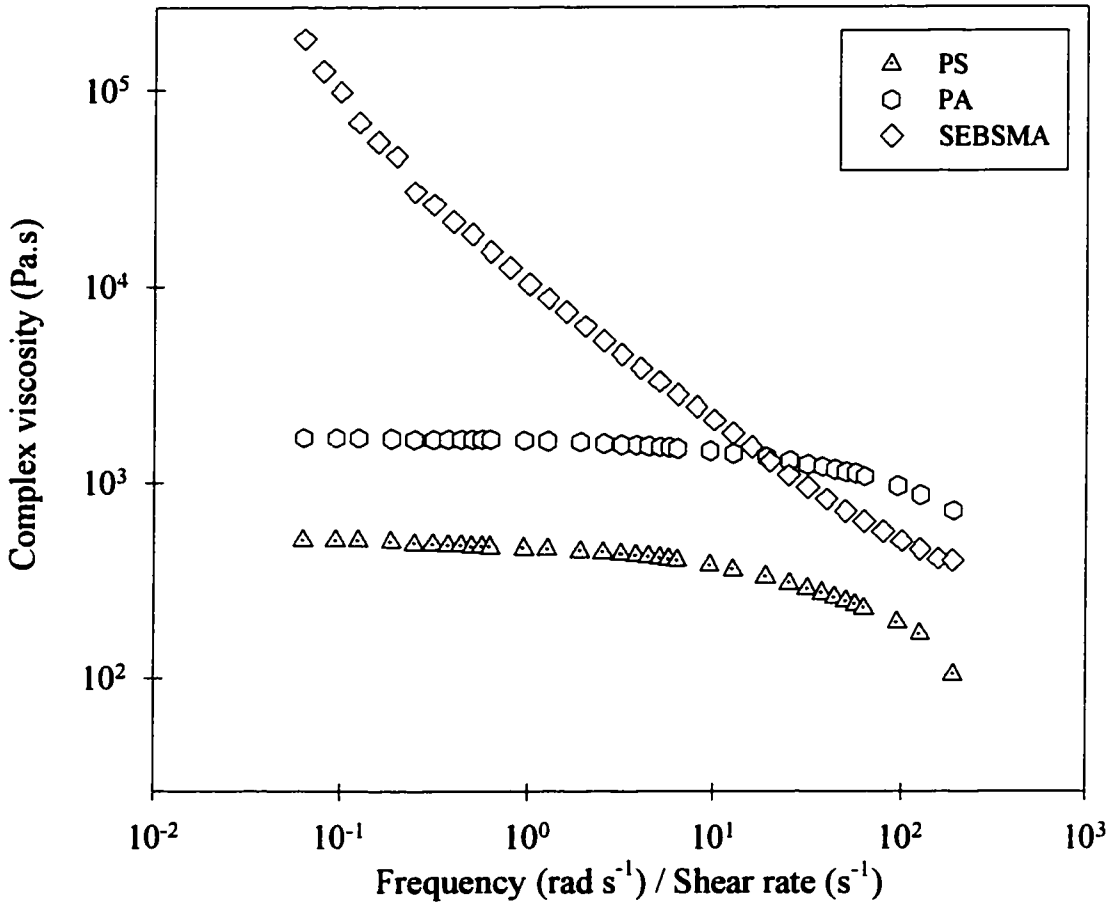

Figure 1. Complex viscosity-frequency/shear rate relationship for PA, PS and SEBS-g-MA at 250°C

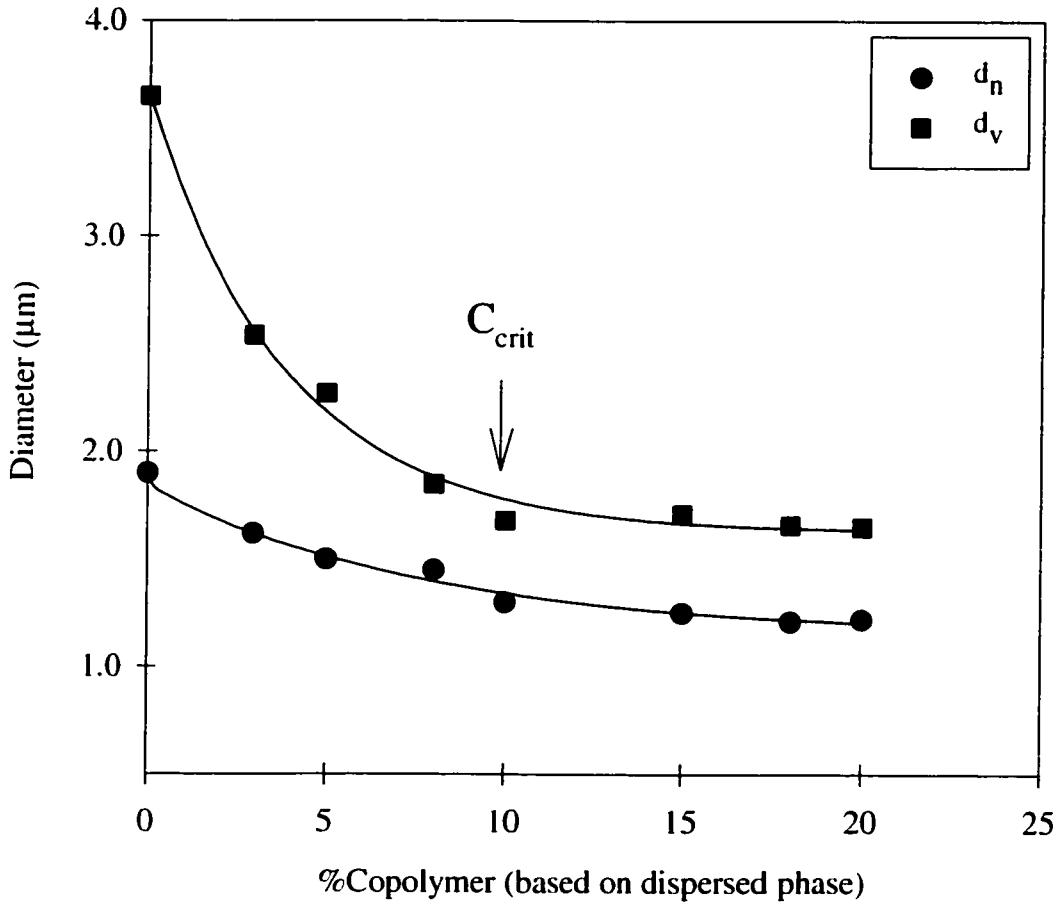

Figure 2 Emulsification curve for 10%PA/90%PS blend modified by SEBS-g-MA copolymer.

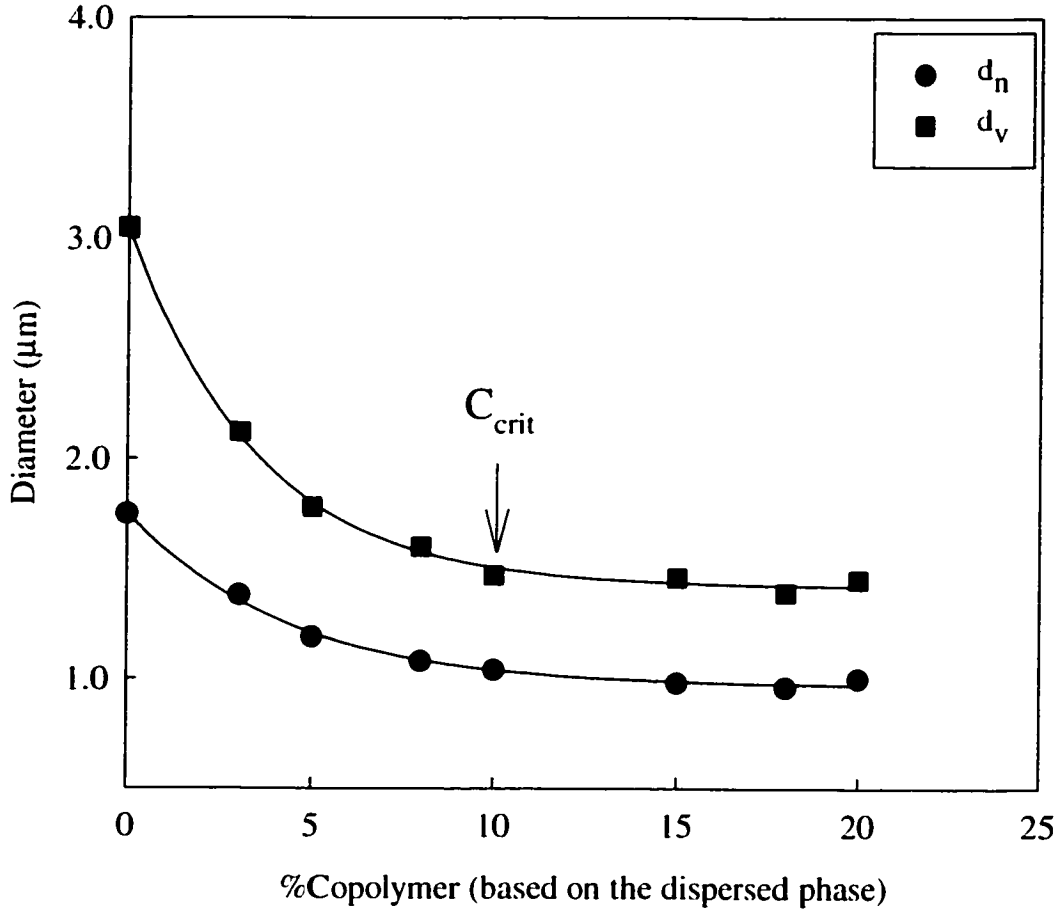

Figure 3 Emulsification curve for 90%PA/10%PS blend modified by SEBS-g-MA copolymer.

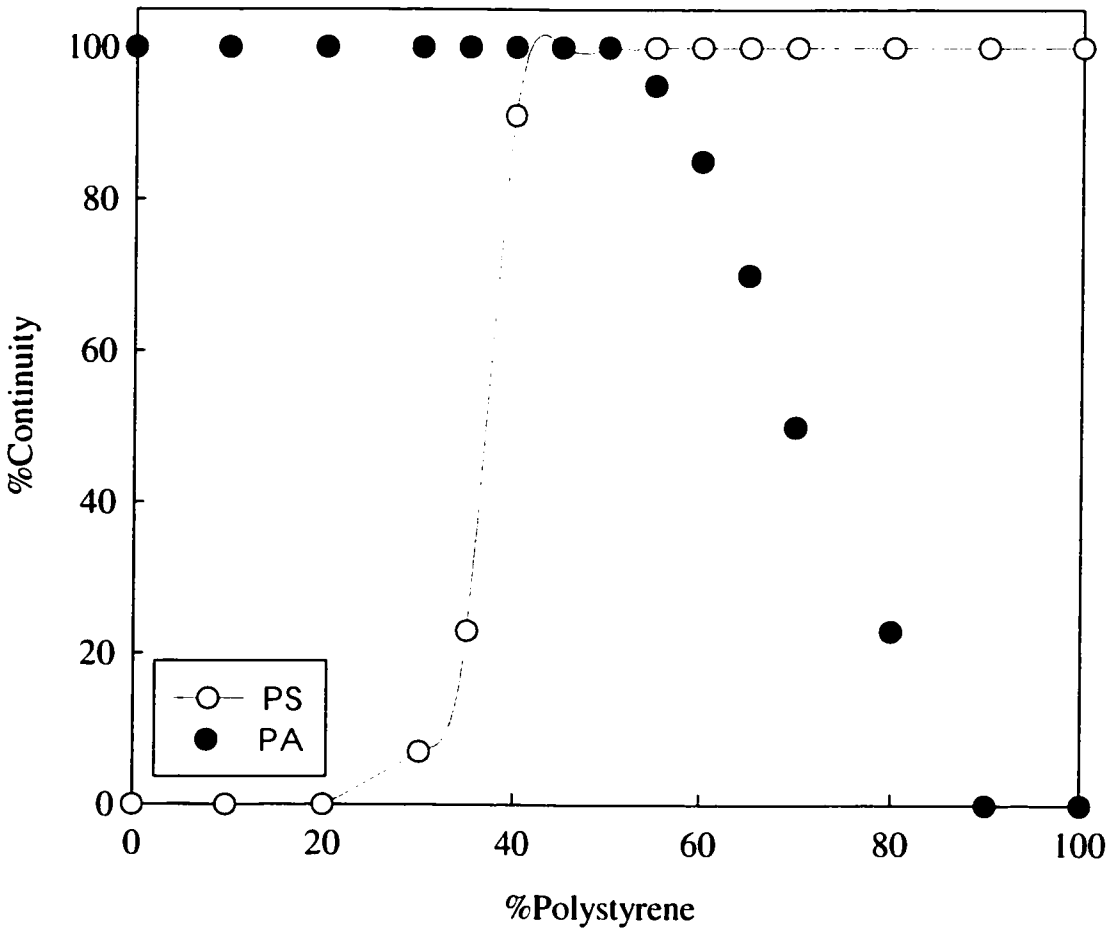

Figure 4 Continuity-composition relationship for non-compatibilized PA/PS blends

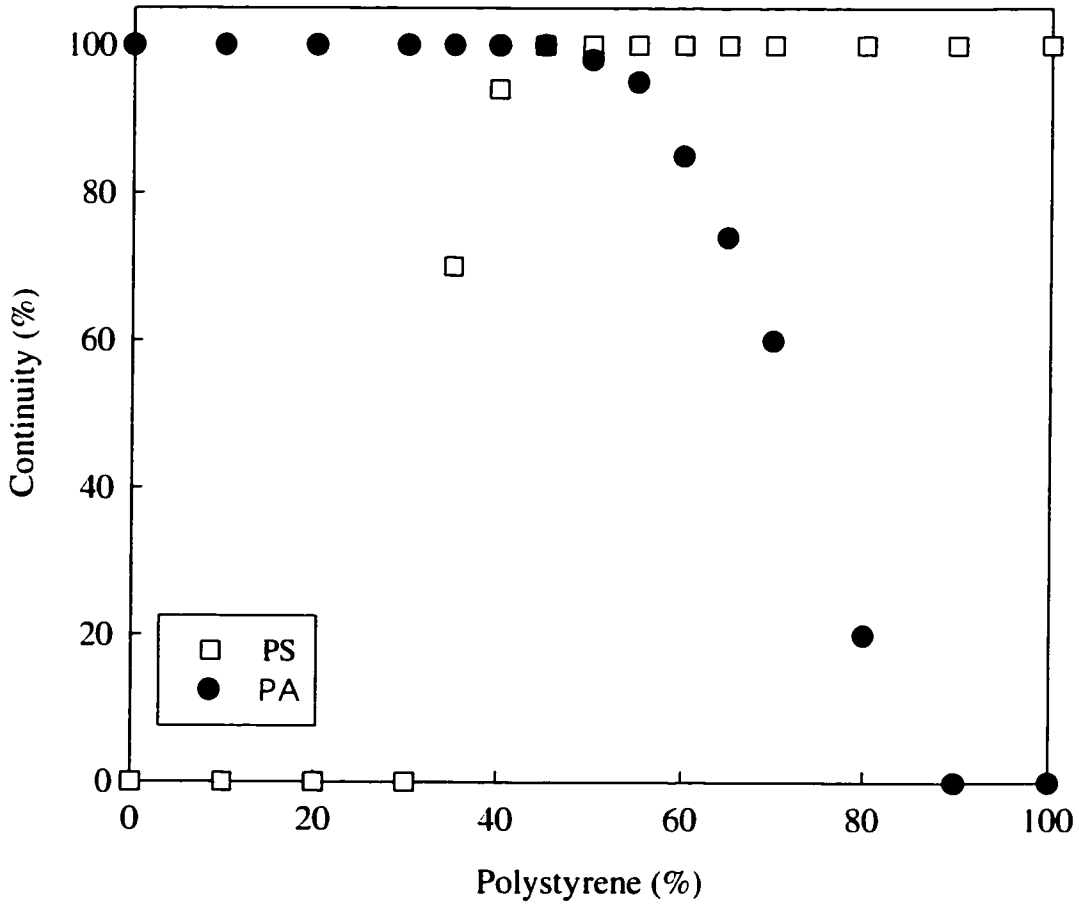

Figure 5 Continuity-composition relationship for compatibilized PA/PS blends.

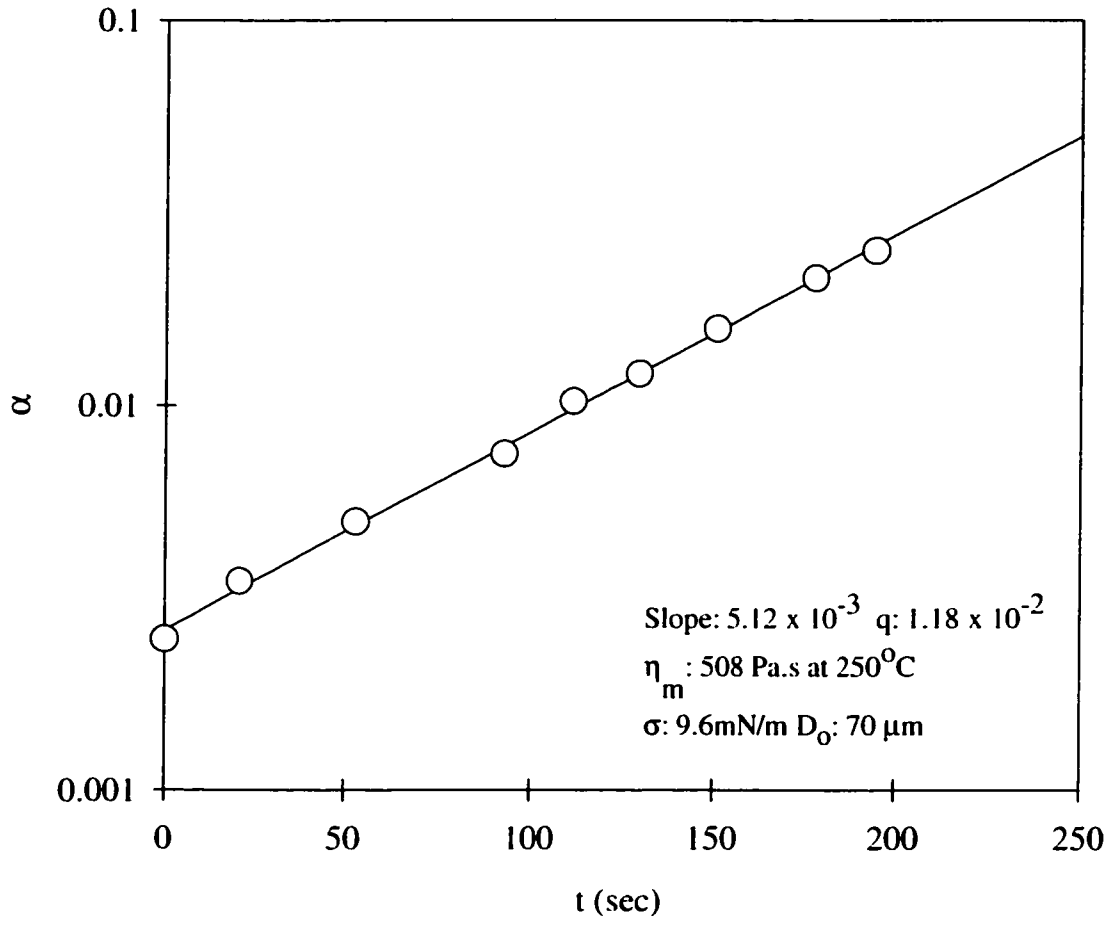

Figure 6 Relative distortion amplitude versus time for PA thread imbeded in a PS matrix.

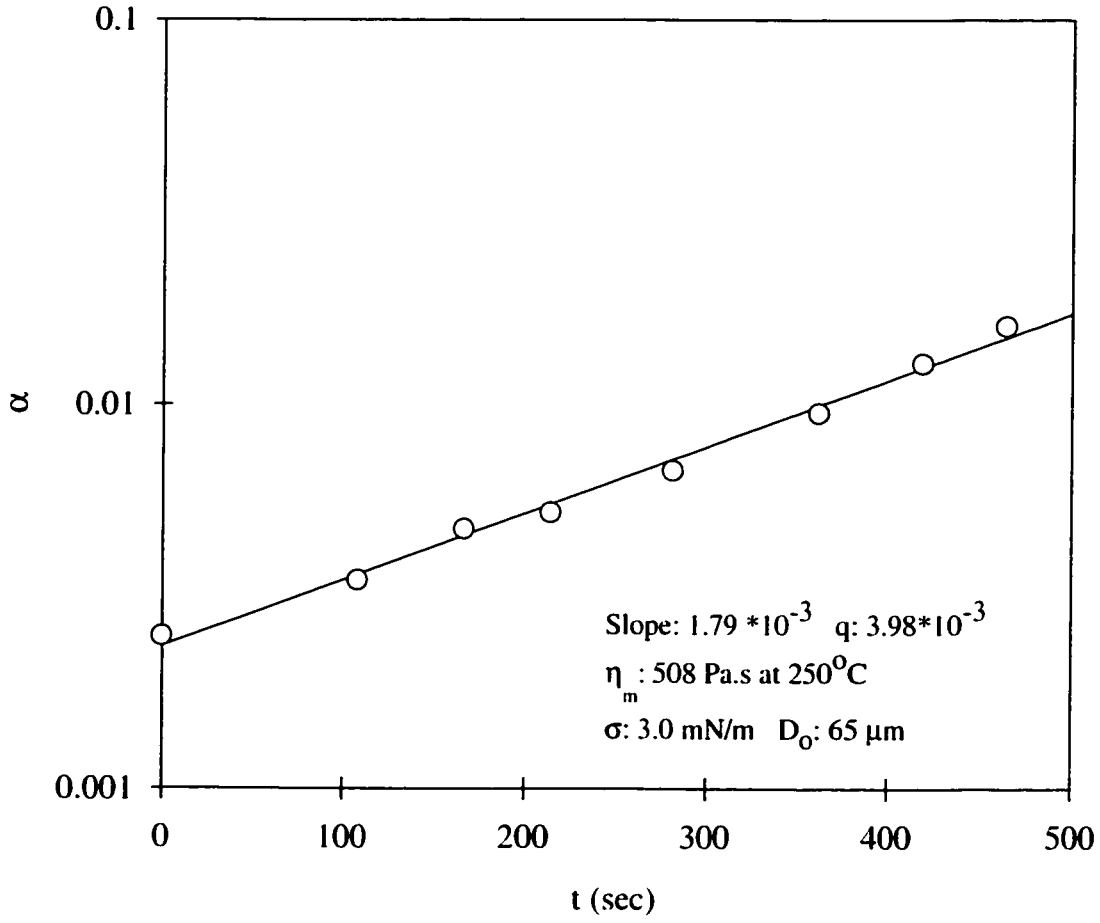

Figure 7 Relative distortion amplitude for PA thread containing SEBS-g-MA copolymer imbeded in a PS matrix

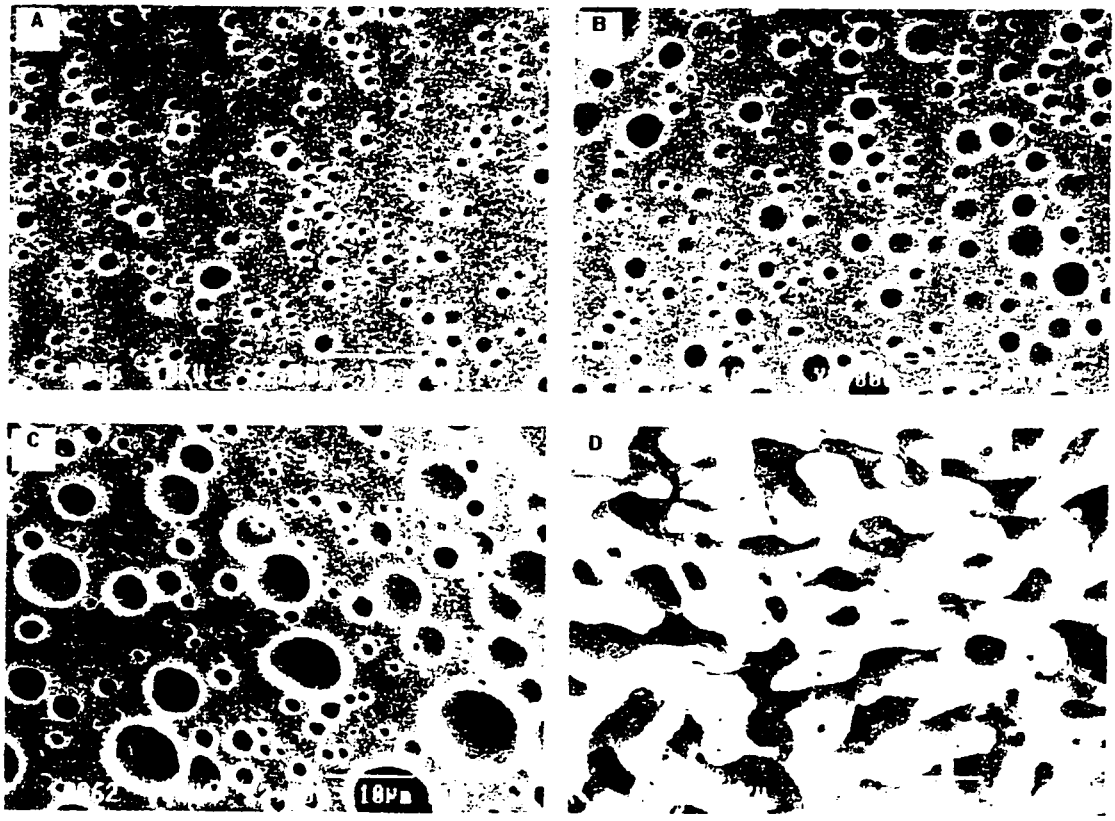

Figure 8. SEM micrographs for noncompatibilized PA/PS blends at 250°C. (A)10%PA/90%PS, (B) 20%PA/80%PS, (C) 30%PA/70%PS and (D) 45%PA/55%PS

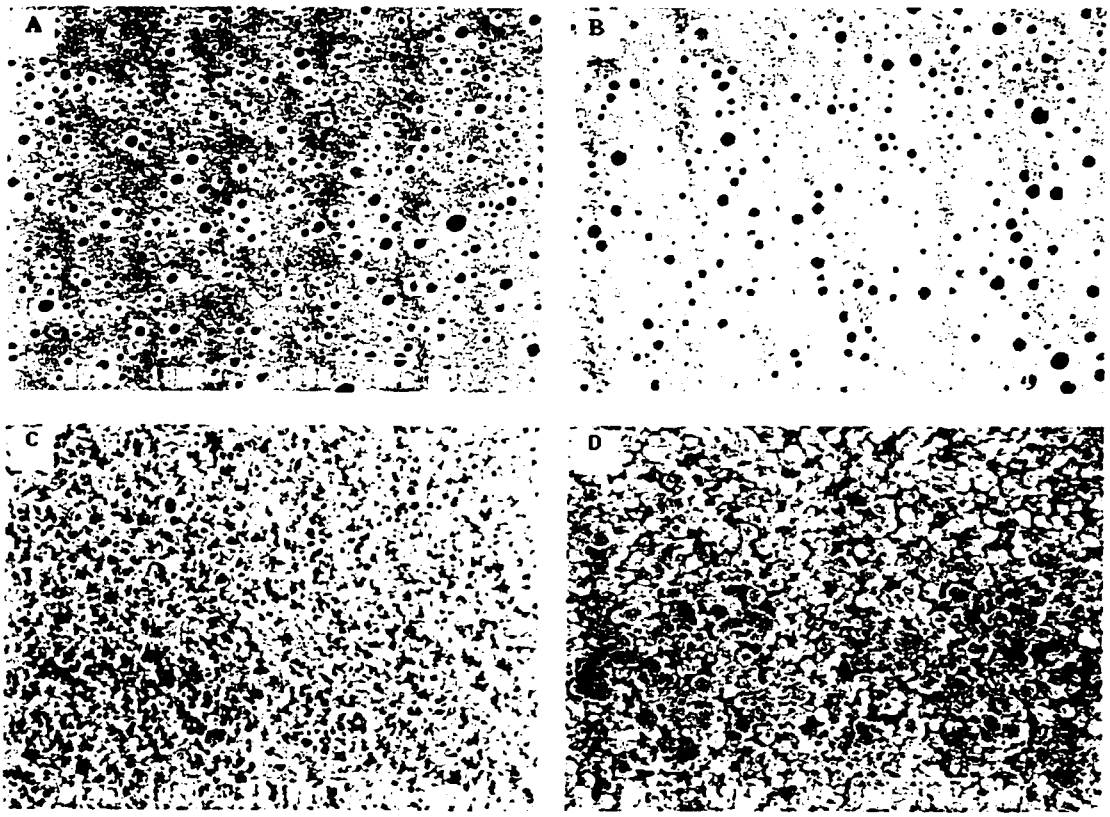

Figure 9. SEM micrographs for compatibilized PA/PS blends at 250°C.
(A) 10%PA/90%PS/20%SEBS-g-MA, (B) 20%PA/80%PS/20%SEBS-g-MA,
(C) 45%PA/55%PS/20%SEBS-g-MA and (D) 60%PA/40%PS/20%SEBS-g-MA

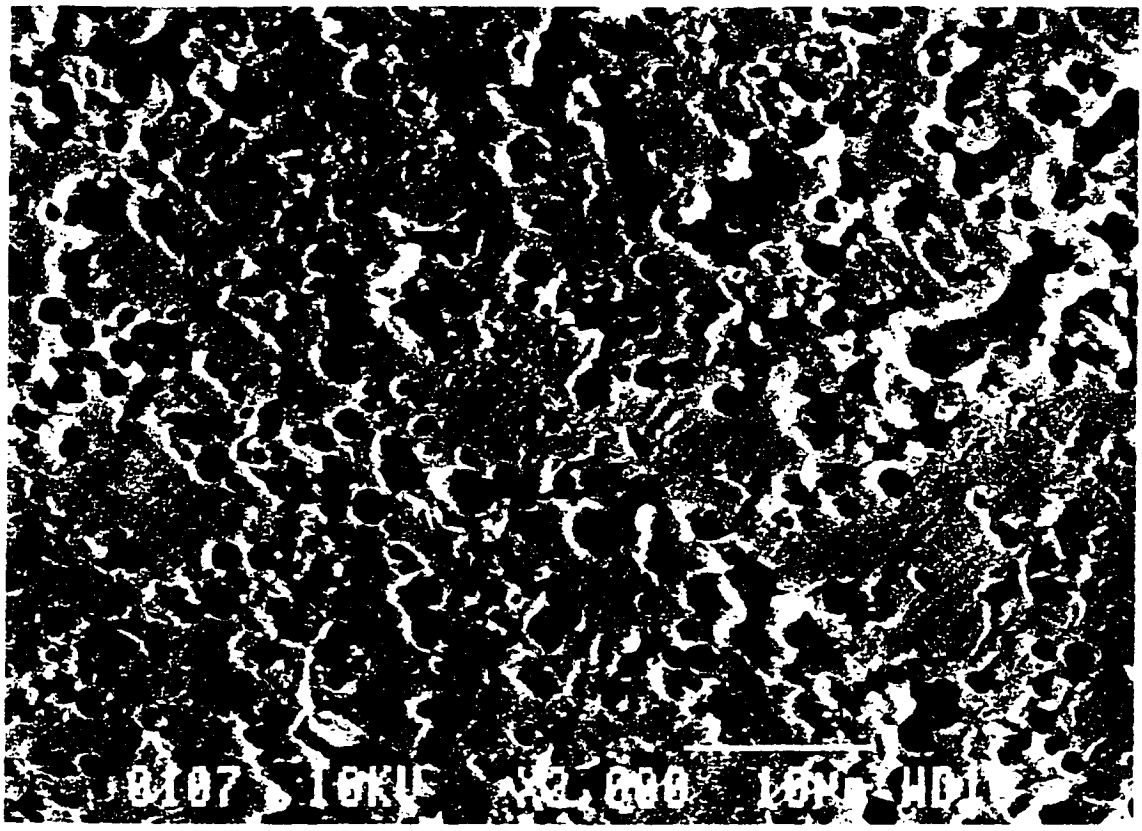

Figure 10. SEM micrograph for a 30%PA/70%PS/20%SEBS-g-MA blend at 250°C.

Table 1 Characteristic properties of materials

	Polyamide	Polystyrene	SEBS-g-MA
M_w	33,000	215,000	---
M_n	---	100,000	S=7500 EB=35000
Density (20°C) (g/cm^3)	1.13	1.04	0.910
Supplier	BASF	Dow	Shell

Table 2 The rheological behavior of PA, PS and SEBS-g-MA (rpm = 50, $\dot{\gamma} = 50\ s^{-1}$, T = 250°C)

	η^* (Pa.s)	η_d^*/η_m^*
PA	$1.0*10^3$	1
PS	$2.3*10^2$	4.3 (0.23)
SEBS-g-MA	$6.3*10^2$	1.6 (0.6)